Title
Identification of Novel Cellular Responses to Metal Homeostasis in Saccharomyces cerevisiae

Author
Lee, Yueh-Jung

Publication Date
2012

Peer reviewed|Thesis/dissertation

UNIVERSITY OF CALIFORNIA

Los Angeles

Identification of Novel Cellular Responses to Metal Homeostasis in *Saccharomyces cerevisiae*

A dissertation submitted in partial satisfaction of the
requirements for the degree Doctor of Philosophy
in Biochemistry and Molecular Biology

by

Yueh-Jung Lee

2012

ABSTRACT OF THE DISSERTATION

Identification of Novel Cellular Responses to Metal Homeostasis
in *Saccharomyces cerevisiae*

by

Yueh-Jung Lee

Doctor of Philosophy in Biochemistry and Molecular Biology
University of California, Los Angeles, 2012

Professor Guillaume F. Chanfreau, Chair

Among the essential transition metals, iron and zinc are the most studied and much is understood about the effect and regulation of these important cofactors. Yet much still remains unknown about the biochemical mechanisms which are required for cellular homeostasis of these metals. My studies have focused on identifying novel cellular responses to iron toxicity and to zinc deficiency in the budding yeast, *Saccharomyces cerevisiae*.

The first part of my research focuses on identifying suppressor genes which, when over-expressed, can protect cells against iron toxicity. Suppressor screens were performed

using a genomic library in a multicopy vector. The screen identified *ORM2* and *ORM1* as both were shown to rescue cell growth in high iron conditions. Both Orm1/2 are transmembrane proteins localized at the endoplasmic reticulum (ER). It was previously known that both Orm2 and Orm1 are negative regulators for sphingolipid biosynthesis and that they also play roles in protein quality control. Thus, cells show resistance to iron toxicity when sphingolipid synthesis is inhibited by the over-expression of Orm2/1 or by the treatment with myriocin, a potent inhibitor of sphingolipid synthesis. By measuring sphingolipid LCB levels with and without high iron, high iron was shown to induce sphingolipid biosynthesis and that over-expression of *ORM2/1* can reduce sphingolipid levels, which protects cells from iron toxicity. Furthermore, data indicate that iron toxicity is mediated by sphingolipid-activated protein kinases Pkh1 and Ypk1 and by a transcriptional factor Smp1. Contrary to general belief that iron toxicity results from oxidative damage, my study shows that iron toxicity involves activation of sphingolipid signaling.

The second part of my research focuses on elucidation of a novel cellular mechanism which yeast cells have developed in response to zinc deficiency. It was discovered that subunits of RNA polymerase I undergo degradation during zinc starvation. The observed degradation is specific to RNA polymerase I (RNAPI) and its associated proteins. Furthermore, this down-regulation of RNAPI is dependent on vacuolar proteases Pep4 and Prb1. Inactivation of the vacuolar proteases rescues the down-regulations of RNAPI as well

as its associated proteins during zinc starvation. RNAPI complex is transported out of the nucleus as a complex and this process is mediated by the exportin Xpo1. Data also suggest that de-ubiquitination of RNAPI is required for its down-regulation during zinc starvation. It is hypothesized that the down-regulation of RNAPI, which is responsible for transcribing ribosomal RNAs and accounts for most transcriptional activities in yeast cells, can conserve energy used for ribosome biogenesis during zinc starvation. Moreover, several subunits of RNAPI are zinc-binding proteins. By degrading RNAPI in the vacuole, yeast cells can conserve and recycle zinc atoms for other important cellular functions during zinc deficiency.

The dissertation of Yueh-Jung Lee is approved.

Arnold J. Berk

Catherine F. Clarke

Alison R. Frand

Jay D. Gralla

Guillaume F. Chanfreau, Committee Chair

University of California, Los Angeles

2012

DEDICATION

I would like to dedicate this dissertation to my mother and father for their support and love and in memory of my brother, Yueh-Hsien Lee.

TABLE OF CONTENTS

LIST OF FIGURES AND TABLES

ACKNOWLEDGEMENTS

Foremost, I would like to thank my advisor Dr. Guillaume F. Chanfreau for giving endless support during my graduate years at UCLA. Without his guidance and encouragement, I would not have been able to achieve the work I present in this dissertation. I would also like to thank all my committee members for being supportive and patient and for all their professional advice and criticism.

I would like to thank *Cell Metabolism* for allowing me to use the reprint of the article entitled "Sphingolipid Signaling Mediates Iron Toxicity" as Chapter 2 in the dissertation. I would also like to thank the co-authors in the work presented in Chapter 2. First, I would like to thank Xinhe Huang and Dr. Robert C. Dickson from University of Kentucky College of Medicine for performing LCB sphingolipid analysis (Figures 3B, 3C in Chapter 2). I would also like to thank Janette Kropat and Dr. Sabeeha S. Merchant from UCLA for performing ICP-MS to measure metal concentrations (Figure 3A). Finally I would like to thank Anthony Henras for generating the genomic library which was used to screen for suppressors.

I would like to thank the co-authors of the manuscript shown in Chapter 3, which is in preparation for submission. First, I would like to thank Chrissie Y. Lee for establishing the foundation of this research. She discovered that the down-regulation of RNA Polymerase I during zinc deficiency is specific to RNAPI subunits and to zinc depletion (Figures 1B-E). She also discovered that this RNAPI down-regulation is mediated by vacuolar proteases

(Figure 2B). I would like to thank Agnieszka Grzechnik for her contribution showing that RNAP associated proteins are also subject to down-regulation during zinc deficiency (Figure 2E). I also want to thank Fernando Gonzales-Zubiate for performing Northern blot analysis of ribosomal RNAs and Pulse-chase analysis of rRNAs and tRNAs (Figure 6). I would like to thank Albert Lee for performing Western blot analysis of Rnt1 expression during zinc deficiency (Figure 1A). Finally, I would like to thank Ajay A. Vashisht and Dr. James Wohlschlegel for performing Mass Spectrometric analysis of RNAPI subunits.

I would also like to thank my friends Brenda Beck and Michael Janis for giving me tremendous support throughout my graduate years. And most importantly, I would like to thank my family. Without their support, I would not have been able to have the opportunity and courage to pursue my interest in science and research.

VITA

EDUCATION

UNIVERSITY OF CALIFORNIA, LOS ANGELES, CA

B.S. Biochemistry, **2003-2005**

AZUSA PACIFIC UNIVERSITY, CA

Bachelor's program in Biology, **2001-2003**

RESEARCH EXPERIENCE

GRADUATE RESEARCH - Laboratory of Dr. Guillaume F. Chanfreau

2007-PRESENT

UNDERGRADUATE RESEARCH

2005-2006

Laboratory of Dr. **James U. Bowie**, Department of Chemistry and Biochemistry

Part of a research project led by Dr. **Sehat Nauli**.

POSTER PRESENTATIONS AT SCIENTIFIC MEETINGS

TRACE ELEMENT METABOLISM IN BIOLOGY & MEDICINE (JUNE, 2010)

FASEB SUMMER RESEARCH CONFERENCE

TEACHING AND MENTORING EXPERIENCE

UNIVERSITY OF CALIFORNIA, LOS ANGELES: DEPARTMENT OF CHEMISTRY AND BIOCHEMISTRY

TEACHING ASSISTANT

1/2007-6/2008

Assisted in teaching undergraduate biochemistry courses. The courses were advanced biochemistry laboratory courses, in which undergraduate students worked as teams to complete two project assignments throughout the course. The techniques used in the projects included cloning, protein expression, protein purification, Western blot analysis, enzyme kinetics, and lipid extraction and analysis. Duties included assisting and guiding students carrying out experiments and grading exams and lab reports.

PUBLICATIONS

Yueh-Jung Lee, Xinhe Huang, Janette Kropat, Anthony Henras, Sabeeha S. Merchant, Robert C. Dickson, and Guillaume F. Chanfreau. Sphingolipid signaling mediates iron toxicity. *Cell Metabolism*, 2012; 16: 90-96

Yueh-Jung Lee, Chrissie Young Lee, Agnes Grzechnik, Fernando Gonzales-Zubiate, Aja A. Vashisht, Albert Lee, James Wohlschlegel, and Guillaume F. Chanfreau. Vacuolar Autophagy of RNA polymerase I during zinc deficiency (**manuscript in preparation**)

Sehat Nauli, Saman Farr*, **Yueh-Jung Lee***, Hye-Yeon Kim, Salem Faham, James U. Bowie. Polymer-driven crystallization. *Protein Science*, 2007; 16(11): 2542-51. (*these authors contributed equally)

CHAPTER 1

INTRODUCTION

Many transition metals are essential trace elements in all living organisms. These metals function as important cofactors for critical cellular molecules, such as nucleic acids, enzymes, proteins and lipids. Without sufficient amounts of these transition metals, most biological processes are significantly affected. However, these metals are potentially toxic to the cells when in excess. Therefore, cells have evolved different mechanisms to maintain metal homeostasis. Many of these cellular mechanisms involve regulations of metal uptake, efflux and distribution systems. Some of them involve regulating metal storage as well as preventing metal-induced oxidative stress. Extensive studies have been done to understand mechanisms by which the budding yeast, *Saccharomyces cerevisiae*, balances metal homeostasis, especially iron and zinc; however, there is still much that remains unknown and requires further investigation.

IRON HOMEOSTASIS AND IRON TOXICITY

Among many transition metals in living organisms, iron is one of the most important metals. Iron can exist in one of two reduction-oxidation, or redox forms: the reduced form, Fe^{2+}, and the oxidized form, Fe^{3+}. Because of this redox characteristic, iron acts as a cofactor for many metalloenzymes. It is also this redox ability that can lead to substantial cellular damage in

high iron concentrations. In cells, "free" iron (Fe^{2+}) is toxic due to its ability to participate in Fenton chemistry to generate reactive oxygen species (ROS) which can cause serious damage to proteins, lipids and nucleic acids. Therefore, excess of cellular iron can result in iron overload/ iron toxicity. Many diseases are related to iron overload/ iron toxicity, including hemochromatosis, Parkinson's disease, and Fredreich's ataxia (Rausch et al, 1988; Radisky et al, 1999).

Iron Uptake

In *Saccharomyces cerevisiae,* one of the mechanisms cells use to maintain iron homeostasis is regulation of iron uptake from the environment. Unlike other eukaryotes, yeast cells do not have iron export systems to remove an excess of iron. Therefore, they can only regulate the amount of iron being taken from the environment or stored in vacuoles. In aerobic conditions, iron exists predominately in its ferric, or oxidized form (Fe^{3+}), which is insoluble in water at neutral pH; however, most iron transporters require ferrous, or reduced Fe^{2+} as their substrates. Therefore, yeast cells employ two parallel pathways for iron uptake from the environment: the reductive pathway and non-reductive pathway. The reductive pathway requires reduction of ferric iron to ferrous iron and the non-reductive pathway requires soluble siderophore-Fe^{3+} chelates (Philpott and Protchenko, 2008; Kaplan and Kaplan, 2009).

In the reductive uptake pathway, before being transported into the cells, the oxidized ferric iron needs to be reduced to ferrous iron by metalloreductases, such as Fre1 and Fre2 in the cell membrane (Dancis et al, 1990; Anderson et al, 1992; Georgatsou and Alexandraki, 1994). Once iron is reduced, it becomes a suitable substrate for two main iron transport systems: the low-affinity iron transporter Fet4 and the high-affinity iron transporter Fet3/Ftr1 (Dix et al, 1994; Askwith et al, 2994; Stearman et al, 1996). The low-affinity transporter Fet4 is a plasma membrane permease and functions as the major iron uptake system when cellular iron concentration is relatively high (Dix et al, 1997). The high-affinity iron transporter consists of two proteins, Fet3 and Ftr1. Fet3 is a multicopper oxidase and can oxidize ferrous ions to ferric ions. The oxidized ferric ions can then become a substrate for the transmembrane permease Ftr1 and are transported into the cytosol. In contrast to Fet4, the high affinity iron transporter Fet3/Ftr1 is responsible for the majority of iron uptake in iron-depleted yeast cells (Eide et al, 1992). Fet3 requires copper ions for its oxidase activity. It has been shown that, in copper-depleted conditions, the amounts of ferrous ions transported into the cells decrease due to the non-functional Fet3 (Askwith et al, 1994). Thus, there is an interconnection between iron homeostasis and copper homeostasis.

Both iron transporters are regulated primarily at the transcriptional level. *FET3/FTR1*, *FET4* and the metalloreductases *FRE1/FRE2* are all part of the iron regulon (Yamaguchi-Iwai et al,

1995; Waters and Eide, 2002; Jensen et al, 2002). The yeast iron regulon is a group of iron-uptake-related genes that are regulated by transcriptional activators Aft1 and Aft2 (Yamaguchi-Iwai et al, 1995; Blaiseau et al, 2001; Rutherford et al, 2001). Aft1p induces the expression of the iron regulon by localizing to the nucleus and binding to the promoter regions of the iron regulon genes when intracellular iron concentration is low. With an excess of iron in the cell, Aft1 does not localize to the nucleus and, therefore, does not induce the expression of genes involved in iron uptake (Yamaguchi-Iwai et al, 2002). Aft2 is another transcriptional activator involved in maintaining iron homeostasis. Evidence shows that, in response to low iron conditions, Aft2 can activate iron-responsive genes in the absence of Aft1 (Blaiseau et al, 2001). Moreover, it was demonstrated from microarray data that Aft2 can activate a group of genes which are not activated by Aft1 (Courel et al, 2005). In addition to the transcriptional regulation of the iron transporters, iron transporters can also be regulated at the post-translational level. When intracellular iron concentration is too high, Ftr1 is ubiquitinated and then the ubiquitinated Ftr1/Fet3 complex undergoes internalization and is targeted for degradation (Felice et al, 2005). Thus, when cellular iron levels are high, yeast cells inhibit expression of iron uptake genes and simultaneously down-regulate existing iron transporters located at the plasma membrane to prevent further iron uptake.

In the non-reductive pathway, yeast cells utilize siderophore-bound iron. Siderophores are

low molecular-weight compounds which can dissolve insoluble ferric ions via chelation to a soluble Fe^{3+} compound (Neilands, 1995). *S. cerevisiae* does not synthesize siderophore compounds and yet it can recognize and utilize different siderophore-Fe^{3+} compounds secreted by other microorganisms. The siderophore-Fe^{3+} complex can be transported across the plasma membrane by the ARN family of transporters Arn1-4 with the help of the facilitators Fit1-3 (Yun et al, 2000; Protchenko et al, 2001). The mRNA levels of iron transporters Arn1-4 and the facilitators Fit1-3 were shown to be regulated by Rnt1, a double-stranded RNA endonuclease of RNAase III family (Lee et al, 2005). In high iron conditions, Rnt1 can cleave the mRNAs of Arnt1-4 and Fit1-3, which results in the degradation of the cleaved mRNAs by 5'-3' exonuclease Xrn1 and Rat1(Lee et al, 2005). This down-regulation of siderophore- Fe^{3+} transporters and facilitators can prevent excess of iron being transported into cells in high iron conditions. Moreover, it has been shown recently that upon oxidative stress, yeast cells favor the non-reductive pathway in order to minimize the oxidative damage caused by ferrous iron from the reductive iron-uptake pathway (Castells-Roca et al, 2011).

Vacuolar Iron Storage

Another mechanism yeast cells utilize to maintain iron homeostasis is iron storage. Unlike other eukaryotes, yeast cells do not have iron storage proteins such as ferritin. Instead, iron is

stored in the cell vacuole. Iron transporters in the vacuolar membrane transport iron in and out of the vacuole. Ccc1 is the only identified vacuolar iron importer and Fet5/Fth1 and Smf3 are the high-affinity and low-affinity iron exporters respectively (Li et al, 2001; Urbanowski and Piper, 1999; Portnoy, 2000). When cytosolic iron is low, *CCC1* is post-transcriptionally down-regulated to prevent further iron import to the vacuole. The down-regulation of *CCC1* involves an mRNA-binding protein Cth2. *CTH2* and its homolog *CTH1* are part of the Aft1 iron regulon and the expression is induced under iron deprivation. Both Cth1 and Cth2 down-regulate mRNA of Fe-dependent pathways at the post-transcriptional level (Puig et al, 2005; Puig et al, 2008). Cth2 binds to AU-rich Element (ARE) within the 3' untranslated region of target mRNA to mediate its degradation. The down-regulation of *CCC1* is mediated by Cth2 during iron deprivation (Puig et al, 2005). Simultaneously, both vacuolar iron exporters including Fet5/Fth1 (high affinity transporter complex) and Smf3 (low affinity transporter) are also up-regulated by Aft1 and Aft2 in iron-depleted yeast cells (Courel et al 2005; Rutherford and Bird 2004). This up-regulation of the vacuolar exporters and down-regulation of the iron importer insure that only the stored iron is being transported from the vacuole to the cytosol when iron is needed.

In contrast to the iron limiting conditions, high levels of cytosolic iron will induce expression of the iron importer *CCC1* to increase iron storage in the vacuole. Yap5, an iron-responsive

transcriptional activator, is responsible for the induction of *CCC1* when cellular iron concentrations are too high (Li et al, 2008). The iron stored in the vacuole can be transported out to the cytosol when needed, and excess of iron in the cytosol can be transported into the vacuole for later use and to prevent iron-related oxidative stress.

Iron-Sulfur (Fe-S) Cluster Biosynthesis

Iron-Sulfur cluster biosynthesis is one of the major iron metabolic functions of mitochondria. Several studies have demonstrated that iron-sulfur (Fe-S) cluster synthesis plays an important role in regulating the Aft1/Aft2-mediated iron regulon in yeast cells. The decrease in Fe-S cluster biosynthesis due to insufficient cellular iron can signal the Aft1/2 transcriptional activators to up-regulate the iron regulon (Chen et al, 2004; Rutherford et al, 2005). More studies have been done to further investigate the mechanism involved in the regulation of Aft1/Aft2. Instead of responding to cytosolic iron, Aft1 and Aft2 respond directly to mitochondrial iron-sulfur cluster biogenesis by interacting with the cytosolic proteins, Grx3/4 and Fra2 (Ojeda et al, 2006; Pujol-Carrion et al, 2006; Kumanovics et al, 2008). Evidence suggests that Grx3/4 and Fra2 can form a complex with iron-sulfur clusters and this complex is essential for regulating Aft1/2 in response to cellular iron status (Li et al, 2009).

Furthermore, it has been shown recently that over-expression of mitochondrial iron transporters, Mrs3/4, can suppress iron toxicity (Lin et al, 2011). In addition, another study demonstrated that the transcriptional activator Yap5 can activate the expression of a Fe-S cluster enzyme under high iron condition (Li et al, 2011). Both pieces of evidence suggest that yeast cells can incorporate excess iron into Fe-S cluster proteins in order to prevent iron toxicity by up-regulating the mitochondrial iron transport and the iron-sulfur cluster synthesis. Therefore, iron-sulfur cluster biosynthesis not only acts as a sensor for cellular iron availability but also serves as an iron reservoir in which excess of iron can be stored, in addition to the vacuole.

Cellular Responses to Iron Toxicity

As mentioned above, yeast cells induce changes in iron transporter pathways, iron storage systems and iron-sulfur biosynthesis in response to cellular iron levels. In high iron conditions, yeast cells utilize homeostatic responses, including down-regulation of iron uptake from the environment and up-regulation of iron storage in the vacuoles to prevent iron toxicity. As mentioned earlier, its ability to participate in Fenton chemistry to generate reactive oxygen species makes iron toxic to cells. Therefore, as an adaptive response to iron toxicity, yeast cells up-regulate antioxidant proteins, including superoxide dismutases (SODs) and peroxidases, to repair damage caused by iron-induced oxidative stress. In addition, a

recent study has shown that, upon oxidative stress, expression of the iron regulon was induced by Aft1 localizing to the nucleus (Castells-Roca et al, 2011). The induced iron regulon includes genes from reductive iron uptake pathways such as *FET3* and *FTR1* and from non-reductive pathways, such as *FIT3*. The *FIT3* mRNA remains stable, while the *FET3* and *FTR1* mRNAs become rapidly degraded (Castells-Roca et al, 2011). This suggests that in response to iron induced oxidative stress, cells prefer the non-reductive iron-uptake pathway in order to prevent oxidative damage caused by the reductive iron-uptake pathway.

It is believed, in the present paradigm, that the production of reactive oxygen species generated from high cellular iron concentration is the major cause of iron toxicity. However, recent work has shown that, in the anaerobic condition, iron is still toxic to yeast cells and that there is no induction of antioxidant transcripts in high iron condition (Lin et al, 2011). This suggests that oxidative damage resulting from reactive oxygen species may not be the major cause to iron toxicity. Even though many studies have been done to uncover the mystery of iron toxicity, much remains unknown and requires further investigation.

ZINC HOMEOSTASIS AND ZINC DEFICIENCY

Zinc is another essential trace element in all organisms. Many enzymes and proteins, including the zinc-finger proteins, zinc-binding transcriptional factors and RNA polymerases, require zinc as an important cofactor for their cellular function and structural stability. In addition, it was shown recently that zinc may serve as a signaling molecule in various signal transduction pathways (Hirano et al, 2008). Therefore, cells need to tightly regulate intracellular zinc homeostasis in response to zinc availability from the environment. Zinc deficiency is common in many organisms, including human, and is associated with many diseases, including chronic liver disease, sickle cell disease, and diabetes (Tuerk and Fazel, 2009).

Zinc Uptake

In *Saccharomyces cerevisiae*, zinc uptake is the major mechanism for maintaining cellular zinc homeostasis. In yeast, high-affinity and low-affinity zinc transporters can mediate zinc uptake in the plasma membrane. *ZRT1* and *ZRT2* genes encode Zn^{2+} specific high-affinity and low-affinity transporters respectively (Zhao and Eide, 1996a; Zhao and Eide, 1996b). Both Zrt1 and Zrt2 belong to the ZIP family of metal transporters. Members of the ZIP family play roles in transporting metal ions and are found in different eukaryotes (Eng et al, 1998).

In addition, Fet4, the low-affinity iron transporter, can also transport zinc as well as copper (Waters and Eide, 2002; Hassett et al, 2000). Zrt1 has a higher affinity for zinc, and therefore, is responsible for the majority of zinc uptake during severe zinc deficiency. Both Zrt2 and Fet4 have lower affinity for zinc and are used for zinc uptake in milder low-zinc conditions. As with the regulation of iron uptake systems, zinc transporters are regulated at both the transcriptional and post-translational levels (Zhao and Eide, 1997; Lyons et al, 2000; Gitan et al, 1998; Gitan and Eide, 2000).

When extracellular zinc is limited, the expression of *ZRT1*, *ZRT2* and *FET4* is induced by Zap1 transcriptional factor in order to increase zinc uptake (Zhao and Eide, 1997; Lyons et al, 2000). Zap1 is a metalloprotein and can act as a transcriptional activator as well as a repressor. Zap1 activates or represses transcription by binding to zinc-responsive elements (ZREs) in the promoter regions of its target genes (Zhao et al, 1998). Zap1 contains two domains, AD1 and AD2, which are responsible for activating transcription of its target genes (Bird et al, 2000). Among its target genes, Zap1 can activate its own transcription during zinc-limited conditions, which increases Zap1 levels to further activate transcription of zinc uptake genes (Zhao et al, 1998). In addition to the ability to activate its target genes, Zap1 can also repress expression by binding to the promoter of its target genes. *ZRT2*, a low affinity zinc transporter, is one of the genes whose expressions can be repressed by Zap1 (Bird et al, 2004). As mentioned above, *ZRT2* expression is induced by Zap1 in low zinc conditions; however,

when yeast cells experience severe zinc deficiency, *ZRT2* expression is repressed. Unlike other Zap1 target genes, *ZRT2* contains three ZRE sites at its promoter region. Two of the ZRE sites have higher affinity for Zap1 and one has lower affinity for Zap1 (Bird et al, 2004). This lower affinity ZRE is located downstream of the TATA box in *ZRT2*. When Zap1protein levels increase due to its autoregulation in severe zinc deficiency, Zap1 can bind to the low affinity ZRE site and inhibit *ZRT2* transcription (Bird et al, 2004). This repression of ZRT2 ensures that yeast cells do not express the low-affinity Zrt2 transporter when it cannot contribute to zinc uptake during severe zinc deficiency.

On the other hand, when cellular zinc concentration is high, zinc atoms can bind to AD1 and AD2 domains and inhibit the ability of Zap1 to activate transcription (Bird et al, 2000; Herbig et al, 2005; Bird et al, 2003). Therefore, Zap1 can function as a direct sensor for cellular zinc availability. In addition to the transcriptional regulation by Zap1, some studies have shown that the zinc transporters Zrt1 and Zrt2 are both down-regulated post-translationally in high zinc conditions (Gitan et al, 1998; Gitan and Eide, 2000). This down-regulation is mediated by ubiquitin-mediated endocytosis (Gitan et al, 1998; Gitan and Eide, 2000). It has been shown that to prevent over-accumulation of cellular zinc atoms, zinc triggers ubiquitination of zinc transporters, which are removed from the plasma membrane by endocytosis (Gitan et al, 1998; Gitan and Eide, 2000). Thus, to maintain cellular zinc homeostasis, cells have

evolved multiple mechanisms in regulating zinc uptake systems.

Vacuolar Zinc Storage

Another cellular mechanism yeast cells utilize to maintain zinc homeostasis is zinc storage in the vacuole. As with iron, an excess of zinc can be stored in the vacuole for later use. Zinc transporters are localized in the vacuolar membrane to transport zinc into or out of the vacuole in response to cytosolic zinc levels. Zrt3, the vacuolar zinc exporter, is responsible for transporting zinc atoms out of the vacuole. Similar to Zrt1 and Zrt2, Zrt3 also belongs to the ZIP family of metal transporters (MacDiarmid et al, 2000). Under zinc-limited conditions, Zrt3 expression is up-regulated by Zap1, which results in an increase in the efflux of zinc atoms from the vacuole to the cytosol (MacDiarmid et al, 2000). When cytosolic zinc levels are high, on the other hand, the vacuolar zinc importers Zrc1 and Cot1 can transport excess zinc into the vacuole for storage (Kamizono et al, 1989; MacDiarmid et al, 2000). Both Zrc1 and Cot1 are members of CDF (Cation Diffusion Facilitator) family. CDF transporters are ubiquitous in eukaryotic organisms and are involved in heavy metal transport. Zrt1 and Cot1 are closely related proteins and can transport both zinc and cobalt in yeast cells (Conklin et al, 1992; Conklin et al, 1994).

In addition to its role in up-regulating vacuolar zinc storage in zinc-replete conditions, Zrc1

also plays an important role in zinc shock tolerance during zinc starvation. When cytosolic zinc levels are low, cells induce expression of zinc transporters, such as Zrt1, in the plasma membrane, which leads to an accumulation of substantial amounts of zinc in the cytosol. This rapid accumulation of zinc in the cytosol is referred to as "zinc shock." In order to withstand zinc shock, yeast cells induce *ZRC1* expression by Zap1 transcriptional factors and promote the transport of excess cytosolic zinc into the vacuole (Miyabe et al, 2000; MacDiarmid et al, 2003). Therefore, yeast vacuoles play an important role in maintaining zinc homeostasis by storage and detoxicification of excess zinc.

Cellular Responses to Zinc Deficiency

Many important cellular proteins and enzymes rely heavily on zinc atoms for their catalytic and structural functions. When intracellular zinc concentration is not sufficient for normal cellular functions, cells can initiate several homeostatic responses, including increasing zinc uptake by up-regulating Zrt1 transporters and by mobilizing stored zinc from vacuoles by up-regulating vacuolar Zrt3 exporters. In addition to these cellular responses during zinc starvation, yeast cells can also conserve limited zinc atoms for other important cellular functions by down-regulating zinc-binding proteins. One particular class of zinc-binding proteins is alcohol dehydrogenase. Adh1 and Adh3 are the major zinc-containing alcohol dehydrogenases in cytosol and mitochondria respectively. Zinc atoms are essential for their

catalytic function and structural stability. During zinc starvation, both *ADH1* and *ADH3* have been shown to be repressed by Zap1 (Bird et al, 2006). Zap1 represses the *ADH1/3* expression by binding to the ZRE sites upstream of the promoter regions and activating the transcription of intergenic transcripts which overlap the promoter of *ADH1* and *ADH3*. These intergenic transcripts prevent binding of transcriptional factors that are required for expression of *ADH1* and *ADH3* (Bird et al, 2006). Thus, by repressing expression of zinc-dependent proteins, yeast cells can conserve zinc for more important uses during zinc deficiency.

Several studies have shown that, in mammalian cells, zinc deficiency can lead to oxidative stress (Powell, 2000). Recent study has confirmed that yeast cells experience more oxidative stress during zinc-limited conditions (Wu et al, 2007). One mechanism, which yeast cells have adapted to protect themselves from the oxidative stress induced by zinc deficiency, is to up-regulate the expression of an antioxidant protein Tsa1. *TSA1*, which encodes a cytosolic thioredoxin-dependent peroxidase, catalyzes the breakdown of hydrogen peroxide and organic hydroperoxides (Rhee et al, 2005). Tsa1 was found to be a direct target of Zap1 and is important for cell growth during zinc-limited conditions. In the absence of Tsa1, cells show higher sensitivity to hydrogen peroxide and accumulate higher amounts of reactive oxygen species (ROS) (Wu et al, 2007). Thus, by inducing an antioxidant protein Tsa1, yeast has

evolved to protect itself from oxidative stress generated from zinc deficiency.

Over the last decade, our understanding of zinc deficiency in yeast and other organisms has advanced significantly. Many studies have uncovered novel cellular mechanisms in response to zinc deficiency and provided new insights into zinc homeostasis within different organisms. These studies have also set a foundation for future studies by uncovering novel mechanisms involved in maintaining cellular zinc homeostasis.

CONTRIBUTION OF MY STUDIES TO METAL HOMEOSTASIS IN *SACCHAROMYCES CEREVISIAE*

The Novel Role of Sphingolipid in Iron Toxicity

As mentioned above, under anaerobic conditions, iron is still toxic to yeast cells and that there is no induction of antioxidant transcripts in high iron conditions (Lin et al, 2011). This suggests that oxidative damage resulting from reactive oxygen species may not be the major cause of iron toxicity. We were interested in understanding novel cellular responses to iron toxicity in the budding yeast, *Saccharomyces cerevisiae*. A suppressor screen was performed to identify genes which, when over-expressed, can protect cells from iron toxicity. We identified *ORM1* and *ORM2*, as both, when over-expressed, were shown to rescue cell growth

in high iron condition. Both yeast *ORM1* and *ORM2* belong to a family of conserved *ORMDL* genes, including *ORMDL1/2/3* in humans (Hjelmqvist et al, 2002). Members of the *ORMDL* family encode transmembrane proteins localized to endoplasmic reticulum (ER). It has been shown that the human *ORMDL3* gene is a potential risk factor for childhood asthma (Moffatt et al, 2007). Several studies have demonstrated that, in yeast cells, both Orm1 and Orm2 proteins play important roles in regulating sphingolipid homeostasis and protein quality control (Breslow et al, 2010; Han et al, 2010). Orm1 and Orm2 act as negative regulators of serine palmitoyltransferase, an essential enzyme that catalyzes the first step in sphingolipid biosynthesis (Breslow et al, 2010). Sphingolipids are essential structural components of cell membranes. Sphingolipid biosynthesis starts in the endoplasmic reticulum (ER), where serine palmitoyltransferase catalyzes the condensation of palmitoyl-CoA and serine as shown in Figure 2. Many sphingolipid intermediates, such as long-chain bases, ceramides and complex sphingolipids, play important roles in regulating essential cellular processes by acting as signaling molecules (reviewed in Dickson, 2008).

We found that a higher level of sphingolipids intermediates was observed in yeast cells grown in high iron conditions. In addition, by over-expressing Orm1/2 or by the use of myriocin, a potent inhibitor of serine palmitoyltransferase, yeast cells become more resistant to high iron. Furthermore, inactivation of sphingolipid-activated kinases, Phk1 and Ypk1, and of the downstream transcriptional factor, Smp1, can confer resistance to iron toxicity. Thus,

contrary to general belief that iron toxicity results from oxidative damage, our work shows that iron toxicity is mediated by sphingolipid signaling.

Vacuolar Autophagy of RNAPI in Response to Zinc Deficiency

As mentioned above, during zinc starvation, cells can conserve limited zinc for important cellular functions by down-regulating the expression of zinc-dependent proteins, such as Adh1/3 (Bird et al, 2006). We were interested in finding novel mechanisms which yeast cells have developed in response to zinc starvation. We discovered that the subunits of RNA polymerase I and other associated proteins are degraded during zinc deficiency. This down-regulation of the RNAPI complex is specific to zinc starvation and is mediated by the nuclear exportin Xpo1 and vacuolar proteases Pep4 and Prb1. Once the RNAPI complex is out of the nucleus, it is then transported into the vacuole for degradation by vacuolar proteases Pep4 and Prb1. Fluorescence microscopy showed that RNAPI was sequestered inside the vacuole in the absence of vacuolar proteases in low zinc conditions. Furthermore, our data suggests that de-ubiquitination of the RNAPI is required for the down-regulation and vacuolar import of RNAPI during zinc starvation. Moreover, several subunits of RNAPI complex require zinc atoms for their function and/or structure stability (Treich et al, 1991;

Naryshkina et al, 2003). Mutations in zinc-containing subunits, such as Rpa135 and Rpa12, affected the down-regulation of RNAPI during zinc starvation. This suggests that zinc-binding subunits of RNAPI may function as zinc sensors in response to intracellular zinc content.

During zinc deficiency, cell growth is limited by the lack of intracellular zinc atoms. In order for cells to survive in growth-limited conditions, they need to conserve energy by down-regulating the cellular process that uses the most energy: ribosome biosynthesis. RNA polymerase I (RNAPI) is responsible for synthesizing ribosomal RNAs (rRNAs), which account for nearly 60% of the total transcription in yeast (Warner, 1999). Thus, our data suggest that, by degrading the RNAPI complex during zinc deficiency, cells can down-regulate ribosome biosynthesis. In addition to energy conservation, the degradation of the RNAPI complex in the vacuole might also contribute to the recycling of zinc atoms bound to the subunits of RNAPI. Taken together, our data demonstrate that the RNAPI complex undergoes vacuolar autophagy in response to zinc starvation in order to down-regulate the most energy-consuming cellular machinery and to conserve/redistribute limited zinc atoms for other important cellular functions.

Figure 1. Iron and Zinc Homeostasis in *Saccharomyces cerevisiae*.
A. Iron homeostasis in *Saccharomyces cerevisiae* **B.** Zinc homeostasis in *Saccharomyces cerevisiae*.

Figure 1

A.

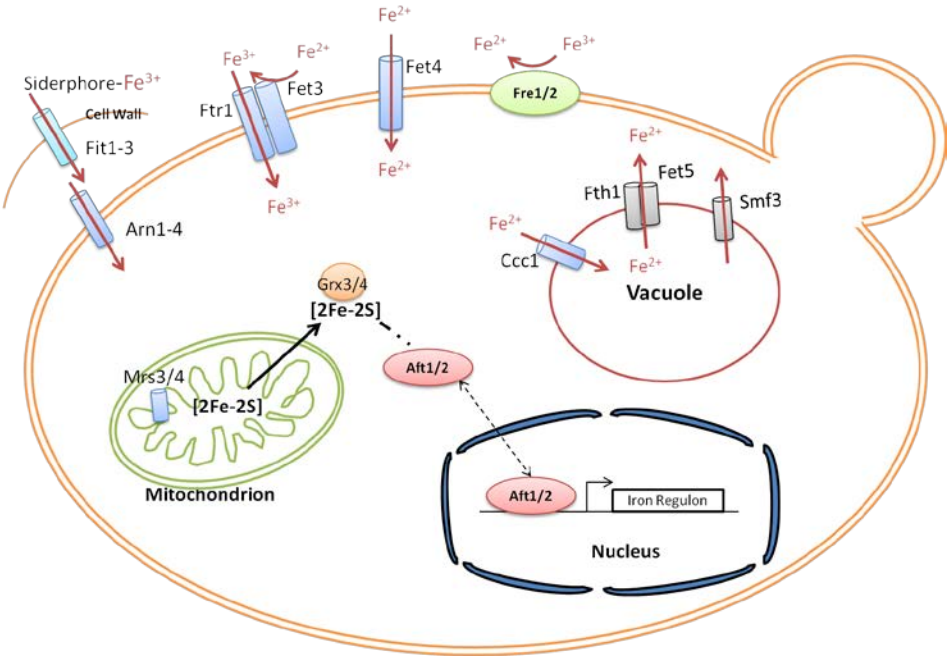
Siderphore-Fe3+
Cell Wall
Fit1-3
Arn1-4
Fe3+
Fe2+
Ftr1
Fet3
Fe2+
Fet4
Fe2+
Fe2+
Fe3+
Fre1/2
Fe2+
Fth1
Fet5
Smf3
Fe2+
Ccc1
Fe2+
Vacuole
Grx3/4
[2Fe-2S]
Aft1/2
Mrs3/4
[2Fe-2S]
Mitochondrion
Aft1/2
Iron Regulon
Nucleus

B.

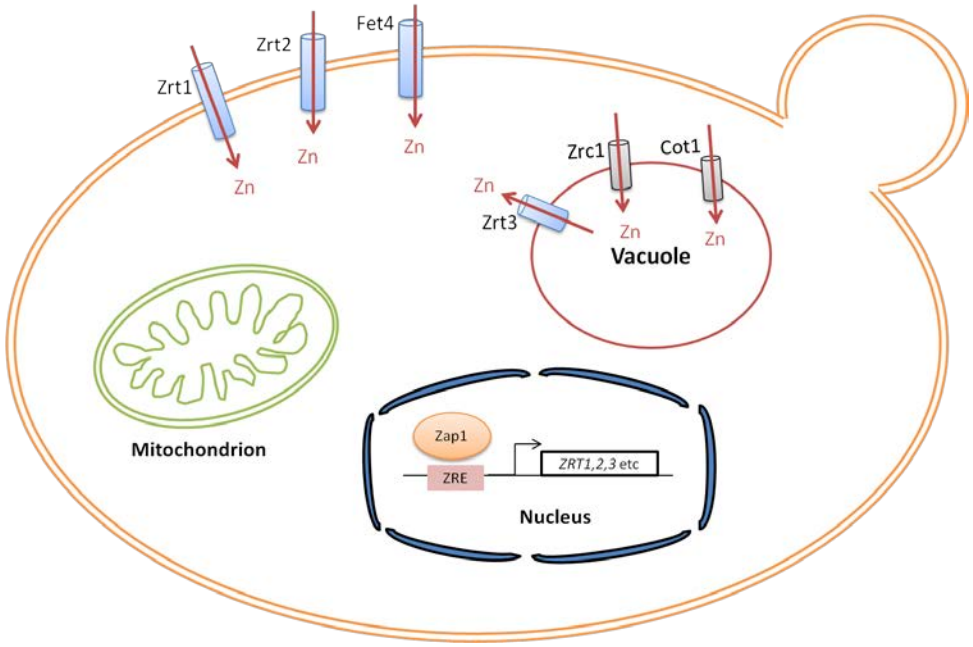
Zrt1
Zn
Zrt2
Zn
Fet4
Zn
Zrc1
Cot1
Zn
Zrt3
Zn
Zn
Vacuole
Mitochondrion
Zap1
ZRE
ZRT1,2,3 etc
Nucleus

Figure 2. Outline of sphingolipid biosynthesis in *Saccharomyces cerevisiae*.

Figure 2

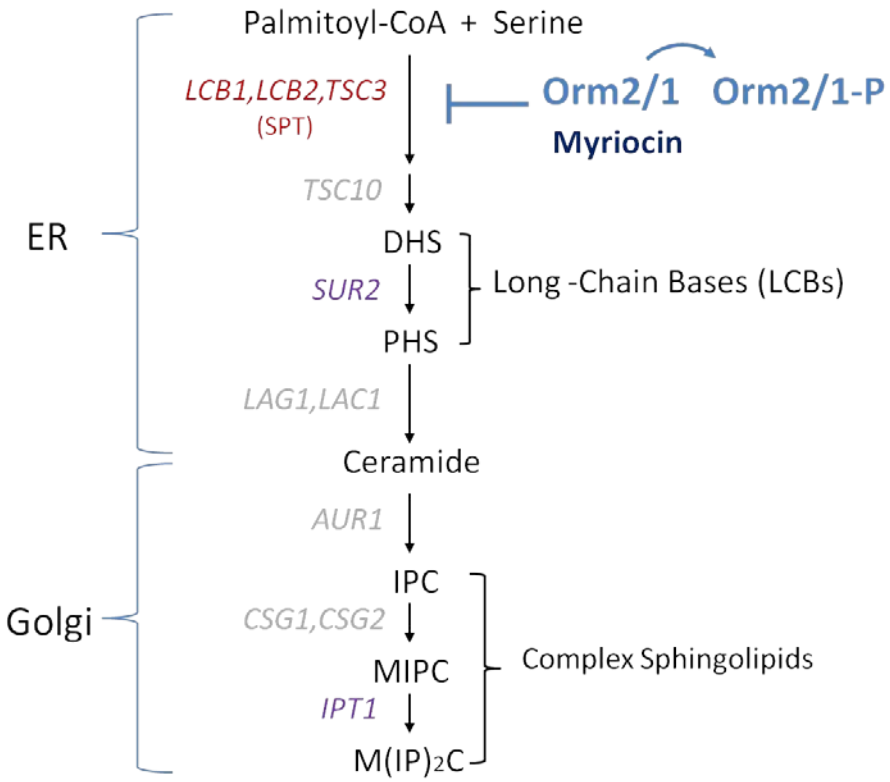
Palmitoyl-CoA + Serine
LCB1,LCB2,TSC3
(SPT)
Orm2/1
Orm2/1-P
Myriocin
TSC10
ER
DHS
SUR2
Long -Chain Bases (LCBs)
PHS
LAG1,LAC1
Ceramide
AUR1
IPC
Golgi
CSG1,CSG2
MIPC
Complex Sphingolipids
IPT1
M(IP)2C

REFERENCES

Anderson, G.J., Lesuisse, E., Dancis, A., Roman, D.G., Labbe, P., and Klausner, R.D. (1992) Ferric iron reduction and iron assimilation in *Saccharomyces cerevisiae*. *J Inorg Biochem* 47(3-4):249-55

Askwith. C., Eide. D., Van Ho, A., Bernard, P.S., Li, L., Davis-Kaplan, S., Sipe, D.M., Kaplan, J (1994) The FET3 gene of *S. cerevisiae* encodes a multicopper oxidase required for ferrous iron uptake. *Cell* 76(2):403-10

Bird, A.J., Blankman, E., Stillman, D.J., Eide, D.J., and Winge, D.R. (2004) The Zap1 transcriptional activator also act as a repressor by binding downstream of the TATA box in ZRT2. *EMBO J* 23(5):1123-32

Bird, A.J., Gordon, M., Eide, D.J., and Winge, D.R. (2006) Repression of ADH1 and ADH3 during zinc deficiency by Zap1-induced intergenic RNA transcripts. *EMBO J* 25(24):5726-34

Bird, A.J., McCall, K., Kramer, M., Blankman, E., Winge, D.R., and Eide, D.J. (2003) Zinc fingers can act as Zn2+ sensors to regulate transcriptional activation domain function. *EMBO J* 22(19): 5137-46

Bird, A.J., Zhao, H., Jensen, L.T., Srinivasan, C., Evans-Galea, M., Winge, D.R., and Eide, D.J. (2000) A dual role for zinc fingers in both DNA binding and zinc sensing by the Zap1 transcriptional activator. *EMBO J* 19(14): 3704-13

Blaiseau, P.-L., Lesuisse, E., and Camadro, J.-M. (*2001*) *Aft2p, a novel iron-regulated transcription activator that modulates, with Aft1p, intracellular iron use and resistance to oxidative stress in yeast. J. Biol. Chem.* 276, 34221–*34226*

Breslow, D.K., Collin, S.R., Bodenmiller, B., Aebersold, R., Simon, K., Shevchnko, A., Ejsing, C.S., and Weissman, J.S. (2010) Orm family proteins mediate sphingolipid homeostasis. *Nature* 463(7284):1048-53

Castells-Roca, L., Muhlenhoff, U., Lill, R., Herrero, E., and Belli, G. (2011) The oxidative stress reponse in yeast cells involves changes in the stability of Aft1 regulon mRNAs. *Mol Microbiol* 81(1):232-48

Chen, O. S., Crisp, R. J., Valachovic, M., Bard, M., Winge, D. R., and Kaplan, J. (2004) Transcription of the yeast iron regulon does not respond directly to iron but rather to iron-sulfur cluster biosynthesis. *J. Biol. Chem.* 279, 29513–29518

Conklin, D.S., Culbertson, M.R., and Kung, C. (1994) Interactions between gene products involved in divalent cation transport in Saccharomyces cerevisiae. *Mol Gen Genet.* 244(3):303-11

Conklin, D.S., McMaster, J.A., Culbertson, M.R., and Kung, C. (1992) COT1, a gene involved in cobalt accumulation in Saccharomyces cerevisiae. *Mol Cell Biol* 12(9):3678-88

Courel, M., Lallet, S., Camadro, J.M., and Blaiseau, P.L. (2005) Direct activation of genes involved in intracellular iron use by the yeast iron responsive transcription factor Aft2 without its paralog Aft1. *Mol. Cell. Biol.* 25:6760–6771

Dancis, A., Klausner, R.D., Hinnebusch, A.G., and Barriocanal, J.G. (1990) Genetic evidence that ferric reductase is required for iron uptake in *Saccharomyces cerevisiae*. *Mol Cell Biol* 10(5):2294-301

Dickson, R.C. (2008) New insights into sphingolipid metabolism and function in budding yeast. *J. Lipid Res* 49: 909-21

Dix, D.R., Bridgham, J.T., Broderius, M.A., Byersdorfer, C.A., Eide, D.J. (1994) The FET4 gene encodes the low affinity Fe(II) transport protein of *Saccharomyces cerevisiae*. *J Biol Chem* 269(42):26092-9

Dix, D.R., Bridgham, J., Broderius, M., and Eide, D.J. (1997) Characterization of the FET4 protein of yeast. Evidence for a direct role in the transport of iron. *J. Biol. Chem.* 272:11770–77

Eide, D.J., Davis-Kaplan, S., Jordan, I., Sipe, D., and Kaplan, J. (1992) Regulation of iron uptake in *Saccharomyces cerevisiae*. The ferrireductase and Fe(II) transporter are regulated independently. *J. Biol. Chem.* 267:20774–81

Eng, B.H., Guerinot, M.L., Eide, D., Saier, M.H. Jr. (1998) Sequence analyses and phylogenetic characterization of the ZIP family of metal ion transport proteins. *J Membr Biol* 166(1):1-7

Felice, M.R., De Domenico, I., Li, L., Ward, D.M., Bartok, B., Musci, G., and Kaplan, J. (2005) Post-transcriptional regulation of the yeast high affinity iron transport system. *J Biol Chem*. 280(23):22181-90

Georgatsou, E., and Alexandraki, D. (1994) Two distinctly regulated genes are required for ferric reduction, the first step of iron uptake in *Saccharomyces cerevisiae*. *Mol Cell Biol* 14(5):3065-73

Gitan, R.S., and Eide, D.J. (2000) Zinc-regulated ubiquitin conjugation signals endocytosis of the yeast ZRT1 zinc transporter. *Biochem J* 346:329-36

Gitan, R.S., Lou, H., Rodgers, J., Broderius, M., and Eide, D. (1998) Zinc-induced inactivation of the yeast ZRT1 zinc transporter occurs through endocytosis and vacuolar degradation. *J Biol Chem* 273: 28617-24

Han, S., Lone, M.A., Schneiter, R., and Chang A. (2010) Orm1 and Orm2 are conserved endoplasmic reticulum membrane proteins regulating lipid homeostasis and protein quality control. *Proc Natl Acad Sci USA* 107(13):5851-6

Hassett, R., Dix, D.R., Eide, D.J., and Kosman, D.J. (2000) The Fe(II) permease Fet4p functions as a low affinity copper transporter and supports normal copper trafficking in Saccharomyces cerevisiae. *Biochem J* 351 pt2:477-84

Herbig, A., Bird, A.J., Swierczek, S., McCall, K., Mooney, M., Wu, C.Y., Winge, D.R., and Eide, D.J. (2005) Zap1 activation domain 1 and its role in controlling gene expression in response to cellular zinc status. *Mol Microbiol* 57(3): 834-46

Hirano, T., Murakami, M., Fukada, T., Nishida, K., Yamasaki, S., and Suzuki, T. (2008) Roles of zinc and zinc signaling in immunity: zinc as an intracellular signaling molecule. *Adv immunol* 97:149-76

Hjelmqvist, L., Tuson, M., Marfany, G., Herrero, E., Balcells, S., and Gonzalez-Duarte, R. (2002) ORMDL proteins are a conserved new family of endoplasmic reticulum membrane proteins. *Genome Biol* 3(6):RESEARCH0027

Jensen, L.T., and Culotta, V.C. (2002) Regulation of *Saccharomyces cerevisiae* FET4 by oxygen and iron. *J Mol Biol* 318(2):251-60

Kamizono, A., Nishizawa, M., Teranishi, Y., Murata, K., and Kimura, A. (1989) Identification of a gene conferring resistance to zinc and cadmium ions in the yeast Saccharomyces cerevisiae. *Mol Gen Genet* 219:161-7

Kaplan, C.D.*, and* Kaplan, J. *(*2009*)* Iron acquisition and transcriptional regulation*. Chem Rev* 109*:* 4536–4552

Kumanovics, A., Chen, O.S., Li, L., Bagley, D., Adkins, E.M., Lin, H., Dingra N.N., Outten, C.E., Keller, G., Winge, D., Ward, D.M., and Kaplan, J. (2008) Identification of FRA1 and FRA2 as genes involved in regulating the yeast iron regulon in response to decreased mitochondrial iron-sulfur cluster synthesis. *J Biol Chem.* 283:10276-86

Lee, A., Henras, A.K., and Chanfreau, G. (2005) Multiple RNA surveillance pathways limit aberrant expression of iron uptake mRNAs and prevent iron toxicity in S. cerevisiae. *Mol. Cell* 19:39-51

Li, L., Bagley, D., Ward, D.M., and Kaplan, J. (2008) Yap5 is an iron-responsive transcriptional activator that regulates vacuolar iron storage in yeast. *Mol. Cell. Biol.* 28:1326-1337

Li, L., Chen, O.S., McVey Ward, D., and Kaplan, J. (2001) CCC1 is a transporter that mediates vacuolar iron storage in yeast. *J. Biol. Chem.* 276:29515–19

Li, L., Jia, X., Ward, D.M., and Kaplan, J. (2011) Yap5 protein-regulated transcription of the *TYW1* gene protects yeast from high iron toxicity. *J Biol. Chem.* 286:38488-97

Li, H., Mapolelo, D.T., Dingra, N.N., Naik, S.G., Lees, N.S., Hoffman, B.M., Riggs-Gelasco, P.J., Huynh, B.H., Johnson, M.K., and Outten, C.E. (2009) The yeast iron regulatory protein Grx3/4 and Fra2 form heterodimeric complex containing a [2Fe-2S] cluster with cysteinyl and histidyl ligation. *Biochemistry.* 48:9569-81

Lin, H., Li, L., Jia, X., Ward, D.M., and Kaplan, J. (2011) Genetic and biochemical analysis of high iron toxicity in yeast. Iron toxicity is due to the accumulation of cytosolic iron and occurs under both aerobic and anaerobic conditions. *J Biol. Chem.* 286:3851-62

Lyons, T.J., Gasch, A.P., Gaither, L.A., Botstein, D., Brown, P.O., and Eide, D.J. (2000) Genome-wide characterization of the Zap1p zinc-responsive reguln in yeast. *Proc Natl Acad Sci USA* 97(14):7957-62

MacDiarmid, C.W., Gaither, L.A., and Eide, D. (2000) Zinc transporters that regulate vacuolar zinc storage in Saccharomyces cerevisiae. *EMBO J* 19(12):2845-55

MacDiarmid, C.W., Milanick, M.A., and Eide, D.J. (2003) Induction of the ZRC1 metal tolerance gene in zinc-limited yeast confers resistance to zinc shock. *J Biol Chem* 278(17):15065-72

Miyabe, S., Izawa, S., and Inoue, Y. (2000) Expression of ZRC1 coding for suppressor of zinc toxicity is induced by zinc-starvation stress in Zap1-dependent fashion in Saccharomyces cerevisiae. *Biochem Biophys Res Commun* 276(3): 879-84

Moffatt, M.F., Kabesch, M., Liang, L., Dixon, A.L., Strachan, D., Heath, S., Depner, M., von Berg, A., Bufe, A., Rietschel, E., Heinzmann, A., Simma, B., Frischer, T., Willis-Owen, S.A., Wong, K.C., Illiq, T., Vogelberg, C., Weiland, S.K., von Mutius, E., Abecasis, G.R., Farrall, M., Gut, I.G., Lathrop, G.M., and Cookson, W.O. (2007) Genetic variants regulating ORMDL3 expression contribute to the risk of childhood asthma. *Nature* 448:470-3

Naryshkina, T., Bruning, A., Gadal, O., and Severinov, K. (2003) Role of second-largest RNA polymerase I submit Zn-binding domain in enzyme assembly. *Eukaryot Cell* 2(5):1046-52

Neilands, J.B. (1995) Siderophores: structure and function of microbial iron transport compounds. *J Biol Chem* 270:26723-26726

Ojeda, L., Keller, G., Muhlenhoff, U., Rutherford, J.C., Lill, R., and Winge, D.R. (2006) Role of glutaredoxin-3 and glutaredoxin-4 in the iron regulation of the Aft1 transcriptional activator in Saccharomyces cerevisiae. *J Biol Chem.* 281:17661-669

Philpott, C.C.*, and* Protchenko, O. *(*2008*)* Response to iron deprivation in *Saccharomices cerevisiae. Eukaryot Cell* 7*:* 20–27

Portnoy, M. E., X. F. Liu, and V. C. Culotta 2000 *Saccharomyces cerevisiae* expresses three functionally distinct homologues of the Nramp family of metal transporters. *Mol. Cell. Biol.* 207893-7902

Powell, S.R. (2000) The antioxidant properties of zinc. *J. Nutr.* 130: S1447-S1454

Protchenko, O., Ferea, T., Rashford, J., Tiedeman, J., Brown, P.O., Botstein, D., and Philpott, C.C. (2001) Three cell wall mannoproteins facilitate the uptake of iron in *Saccharomyces cerevisiae*. *J Biol Chem* 276:49244-49250

Puig, S., Askeland, E., and Thiele, D.J. (2005) Coordinated remodeling of cellular metabolism during iron deficiency through targeted mRNA degradation. *Cell* 120:99–110

Puig, S., Vergara, S.V., and Thiele, D.J. (2008) Cooperation of two mRNA-binding proteins drives metabolic adaptation to iron deficiency. *Cell Metab* 7:555-564

Pujol-Carrion, N., Belli, G., Herrero, E., Nogues, A., and de la Torre-Ruiz, M.A. (2006) Glutaredoxins Grx3 and Grx4 regulate nuclear localization of Aft1 and the oxidative stress response in Saccharomyces cerevisiae. *J Cell Sci.* 119:4554-64

Radisky, D.C., Babcock, M.C., and Kaplan, J. (1999) The yeast frataxin homologue mediates mitochondrial iron efflux: evidence for a mitochondrial iron cycle. *J Biol Chem* 274:4497-4499

Rausch, W., Hirata, Y., Nagatsu, T., Riederer, P., and Jellinger, K. (1988) Tyrosine hydroxylate activity in caudate nucleus from Parkinson's disease: effect of iron and phosphorylating agents. *Journal of Neurochemistry* 50:202-208

Rhee, S.G., Chae, H.Z., and Kim, K. (2005) Peroxiredoxins: a historical overview and speculative preview of novel mechanisms and emerging concepts in cell signaling. *Free Radic Biol Med* 38(12):1543-52

Rutherford, J.C., Jaron, S., Ray, E., Brown, P.O., and Winge, D.R. (2001) A second iron-regulatory system in yeast independent of Aft1p. *Proc Natl, Acad Sci U.S.A* 98, 14322-14327

Rutherford, J. C., and A. J. Bird. (2004) Metal-responsive transcription factors that regulate iron, zinc, and copper homeostasis in eukaryotic cells. *Eukaryot. Cell* 3:1–13

Rutherford, J. C., Ojeda, L., Balk, J., Muhlenhoff, U., Lill, R., and Winge, D. R. (2005) Activation of the iron regulon by the yeast Aft1/Aft2 transcription factors depends on mitochondrial but not cytosolic iron-sulfur protein biogenesis. *J. Biol. Chem.* 280, 10135–10140

Roeser, H.P., Lee, G.R., Nacht, S., and Cartwright, G.E. (1970) The role of ceruloplasmin in iron metabolism. J. Clin. Invest. 49: 2408-2417

Rouault, T.A. (2006) The role of iron regulatory proteins in mammalian iron homeostasis and disease. *Nature Chem. Biol.* 2: 406-414

Stearman, R., Yuan, D.S., Yamaguchi-Iwai, Y., Klausner, R.D., and Dancis, A. (1996) A permease-oxidase complex involved in high-affinity iron uptake in yeast. *Science* 271(5255):1552-7

Treich, I., Riva, M., and Sentenac, A. (1991) Zinc-binding subunits of Yeast RNA polymerases. *J. Biol. Chem* 266(32):21971-76

Tuerk, M.J., and Fazel, N. (2009) Zinc deficiency. *Curr Opin Gastroenterol* 25:136-43

Urbanowski, J. L., and R. C. Piper. (1999) The iron transporter Fth1p forms a complex with the Fet5 iron oxidase and resides on the vacuolar membrane. *J. Biol. Chem.* 27438061-38070

Warner, J.R. (1999) The economics of ribosome biosynthesis in yeast. *Trends Biochem. Sci.* 24:437-440

Waters, B.M., and Eide, D.J. (2002) Combinatorial control of yeast FET4 gene expression by iron, zinc, and oxygen. *J Biol Chem* 277(37):33749-57

Wu, C.Y., Bird, A.J., Winge, D.R., and Eide, D.J. (2007) Regulation of the yeast TSA1 peroxiredoxin by ZAP1 is an adaptive response to the oxidative stress of zinc deficiency. *J Biol Chem* 282(4):2184-95

Yamaguchi-Iwai, Y., Dancis, A., and Klausner, R.D. (1995) AFT1: a mediator of iron regulated transcriptional control in *Saccharomyces cerevisiae*. *EMBO J.* 14:1231–39

Yamaguchi-Iwai, Y., Ueta, R., Fukunaka, A., and Sasaki, R. (2002) Subcellular localization of Aft1 transcription factor responds to iron status in *Saccharomyces cerevisiae*. *J. Biol. Chem.* 277:18914–18

Yun, C.W., Ferea, T., Rashford, J., Ardon, O., Brown, P.O., Botstein, D., Kaplan, J., and

Philpott, C.C. *(*2000*)* Desferrioxamine-mediated iron uptake in *Saccharomyces cerevisiae*: evidence for two pathways of iron uptake. *J Biol Chem* 275*:* 10709–10715

Zhao, H., Butler, E., Rodgers, J., Spizzo, T., Duesterhoeft, S., and Eide, D. (1998) Regulation of zinc homeostasis in yeast by binding of the ZAP1 transcriptional activator to zinc-responsive promoter elements. *J Biol Chem* 273(44): 28713-20

Zhao, H., and Eide, D. (1996a) The yeast ZRT1 gene encodes the zinc transporter protein of a high-affinity uptake system induced by zinc limitation. *Proc Natl Acad Sci USA* 93(6):2454-8

Zhao, H., and Eide, D. (1996b) The ZRT2 gene encodes the low affinity zinc transporter in Saccharomyces cerevisiae. *J Biol Chem* 271(38):23203-10

Zhao, H., and Eide, D. (1997) Zap1p, a metalloregulatory protein involved in zinc-responsive transcriptional regulation in Saccharomyces cerevisiae. *Mol Cell Biol* 17(9):5044-52

CHAPTER 2

SPHINGOLIPID SIGNALING MEDIATES IRON TOXICITY

Cell Metabolism
Short Article

Sphingolipid Signaling Mediates Iron Toxicity

Yueh-Jung Lee,[1] Xinhe Huang,[2] Janette Kropat,[1] Anthony Henras,[1,3] Sabeeha S. Merchant,[1] Robert C. Dickson,[2] and Guillaume F. Chanfreau[1,*]
[1]Department of Chemistry and Biochemistry and the Molecular Biology Institute, University of California, Los Angeles, Los Angeles, CA 90095-1569, USA
[2]Department of Molecular and Cellular Biochemistry, University of Kentucky College of Medicine, 741 South Limestone Street, Lexington, KY 40536-0509, USA
[3]Present address: CNRS, LBME and Université de Toulouse, UPS, 31000 Toulouse, France
*Correspondence: guillom@chem.ucla.edu
http://dx.doi.org/10.1016/j.cmet.2012.06.004

SUMMARY

Iron constitutes a major source of toxicity due to its ability to generate reactive oxygen species that can damage cellular macromolecules. However, the precise mechanism by which exposure to high iron concentrations results in cellular toxicity remains unknown. Here we identify sphingolipid synthesis and signaling as a major mediator of iron toxicity in *S. cerevisiae.* Inhibition of sphingolipid synthesis by myriocin treatment or after overexpression of the negative regulator Orm2p confers resistance to high iron. High iron conditions upregulate sphingolipid synthesis, and increasing sphingolipid levels by inactivating Orm2p exacerbates sensitivity to iron. Toxicity is mediated by sphingolipid signaling, as inactivation of the sphingolipid-activated protein kinases Pkh1p and Ypk1p and of the transcription factor Smp1p also enhances resistance to high iron conditions. These results demonstrate an unexpected connection between sphingolipid flux and iron toxicity and show that activation of a signal transduction cascade contributes to iron-mediated cellular toxicity.

INTRODUCTION

Iron (Fe) is a ubiquitous metal in biological systems. However, Fe also represents a potential danger to biological macromolecules due to its ability to generate reactive oxygen species (ROS) (Touati, 2000; Valentine et al., 1998; Valko et al., 2005). In most organisms, the present paradigm in Fe toxicity suggests that the major toxic effect of Fe is the result of the exposure of cellular macromolecules to ROS (Touati, 2000; Valko et al., 2005). Defects in Fe metabolism can result in various pathologies in diseases of Fe overload (Hentze et al., 2004), underscoring the importance of limiting iron toxicity. Thus, iron levels must be regulated to meet the demands of cellular metabolism but also to prevent an overabundance that might result in potential damages. The unicellular eukaryote *S. cerevisiae* has been used as a model system to study Fe transport, metabolism, and toxicity (Philpott, 2006; Van Ho et al., 2002; Chen et al., 2002; Lin et al., 2011). In yeast, exposure of cells to high Fe results in growth defects through inhibition of the cell cycle (Philpott et al., 1998). Some of the protective mechanisms against Fe toxicity include storage of iron in organelles, presumably to limit the exposure of cytosolic or nuclear macromolecules to high iron concentrations (Chen and Kaplan, 2000; Li et al., 2001; Lin et al., 2011). This observation is consistent with the hypothesis that Fe causes toxicity by oxidative damage. However, recent work has shown that some of the toxic effects of Fe in yeast are independent of oxidative stress (Lin et al., 2011), suggesting that the major pathway(s) by which Fe hampers cellular growth remain to be identified. The results presented here show that reducing sphingolipid synthesis and signaling is sufficient to allow yeast cells to grow in otherwise toxic iron conditions, demonstrating that sphingolipid signaling contributes to mediating iron toxicity in *S. cerevisiae*.

RESULTS

Genetic or Chemical Inhibition of Sphingolipid Synthesis Confers Resistance to Iron Toxicity

We showed previously that yeast cells lacking the RNase III Rnt1p are hypersensitive to high Fe (Lee et al., 2005). To further understand the molecular basis of Fe toxicity, we performed a high-copy suppressor screen to identify genes, which, when overexpressed, would allow Rnt1p-deficient cells to grow in high Fe. We constructed a genomic library from the *rnt1*Δ strain in the multicopy vector YEp24 and performed screens in the presence of high Fe to identify suppressors. We could not reproducibly identify genes that allow *rnt1*Δ cells to grow in high Fe, so we redirected our efforts to performing this screen in wild-type cells. We isolated a clone exhibiting growth in high Fe conditions and identified *ORM2* as the gene responsible for this effect. We confirmed that an independently cloned version of *ORM2* could confer resistance to Fe toxicity when overexpressed in wild-type cells (Figure 1A). Orm2p and the closely related Orm1p protein were identified as negative regulators of sphingolipid synthesis and mediators of the endoplasmic reticulum (ER) stress response (Breslow et al., 2010; Breslow and Weissman, 2010; Han et al., 2010). We tested the ability of Orm1p to confer resistance to iron toxicity and found that *ORM2*-overexpressing cells (*ORM2ox*; pORM2 on the figures) grew faster than *ORM1ox* in high Fe conditions, suggesting that Orm2p was a more potent high copy suppressor of Fe toxicity than Orm1p. We monitored Orm1p and Orm2p levels in high Fe conditions, both when the proteins were HA tagged

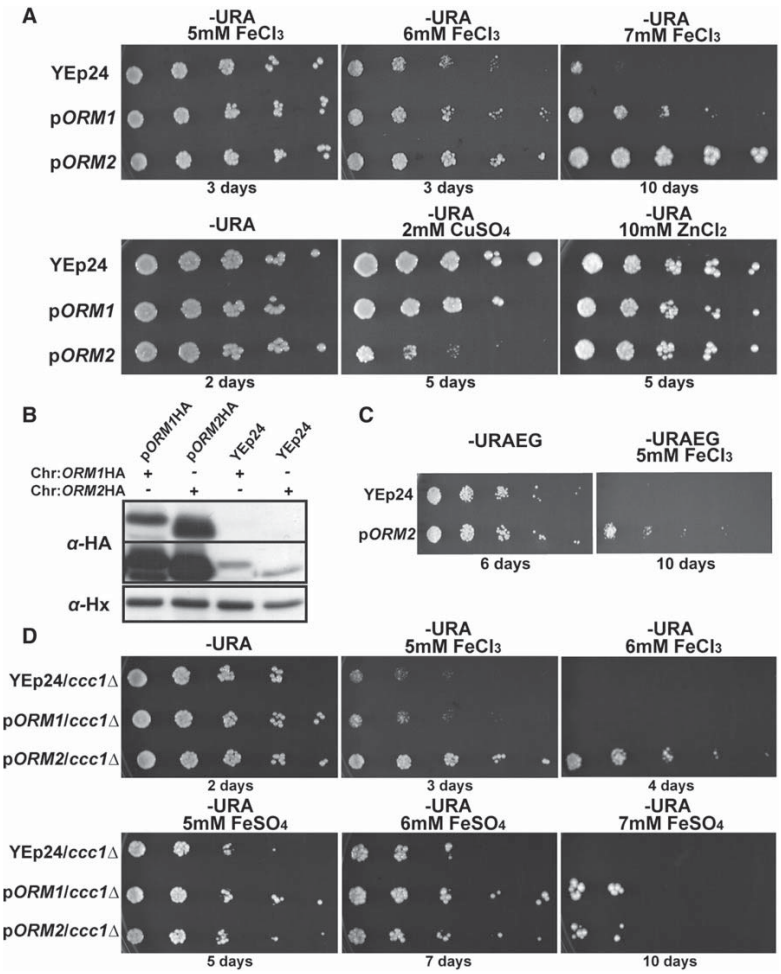

Figure 1. *ORM2* Overexpression Confers Specific Resistance to Iron Toxicity in a Variety of Physiological Contexts

(A) Strains were grown in SD medium lacking uracil (−URA) supplemented with the indicated metals. These and all subsequent assays show 10-fold dilution series from left to right. For the bottom panel, plates were incubated at 30°C.

(B) Cells expressing Orm1p or Orm2p HA-tagged at their chromosomal loci (Chr), transformed with either the YEp24 vector or with plasmids containing HA-tagged Orm1p or Orm2p (p*ORM1*/2-HA), were grown in 7 mM $FeCl_3$, and the levels of Orm1/2p were analyzed by immunoblot. Upper panels are two different exposures to detect endogenous and overexpressed Orm1/2p.

(C) Strains were grown on ethanol-glycerol carbon source lacking uracil (-URAEG), without or with 5 mM $FeCl_3$.

(D) Legends as in (A).

at their respective endogenous loci and when the same HA-tagged proteins were overexpressed (Figure 1B). We found that in this overexpression system, Orm2p was expressed at higher levels than Orm1p in high Fe conditions (Figure 1B) and at levels much higher than the endogenous copy. Thus, the ability of Orm2p to confer better growth in high iron than Orm1p might be linked to higher overexpression levels.

The resistance of *ORM2ox* cells to high Fe was specific to this particular stress. In contrast to high iron, *ORM2ox* cells actually grew slower than wild-type in high copper conditions (Figure 1A). In addition, we found no growth difference between wild-type and *ORM2ox* cells in high zinc (Figure 1A) or oxidative stress conditions (Figure S1A). We also found no differences in the levels of oxidized proteins between wild-type and *ORM2ox* cells in high Fe (Figure S1B) and no growth difference in high salt (Figure S1C) nor in survival after heat shock (Figure S1D). Finally, because media containing high Fe require acidic conditions in order for Fe to be soluble, we also tested the growth of wild-type and *ORM2ox* cells in acidic medium and found no difference (Figure S1E). Thus, *ORM2* overexpression does not confer general resistance to a variety of cellular stresses, but seems specific to Fe toxicity.

The genetic screen identifying *ORM2* was performed in glucose-containing medium, where oxidative stress is low. We found that overexpressing Orm2p conferred resistance to Fe toxicity in media containing the nonfermentable carbon sources ethanol and glycerol (Figure 1C). Thus, Orm2p can also suppress Fe toxicity when oxidative stress is increased by respiration. To further investigate the potency of the suppression of Fe toxicity by Orm2p, we overexpressed Orm2p in a strain deficient for the vacuolar Fe importer Ccc1p. Strains lacking Ccc1p are hypersensitive to high Fe because they cannot store iron in the vacuole (Li et al., 2001; Lin et al., 2011). Overexpression of *ORM2* was sufficient to rescue the growth of *ccc1*Δ cells at 6 mM $FeCl_3$ (Figure 1D), showing that Orm2p can also rescue the growth of cells deficient in iron storage. Overexpressing Orm1p also resulted in some suppression, although this effect was more robust when cells were grown in medium containing $FeSO_4$ (Figure 1D). We do not fully understand why Orm1p seems to be more potent in these conditions, but this effect might be due to differential expression. Collectively, these results show that overexpressing Orm1/2p can suppress Fe toxicity in a variety of physiological contexts and can compensate for defects in vacuolar iron storage. These results also show that the capacity of Orm1/2p to suppress Fe toxicity is not linked to their ability to influence vacuolar iron storage by modulation of the activity of the vacuolar ATPase (Finnigan et al., 2011), since cells lacking Ccc1p cannot store iron in the vacuole. Taken together, these results show that overexpression of Orm2p can suppress Fe toxicity in a variety of physiological contexts.

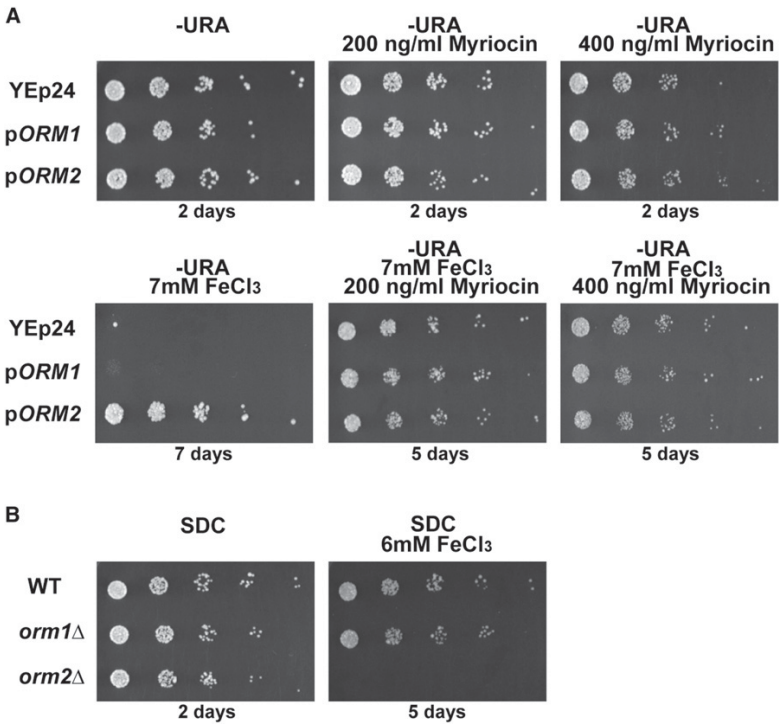

Figure 2. Modulation of Sphingolipid Synthesis Changes Resistance to High Iron

(A) Strains were grown on normal medium or with the indicated concentrations of myriocin and $FeCl_3$.

(B) Strains were grown on normal or 6 mM $FeCl_3$ conditions in minimal medium (SDC).

Based on its cellular functions (Breslow et al., 2010; Han et al., 2010), the ability of Orm2p to enhance resistance to Fe toxicity could be attributed to two distinct pathways: (1) control of ER stress and unfolded protein response (UPR), or (2) inhibition of sphingolipid synthesis. Since metals such as Cd can induce the UPR (Gardarin et al., 2010), we tested whether *ORM2* confers resistance to iron toxicity by modulating the UPR, which might have been activated by high Fe. Splicing of the *HAC1* mRNA, a hallmark of the UPR (Cox and Walter, 1996), was not triggered by growing cells in high Fe (Figure S2A), and no differences in *HAC1* splicing were found when overexpressing *ORM2* (Figure S2A). These results show that in contrast to Cd stress, high Fe conditions do not trigger the UPR, and that Orm2p is unlikely to mediate resistance to high iron by modulating ER stress. To test whether Orm2p confers resistance to Fe toxicity by inhibiting sphingolipid synthesis, we used the chemical inhibitor myriocin, which modulates sphingolipid synthesis through inhibition of the long-chain base (LCB)-synthesizing enzyme serine palmitoyltransferase (Breslow and Weissman, 2010; Cowart and Obeid, 2007; Dickson et al., 2006). If *ORM2* overexpression enhances resistance to iron toxicity by inhibiting sphingolipid synthesis, exposure of cells to subtoxic concentrations of myriocin was predicted to have a similar protective effect. While myriocin at the concentrations used had no effect on overall growth in normal medium, it allowed wild-type cells to survive in high Fe conditions (Figure 2A). There seemed to be no cumulative effect of exposing cells to myriocin and overexpressing *ORM2*, consistent with the hypothesis that these two treatments act on the same pathway.

The previous results are consistent with the hypothesis that *ORM2* overexpression and myriocin treatment suppress iron toxicity by reducing sphingolipid levels. To test whether an increase of sphingolipid flux is toxic when combined with high Fe concentrations, we used an *orm2*Δ strain, since *ORM2* inactivation was shown to upregulate sphingolipid synthesis (Breslow et al., 2010; Breslow and Weissman, 2010; Finnigan et al., 2011; Han et al., 2010). As shown in Figure 2B, cells lacking *ORM2* were unable to grow in 6 mM Fe, while wild-type cells were still viable. By contrast, the *orm1*Δ strain did not exhibit any strong growth phenotype (Figure 2B), suggesting a more prominent function for Orm2p in these conditions. These results show that an increase of sphingolipid synthesis confers hypersensitivity to subtoxic Fe concentrations, further correlating sphingolipid flux and Fe-mediated toxicity.

Orm2p Overexpression Does Not Reduce Cellular Iron Levels

Since sphingolipids are integral components of membranes, the capacity of Orm2p to enhance resistance to Fe toxicity could be linked to a potential function in modulating the activity of a transmembrane Fe transporter and Fe import. To test this hypothesis, we measured the iron content of wild-type and *ORM2ox* cells by ICP-MS (Figure 3A). In normal Fe conditions, these strains showed comparable low levels of Fe and of other metals (Figure 3A). In high Fe conditions, both strains exhibited an increase of intracellular Fe, and *ORM2ox* cells showed slightly higher Fe levels than the wild-type (Figure 3A). In contrast, the level of other metals such as Zn or Cu was similar in both strains (Figure 3A), showing that the slightly higher Fe content in *ORM2ox* cells is specific to this metal. Prior work had shown that sphingolipids regulate the expression of Fet3p (Villa et al., 2009), a multicopper oxidase involved in Fe transport. We detected similar levels of the *FET3* mRNA in wild-type and *ORM2ox* cells (Figure S2B) in normal conditions and could not detect *FET3* in high Fe conditions in both strains, suggesting that *ORM2* overexpression in high iron does not change the expression of this key mediator of Fe assimilation. Taken together, these results rule out the hypothesis that Orm2p suppresses cellular Fe toxicity by preventing intracellular iron uptake.

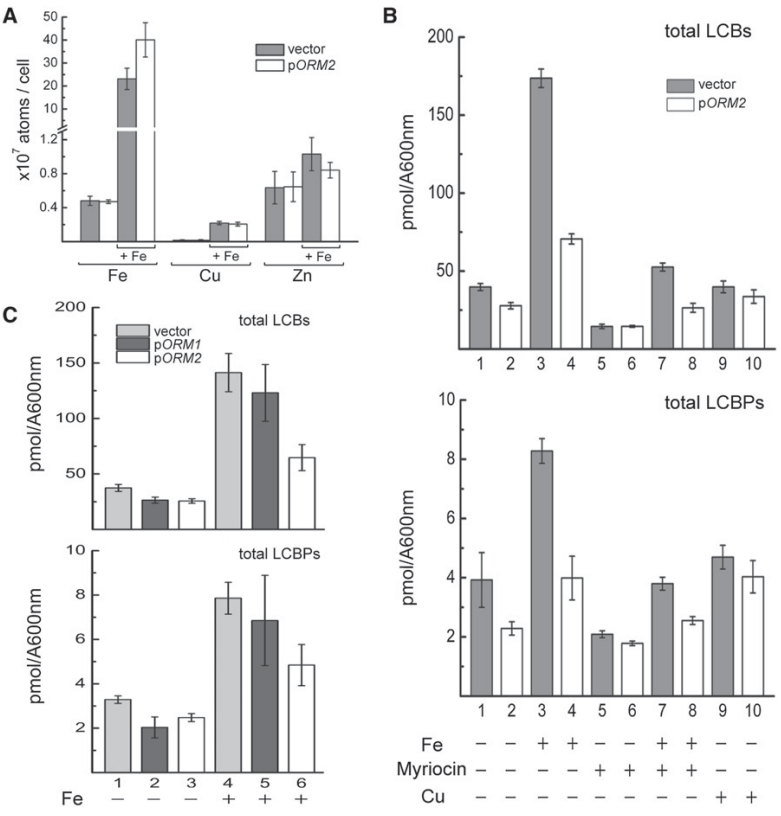

Figure 3. High Iron Conditions Result in Higher Intracellular Iron Concentrations and Sphingolipid LCBs

(A) Intracellular metal content analysis. Strains were grown on SD plates containing a normal concentration of Fe and incubated for 2 days or on SD + 7 mM $FeCl_3$ and incubated for 6 days (p*ORM2*) and 11 days (YEp24) before harvesting for ICP-MS measurement. The results shown are the average of six samples (triplicate samples from two independent experiments), except for pORM2 in normal conditions, which is the average of five samples (three and two samples from two independent experiments).

(B) Sphingolipid analysis in normal, high Fe, and high Cu conditions. Strains were grown either on normal medium, 7 mM $FeCl_3$, 200 ng/ml myriocin, 7 mM $FeCl_3$ + 200 ng/ml myriocin, or 2 mM $CuSO_4$ conditions and incubated at 25°C until colonies reached a similar size before harvesting for LCB analysis. Triplicate samples for LCB analysis were prepared as described in Experimental Procedures. LCB and LCBP levels are indicated as pmol/A_{600}. Statistical analysis is provided in Table S1. Evidence for reproducibility of the effect of high iron conditions and ORM2 overexpression on LCB levels is shown in Figure S3.

(C) Comparison of the effects of Orm1p and Orm2p overexpression on sphingolipid levels. Procedures were the same as in (B), except that cells were transformed with the vector alone (YEp24) or the vector overexpressing Orm1p or Orm2p (p*ORM1/2*) and grown in −URA medium (lanes 1, 2, and 3) or with −URA + 7 mM $FeCl_3$. Shown are the average values of three independent biological samples with the standard deviations.

High Iron Conditions Increase Sphingolipid Synthesis

Since the previous data showed that decreasing sphingolipid synthesis enhances the capacity to grow in high Fe, we investigated whether high Fe conditions trigger an increase in sphingolipid synthesis. We measured the concentration of sphingolipid LCB and long-chain base phosphate (LCBP) metabolic intermediates in wild-type and *ORM2ox* cells, since their level is sensitive to changes in growth rate and environmental stress (Cowart and Obeid, 2007; Dickson et al., 2006). Consistent with previous results (Breslow et al., 2010; Han et al., 2010), overexpression of *ORM2* or myriocin treatment significantly reduced LCB levels in normal medium (Figure 3B; detailed values and statistical analysis shown in Table S1; see also Figures S3 and S4). When grown in high Fe, wild-type cells showed a statistically significant increase in total LCBs and LCBPs compared to normal medium (Figure 3B, Figure S3). These data support the hypothesis that high Fe causes an accumulation of sphingolipid intermediates. Overexpressing Orm2p or myriocin treatment significantly reduced LCBs in Fe-treated cells (Figure 3B, Figure S3), and a stronger reduction was observed when combining Orm2p overexpression and myriocin (Figure 3B, lanes 4 and 8). Similar trends were observed for LCBPs (Figure 3B, Figure S3). The complete analysis for each species of LCB and LCBP is shown in Figure S4 and shows the same tendencies as total LCBs and LCBPs. These effects were specific to Fe, as high Cu was found to have no effect on LCB and LCBP levels (Figure 3B). We also compared the ability of Orm1p and Orm2p to modulate sphingolipid synthesis in high Fe conditions when each of these proteins was overexpressed (Figure 3C). We found that Orm2p overexpression conferred a statistically significant reduction of LCBs and LCBPs in high iron compared to cells transformed with the YEp24 vector (p values of 7.3×10^{-5} and 5.2×10^{-5}, respectively, t test), while Orm1p overexpression did not lead to a significant effect. These results corroborate the suppression analysis showing that Orm2p is a much more potent suppressor of Fe toxicity than Orm1p (Figure 1A). Taken together, these results show that the levels of LCB and LCBP are specifically increased in high Fe conditions and that the capacity of Orm2p or myriocin to enhance resistance to high Fe is correlated with a reduction in LCB and LCBP levels.

Inactivation of Sphingolipid-Mediated Signaling Enhances Resistance to High Iron

Ceramides have been shown to induce apoptosis in mammals (Colombini, 2010). In addition, previous data have shown that exposure of yeast cells to metals such as Cu and Mn can trigger apoptosis (Liang and Zhou, 2007). Thus, the increase in sphingolipid levels detected in high Fe conditions might potentially cause apoptosis through an accumulation of ceramides. To test this

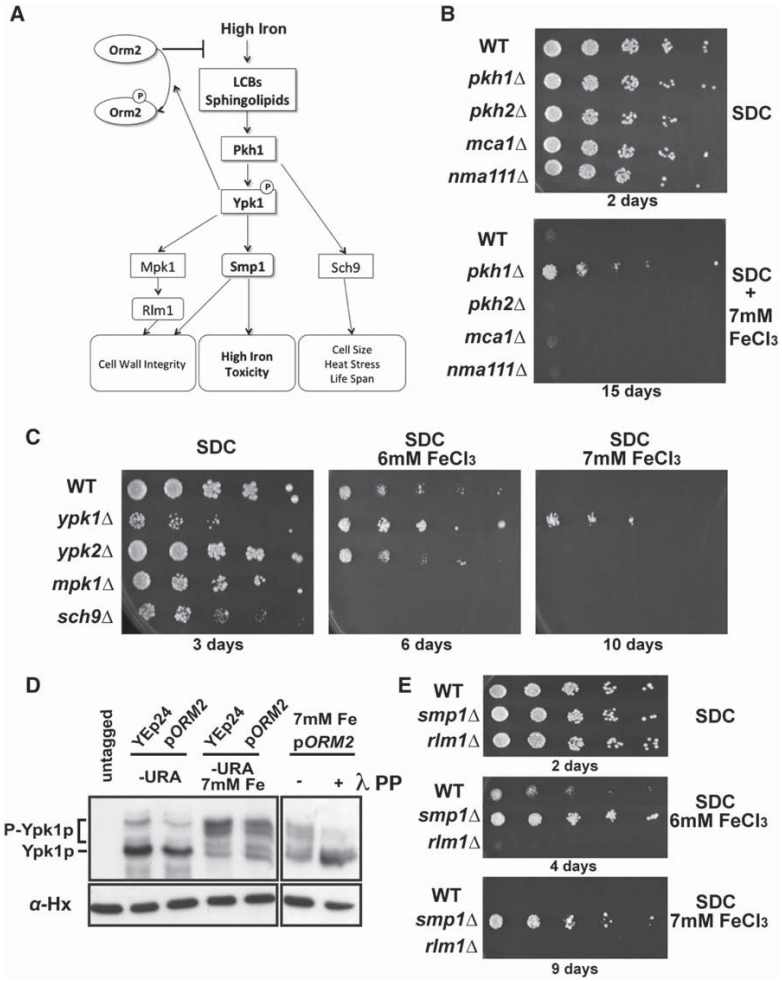

Figure 4. Inactivation of Sphingolipid Signaling Confers Resistance to Iron Toxicity

(A) Yeast sphingolipid-mediated signal transduction pathways.

(B) Strains were grown on normal minimal medium (SDC) or SDC containing 7 mM $FeCl_3$.

(C) Legends as in Figure 1A.

(D) Immunoblot analysis of *myc*-tagged Ypk1p in normal and high iron conditions in wild-type cells or cells overexpressing Orm2p. SDS-PAGE was performed in the presence of 20 μM Phos-tag. To demonstrate that the higher bands corresponded to phospho-Ypk1p, the extracts prepared from cells overexpressing Orm2p were treated with lambda (λ) phosphatase (PP; right lane).

(E) Legends as in (B).

hypothesis, we analyzed a number of mutants in this pathway. Blocking apoptosis by inactivation of the metacaspase Mca1p/Yca1p (Madeo et al., 2002) or of the serine protease Nma111p (Fahrenkrog et al., 2004) did not restore growth in high Fe conditions (Figure 4B). We conclude that unlike Cu or Mn, high Fe is unlikely to mediate toxicity through apoptosis.

In addition to triggering apoptosis, sphingolipids are involved in many cellular functions, as structural components of membranes, but also as signaling molecules during stress (Breslow and Weissman, 2010; Dickson, 2008; Dickson et al., 2006). In *S. cerevisiae* their signaling function is primarily mediated by LCBs, which activate the Pkh1p and Pkh2p protein kinases (Figure 4A) (Liu et al., 2005; Roelants et al., 2002), although other sphingolipids can act as signaling molecules as well (Roelants et al., 2010). If the contribution of LCBs to cellular toxicity in high iron conditions is due to their signaling function, we hypothesized that strains deficient in these kinases might also exhibit resistance to high Fe. Indeed, the *pkh1*Δ strain exhibited increased resistance to high Fe (Figure 4B), while cells lacking Pkh2p did not show this phenotype, suggesting a specific role for Pkh1p. Pkh1p has been shown to activate several signal transduction cascades (Figure 4A). To investigate which cascade is responsible for mediating toxicity in high iron conditions, we inactivated the Mpk1p, Sch9p, Ypk1p, and Ypk2p kinases and assessed the growth of these mutants in high Fe. Strikingly, inactivation of Ypk1p resulted in resistance to high Fe, while none of the other kinase knockout strains exhibited this phenotype (Figure 4C). This suppression phenotype is particularly striking considering that the *ypk1*Δ strain shows a growth defect in normal medium (Figure 4C). We analyzed the expression of some genes known to be controlled by the Pkh1p/Ypk1p kinases, but none of them showed a change in expression in high iron or upon Orm2p overexpression (Figure S2C). Thus, these kinases control other cellular functions besides the expression of known target genes.

To directly demonstrate that sphingolipid signaling is activated during high Fe conditions, we assessed Ypk1p phosphorylation by immunoblot using a strain expressing myc-tagged Ypk1p (Figure 4D). In cells shifted to high Fe, we found increased amounts of slower mobility forms of Ypk1p (Figure 4D). Strikingly, the level of these forms was reduced upon Orm2p overexpression (Figure 4D). These slower mobility bands correspond to phosphorylated forms of Ypk1p, as their mobility was increased upon treatment of extracts with phosphatase prior to fractionation (Figure 4D). This result directly shows that increased sphingolipid levels in high iron activate the Pkh1p/Ypk1p signal transduction cascade and that Orm2p overexpression confers resistance to high iron by inhibiting this response and reducing Ypk1p phosphorylation. While this work was being considered, it was shown that Ypk1p can phosphorylate and inactivate Orm2p (Roelants et al., 2011; Sun et al., 2012). Therefore, the observation that Ypk1p depletion could rescue iron toxicity might indicate that this effect could be due to Orm2p activation

in the absence of Ypk1p-mediated phosphorylation. If this were the case, we would not expect any downstream target of Ypk1p to have any influence on the ability of cells to grow in high iron conditions. However, we found that inactivation of Smp1p also rescued the ability of cells to grow in high iron conditions (Figure 4E). This result contrasts with the observation that Smp1p inactivation usually results in decreased growth in stress conditions, such as high osmolarity (de Nadal et al., 2003). In contrast, inactivation of another transcription factor, Rlm1p, had a negative effect on growth in high iron (Figure 4E). Taken together, these results show that sphingolipid signaling through Pkh1p, Ypk1p, and Smp1p contributes to mediating iron toxicity.

DISCUSSION

In this study, we report the finding that genetic or chemical inhibition of sphingolipid synthesis allows yeast cells to grow in higher iron conditions, showing that sphingolipid levels are limiting the ability of cells to grow in these conditions. We cannot completely exclude that the increased growth of cells overexpressing Orm2p in high iron is due to general effects on cellular viability, or that overexpressing Orm2p can confer resistance to other transition metals. However the effect of Orm2p seems specific to Fe, as overexpressing Orm2p does not confer resistance to Cu or Zn or to all other stresses tested—indeed, the opposite effect is observed for Cu, since cells overexpressing Orm2p are more sensitive to Cu. A link between Fe levels and sphingolipids was shown previously, as Fe deficiency was found to reduce sphingolipids (Shakoury-Elizeh et al., 2010). This effect might be explained by the inactivation in low iron conditions of sphingolipid biosynthetic enzymes that require Fe as an essential cofactor. In contrast, we found that high Fe conditions increase sphingolipid levels. This effect might be due to a general increase of synthesis of these lipids in response to environmental stress, as shown previously (Liu et al., 2005). However, unlike for other cellular stresses such as heat shock, elevated sphingolipids do not confer resistance to high iron conditions, but rather are toxic. Thus there is a unique relationship between sphingolipid levels and iron-mediated cellular toxicity, as preventing upregulation is sufficient to allow cells to survive in high Fe.

Our data indicate that sphingolipids mediate cellular toxicity by acting as signaling molecules. It was shown recently that sphingolipid signaling affects yeast life span (Huang et al., 2012). This effect is mechanistically distinct from those described here, as inactivation of Sch9p increases life span (Huang et al., 2012) but decreases the ability of cells to grow in high Fe (Figure 4C). Thus, sphingolipid signaling can modulate cellular fitness in a variety of mechanisms. Sphingolipid signaling through Pkh1p/Ypk1p was shown to be required for endocytosis (deHart et al., 2002; Friant et al., 2001), and it is known that some divalent cation transporters are endocytosed following exposure to high metal concentrations (Philpott, 2006). However, our data are inconsistent with the idea that these lipids play a role in limiting Fe toxicity by controlling Fe transporter endocytosis, since we found slightly elevated Fe levels in cells overexpressing Orm2p. Instead, sphingolipids play a function in mediating Fe toxicity by triggering a change in cellular properties through the activation of the Pkh1p/Ypk1p signal transduction cascade. Although we favor LCBs as regulators of Pkh1p-Ypk1p signaling in high Fe, we cannot exclude that other sphingolipids are also involved, because their concentration is also affected when serine palmitoyltransferase activity is reduced (Breslow et al., 2010; Huang et al., 2012). This signaling cascade involves the Smp1p transcription factor, as Smp1p inactivation increases resistance to high Fe. Smp1p might mediate downstream events responsible for mediating Fe toxicity, which could include changes in cell cycle events known to be affected in high Fe (Philpott et al., 1998). Alternatively, other molecular events controlled by sphingolipids, such as the activity of aminophospholipid flippases (Roelants et al., 2010), might modify the properties of the membrane or the cell wall and thus make the cells more sensitive to high Fe.

Iron is generally thought to mediate cellular toxicity by virtue of its ability to generate damaging ROS (Touati, 2000; Valko et al., 2005). By contrast, our data show that a significant part of iron toxicity in yeast involves the activation of sphingolipid signaling. This result is in agreement with the pioneer work from Lin and colleagues, who showed that some of the toxic effects of Fe are independent from oxidative stress in yeast and therefore from the ability of Fe to generate ROS (Lin et al., 2011). Taken together, these findings provide a paradigm change by showing that Fe toxicity in a model eukaryotic unicellular system is mediated, at least in part, by the activation of a biological signal transduction cascade. It remains to be investigated if a similar signaling pathway is activated in other eukaryotic cells exposed to high iron conditions.

EXPERIMENTAL PROCEDURES

Strains and Plasmids

S. cerevisiae strains were derived from BMA64 (Lee et al., 2005). Genomic library construction and screening and construction of the plasmids used in this study are described in Supplemental Information. Cells were grown on synthetic defined (SD) medium plates with or without specific concentrations of added $FeCl_3$ or $FeSO_4$ or of other metals, as described in Supplemental Information. Most of the growth assays were performed at 25°C, unless indicated otherwise in the figure legends.

Sphingolipid and Metal Analysis

Preparation of extracts for the analysis of LCB sphingolipids is described in detail in Supplemental Information. Analysis of LCB by HPLC was performed as described (Lester and Dickson, 2001). For measurement of metal content by ICP-MS, cells were washed with 1 mM EDTA and water after harvesting, before digestion with nitric acid. ICP-MS measurement was performed as described (Kropat et al., 2011).

RNA and Protein Analysis

Protein extracts were prepared as described in Supplemental Information. Western blot analysis of strains expressing myc-tagged Ypk1p was performed using anti-myc polyclonal antibody. Western blot analysis of strains expressing Orm1p or Orm2p tagged at the C terminus with the HA epitope was performed using anti-HA monoclonal antibody. Analysis of Ypk1p phosphorylation by phosphatase treatment and fractionation on SDS-PAGE containing Phos-tag is described in Supplemental Information.

Statistical Analysis

Statistical analysis was performed using a two-tailed t test in Excel.

SUPPLEMENTAL INFORMATION

Supplemental Information includes four figures, one table, and Supplemental Experimental Procedures and can be found with this article online at http://dx.doi.org/10.1016/j.cmet.2012.06.004.

ACKNOWLEDGMENTS

We thank S. Covarrubias for help with the construction of the genomic library; I. Toesca for help with initials screens, R. Lester for advice on sphingolipid analyses; and C. Clarke, J. Valentine, and J. Torres for discussions. This work is supported by NIGMS grant GM61518 to G.F.C., grant AG024377 to R.C.D., and grant DOE-DE-FG02- 04ER15529 to S.S.M.

Received: August 2, 2011
Revised: March 4, 2012
Accepted: June 14, 2012
Published online: July 2, 2012

REFERENCES

Breslow, D.K., and Weissman, J.S. (2010). Membranes in balance: mechanisms of sphingolipid homeostasis. Mol. Cell *40*, 267–279.

Breslow, D.K., Collins, S.R., Bodenmiller, B., Aebersold, R., Simons, K., Shevchenko, A., Ejsing, C.S., and Weissman, J.S. (2010). Orm family proteins mediate sphingolipid homeostasis. Nature *463*, 1048–1053.

Chen, O.S., and Kaplan, J. (2000). CCC1 suppresses mitochondrial damage in the yeast model of Friedreich's ataxia by limiting mitochondrial iron accumulation. J. Biol. Chem. *275*, 7626–7632.

Chen, O.S., Hemenway, S., and Kaplan, J. (2002). Genetic analysis of iron citrate toxicity in yeast: implications for mammalian iron homeostasis. Proc. Natl. Acad. Sci. USA *99*, 16922–16927.

Colombini, M. (2010). Ceramide channels and their role in mitochondria-mediated apoptosis. Biochim. Biophys. Acta *1797*, 1239–1244.

Cowart, L.A., and Obeid, L.M. (2007). Yeast sphingolipids: recent developments in understanding biosynthesis, regulation, and function. Biochim. Biophys. Acta *1771*, 421–431.

Cox, J.S., and Walter, P. (1996). A novel mechanism for regulating activity of a transcription factor that controls the unfolded protein response. Cell *87*, 391–404.

de Nadal, E., Casadomé, L., and Posas, F. (2003). Targeting the MEF2-like transcription factor Smp1 by the stress-activated Hog1 mitogen-activated protein kinase. Mol. Cell. Biol. *23*, 229–237.

deHart, A.K., Schnell, J.D., Allen, D.A., and Hicke, L. (2002). The conserved Pkh-Ypk kinase cascade is required for endocytosis in yeast. J. Cell Biol. *156*, 241–248.

Dickson, R.C. (2008). Thematic review series: sphingolipids. New insights into sphingolipid metabolism and function in budding yeast. J. Lipid Res. *49*, 909–921.

Dickson, R.C., Sumanasekera, C., and Lester, R.L. (2006). Functions and metabolism of sphingolipids in Saccharomyces cerevisiae. Prog. Lipid Res. *45*, 447–465.

Fahrenkrog, B., Sauder, U., and Aebi, U. (2004). The S. cerevisiae HtrA-like protein Nma111p is a nuclear serine protease that mediates yeast apoptosis. J. Cell Sci. *117*, 115–126.

Finnigan, G.C., Ryan, M., and Stevens, T.H. (2011). A genome-wide enhancer screen implicates sphingolipid composition in vacuolar ATPase function in Saccharomyces cerevisiae. Genetics *187*, 771–783.

Friant, S., Lombardi, R., Schmelzle, T., Hall, M.N., and Riezman, H. (2001). Sphingoid base signaling via Pkh kinases is required for endocytosis in yeast. EMBO J. *20*, 6783–6792.

Gardarin, A., Chédin, S., Lagniel, G., Aude, J.C., Godat, E., Catty, P., and Labarre, J. (2010). Endoplasmic reticulum is a major target of cadmium toxicity in yeast. Mol. Microbiol. *76*, 1034–1048.

Han, S., Lone, M.A., Schneiter, R., and Chang, A. (2010). Orm1 and Orm2 are conserved endoplasmic reticulum membrane proteins regulating lipid homeostasis and protein quality control. Proc. Natl. Acad. Sci. USA *107*, 5851–5856.

Hentze, M.W., Muckenthaler, M.U., and Andrews, N.C. (2004). Balancing acts: molecular control of mammalian iron metabolism. Cell *117*, 285–297.

Huang, X., Liu, J., and Dickson, R.C. (2012). Down-regulating sphingolipid synthesis increases yeast lifespan. PLoS Genet. *8*, e1002493.

Kropat, J., Hong-Hermesdorf, A., Casero, D., Ent, P., Castruita, M., Pellegrini, M., Merchant, S.S., and Malasarn, D. (2011). A revised mineral nutrient supplement increases biomass and growth rate in Chlamydomonas reinhardtii. Plant J. *66*, 770–780.

Lee, A., Henras, A.K., and Chanfreau, G. (2005). Multiple RNA surveillance pathways limit aberrant expression of iron uptake mRNAs and prevent iron toxicity in S. cerevisiae. Mol. Cell *19*, 39–51.

Lester, R.L., and Dickson, R.C. (2001). High-performance liquid chromatography analysis of molecular species of sphingolipid-related long chain bases and long chain base phosphates in Saccharomyces cerevisiae after derivatization with 6-aminoquinolyl-N-hydroxysuccinimidyl carbamate. Anal. Biochem. *298*, 283–292.

Li, L., Chen, O.S., McVey Ward, D., and Kaplan, J. (2001). CCC1 is a transporter that mediates vacuolar iron storage in yeast. J. Biol. Chem. *276*, 29515–29519.

Liang, Q., and Zhou, B. (2007). Copper and manganese induce yeast apoptosis via different pathways. Mol. Biol. Cell *18*, 4741–4749.

Lin, H., Li, L., Jia, X., Ward, D.M., and Kaplan, J. (2011). Genetic and biochemical analysis of high iron toxicity in yeast: iron toxicity is due to the accumulation of cytosolic iron and occurs under both aerobic and anaerobic conditions. J. Biol. Chem. *286*, 3851–3862.

Liu, K., Zhang, X., Sumanasekera, C., Lester, R.L., and Dickson, R.C. (2005). Signalling functions for sphingolipid long-chain bases in Saccharomyces cerevisiae. Biochem. Soc. Trans. *33*, 1170–1173.

Madeo, F., Herker, E., Maldener, C., Wissing, S., Lächelt, S., Herlan, M., Fehr, M., Lauber, K., Sigrist, S.J., Wesselborg, S., and Fröhlich, K.U. (2002). A caspase-related protease regulates apoptosis in yeast. Mol. Cell *9*, 911–917.

Philpott, C.C. (2006). Iron uptake in fungi: a system for every source. Biochim. Biophys. Acta *1763*, 636–645.

Philpott, C.C., Rashford, J., Yamaguchi-Iwai, Y., Rouault, T.A., Dancis, A., and Klausner, R.D. (1998). Cell-cycle arrest and inhibition of G1 cyclin translation by iron in AFT1-1(up) yeast. EMBO J. *17*, 5026–5036.

Roelants, F.M., Torrance, P.D., Bezman, N., and Thorner, J. (2002). Pkh1 and Pkh2 differentially phosphorylate and activate Ypk1 and Ykr2 and define protein kinase modules required for maintenance of cell wall integrity. Mol. Biol. Cell *13*, 3005–3028.

Roelants, F.M., Baltz, A.G., Trott, A.E., Fereres, S., and Thorner, J. (2010). A protein kinase network regulates the function of aminophospholipid flippases. Proc. Natl. Acad. Sci. USA *107*, 34–39.

Roelants, F.M., Breslow, D.K., Muir, A., Weissman, J.S., and Thorner, J. (2011). Protein kinase Ypk1 phosphorylates regulatory proteins Orm1 and Orm2 to control sphingolipid homeostasis in Saccharomyces cerevisiae. Proc. Natl. Acad. Sci. USA *108*, 19222–19227.

Shakoury-Elizeh, M., Protchenko, O., Berger, A., Cox, J., Gable, K., Dunn, T.M., Prinz, W.A., Bard, M., and Philpott, C.C. (2010). Metabolic response to iron deficiency in Saccharomyces cerevisiae. J. Biol. Chem. *285*, 14823–14833.

Sun, Y., Miao, Y., Yamane, Y., Zhang, C., Shokat, K.M., Takematsu, H., Kozutsumi, Y., and Drubin, D.G. (2012). Orm protein phosphoregulation mediates transient sphingolipid biosynthesis response to heat stress via the Pkh-Ypk and Cdc55-PP2A pathways. Mol. Biol. Cell *23*, 2388–2398.

Touati, D. (2000). Iron and oxidative stress in bacteria. Arch. Biochem. Biophys. *373*, 1–6.

Valentine, J.S., Wertz, D.L., Lyons, T.J., Liou, L.L., Goto, J.J., and Gralla, E.B. (1998). The dark side of dioxygen biochemistry. Curr. Opin. Chem. Biol. *2*, 253–262.

Valko, M., Morris, H., and Cronin, M.T. (2005). Metals, toxicity and oxidative stress. Curr. Med. Chem. *12*, 1161–1208.

Van Ho, A., Ward, D.M., and Kaplan, J. (2002). Transition metal transport in yeast. Annu. Rev. Microbiol. *56*, 237–261.

Villa, N.Y., Kupchak, B.R., Garitaonandia, I., Smith, J.L., Alonso, E., Alford, C., Cowart, L.A., Hannun, Y.A., and Lyons, T.J. (2009). Sphingolipids function as downstream effectors of a fungal PAQR. Mol. Pharmacol. *75*, 866–875.

Cell Metabolism, Volume *16*

Supplemental Information

Sphingolipid Signaling Mediates Iron Toxicity

Yueh-Jung Lee, Xinhe Huang, Janette Kropat, Anthony Henras, Sabeeha S. Merchant, Robert C. Dickson, and Guillaume F. Chanfreau

Supplemental Experimental Procedures

Yeast strains

All *S. cerevisiae* strains used in this study are derived from *BMA64* (Baudin et al., 1993). Strains containing gene knockouts and proteins tagged at the C-termini were generated by PCR-mediated gene deletion and tagging as described in (Longtine et al., 1998).

Media

Yeast cells were grown on synthetic defined (SD) medium plates at 25°C or 30°C. Iron-replete plates were made by adjusting the pH of synthetic media to 5.8 before autoclaving and adding specific concentration of $FeCl_3$ or $FeSO_4$ before pouring. Other metals were added in a similar way. The iron concentration of unsupplemented media was measured at 43 µM for YPD plates, and 35 µM for minimal medium plates (SC or -URA; average of triplicate samples). Therefore the added iron (5 to 7mM) is in large excess of the normal iron concentrations of standard media.

Suppressors screening

The overexpression genomic library was constructed by partial digestion of genomic DNA prepared from the *rnt1Δ* strain with *Sau*3AI. DNA fragments of 3- to 5-kb were size selected by agarose gel electrophoresis, purified, and inserted into YEp24 (Botstein et al. 1979) linearized with *Bam*HI. 10^5 *E.coli* clones were pooled, and the genomic library purified using Qiagen columns. Unamplified library was used for screening for suppressors of iron toxicity, by transforming 10^9 wild-type or *rnt1Δ* cells with 20µg of genomic library DNA. Cells were first plated onto SD–URA plates and incubated at 30°C for a day. Cells were then replica plated onto –URA+ 7mM $FeCl_3$ plates and incubated at 30°C. 100 colonies were picked and confirmed by re-streaking onto –URA plates. Plasmids from positive colonies were isolated and sequenced to identify the ORFs.

Plasmids

Overexpression plasmids containing individual full-length *ORM1* and *ORM2* open-reading frames (ORF) were constructed by amplifying each individual ORF, including its own promoter sequence and 3'-flanking region and cloning these fragments into YEp24. For *ORM1*, 300 nucleotides upstream of the translation start site and 400 nucleotides downstream of the translation stop site were amplified. *Bam*HI and *Sal*I restriction sites were added onto the PCR primers and used for cloning. For *ORM2*, 330 nucleotides upstream and downstream of the translation start and stop sites were amplified. *Bam*HI and *Eag*I restriction sites were added onto the PCR primers and used for cloning. The sequence of each individual ORF was further confirmed by sequencing. To overexpress HA-tagged Orm1p and Orm2p, the sequences of *ORM1* and *ORM2* tagged with the HA-epitope at their endogenous loci were amplified by PCR from genomic DNA using the same sets of primers as described above, and cloned into YEp24.

Protein analysis

In order to analyze Ypk1p-myc levels and phosphorylation state, cells were carefully scraped from plates, resuspended in lysis buffer (20mM Tris-HCl pH 7.5, 125mM Potassium acetate, 0.5mM EDTA, 0.5mM EGTA, 1mM DTT, 0.1% Triton X-100, 12.5% glycerol, protease inhibitor and phosphatase inhibitor cocktails from Roche) and vortexed with glass beads for 3 min at 4°C, and left on ice for 3 min. The procedure was repeated two more times. Soluble supernatants were obtained by centrifugation and the total protein concentrations measured using the Bradford assay. For phosphatase treatment, 800 units of lambda phosphatase (New England Biolabs) were added to 5µg of proteins and incubated/rotated at 30°C for 1.5 hours. Samples were then fractionated on 8% SDS-PAGE containing 40µM $MnCl_2$ and 20µM Phostag (Wako Chemicals). Gels were washed with transfer buffer containing 1mM EDTA for 10 min twice and with transfer buffer without EDTA for 10 min twice before transferring to PVDF membranes. Polyclonal anti-Myc antibody from Santa Cruz biotechnology was used for Western analysis at a dilution of 1:5000. For analysis of Orm1p and Orm2p, cells were resuspended in SDS lysis buffer (50mM Tris-HCl, pH 6.8, 2% SDS, 10% glycerol, protease inhibitor cocktail and phosphatase inhibitor cocktail) and prepared as described above. Samples were analyzed by 10% SDS-PAGE and Western analysis using anti-HA antibody (Santa Cruz Biotechnology) at a dilution of 1:10000.

LCB analysis

Frozen cells scraped from plates were washed with milliQ water and suspended in 500 µl of fresh 80 mM tri-ethylamine (prepared in HPLC-grade absolute ethanol). Samples were sonicated in a water bath for 5 min at 37°C, heated for 30 min at 65°C, centrifuged, and the supernatant (150 µl) transferred to an HPLC sample vial insert. AQC (6-aminoquinolyl-N-hydroxysuccinimidyl carbamate) reagent (30 µl) was added and samples were treated at room temperature for 40 minutes, followed by addition of 20 µl of 1.5 N KOH (made in methanol) and incubation at 37°C for 30 minutes. The pH was adjusted by adding 20 µl of 1.74 M acetic acid (made in methanol) and 40 µl of the sample were assayed by HPLC as described (Lester and Dickson, 2001).

RNA Analysis

Cells were carefully scraped from plates, washed with water, resuspended in RNA lysis buffer (Chanfreau et al., 1998), and RNA extraction was performed as described (Chanfreau et al., 1998). 5 µg of total RNA was denatured in glyoxal and resolved on a 1.2% agarose gel. Hybridization with antisense riboprobes was performed as described previously (Sayani et al., 2008). All riboprobes were generated by T3MAXIscript kit (Ambion) and hybridization was performed at 67°C overnight.

Supplemental References

Baudin, A., Ozier-Kalogeropoulos, O., Denouel, A., Lacroute, F., and Cullin, C. (1993). A simple and efficient method for direct gene deletion in Saccharomyces cerevisiae. Nucleic Acids Res *21*, 3329-3330.

Botstein, D., S. C. Falco, S. E. Stewart, M. Brennan, S. Scherer, D. T. Stinchcomb, K. Struhl, and R. W. Davis. (1979). Sterile host yeasts (SHY): a eukaryotic system of biological containment for recombinant DNA experiments. Gene *8*:17-24.

Chanfreau, G., Rotondo, G., Legrain, P., and Jacquier, A. (1998). Processing of a dicistronic small nucleolar RNA precursor by the RNA endonuclease Rnt1. EMBO J *17*, 3726-3737.

Lester, R.L., and Dickson, R.C. (2001). High-performance liquid chromatography analysis of molecular species of sphingolipid-related long chain bases and long chain base phosphates in Saccharomyces cerevisiae after derivatization with 6-aminoquinolyl-N-hydroxysuccinimidyl carbamate. Anal Biochem *298*, 283-292.

Longtine, M.S., McKenzie, A., 3rd, Demarini, D.J., Shah, N.G., Wach, A., Brachat, A., Philippsen, P., and Pringle, J.R. (1998). Additional modules for versatile and economical PCR-based gene deletion and modification in Saccharomyces cerevisiae. Yeast *14*, 953-961.

Sayani, S., Janis, M., Lee, C.Y., Toesca, I., and Chanfreau, G.F. (2008). Widespread impact of nonsense-mediated mRNA decay on the yeast intronome. Mol Cell *31*, 360-370.

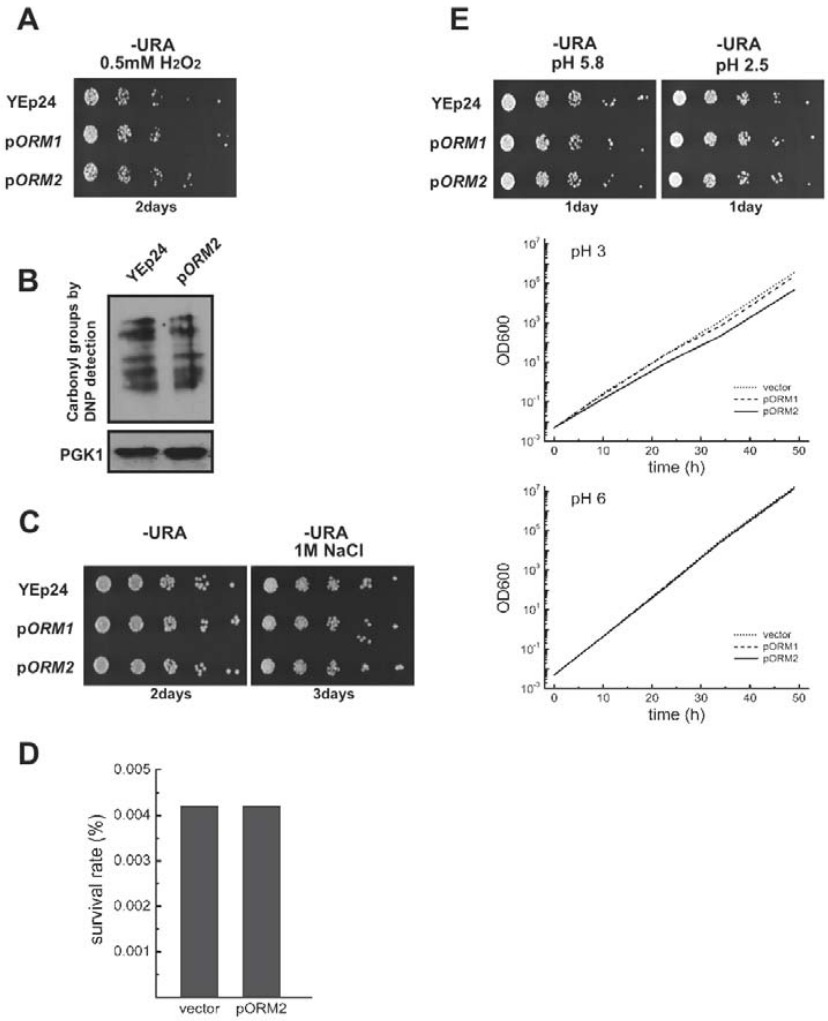

Figure S1 (**related to Figure 1).** ***ORM2*** **Overexpression Does Not Confer Higher Resistance to a Variety of Cellular Stresses and Does Not Affect Oxidized Protein Levels**

(A) Strains were grown without or with 0.5 mM H_2O_2 and incubated for 2 days at 25˚C.

(B) Oxyblot analysis in wild-type and *ORM2ox* cells grown in high iron. C. Strains were grown without or with 1M NaCl and incubated for 2 or 3 days, respectively at 30˚C. D. Strains were grown at 30˚C, heat-shocked at 50˚C for 20 minutes and returned to 30˚C for survival rate calculation. E. Strains were grown on normal (pH 5.8) or low pH (pH 2.5) and incubated for 1 day at 30˚C. The growth curves were also measured for all strains at normal or low pH.

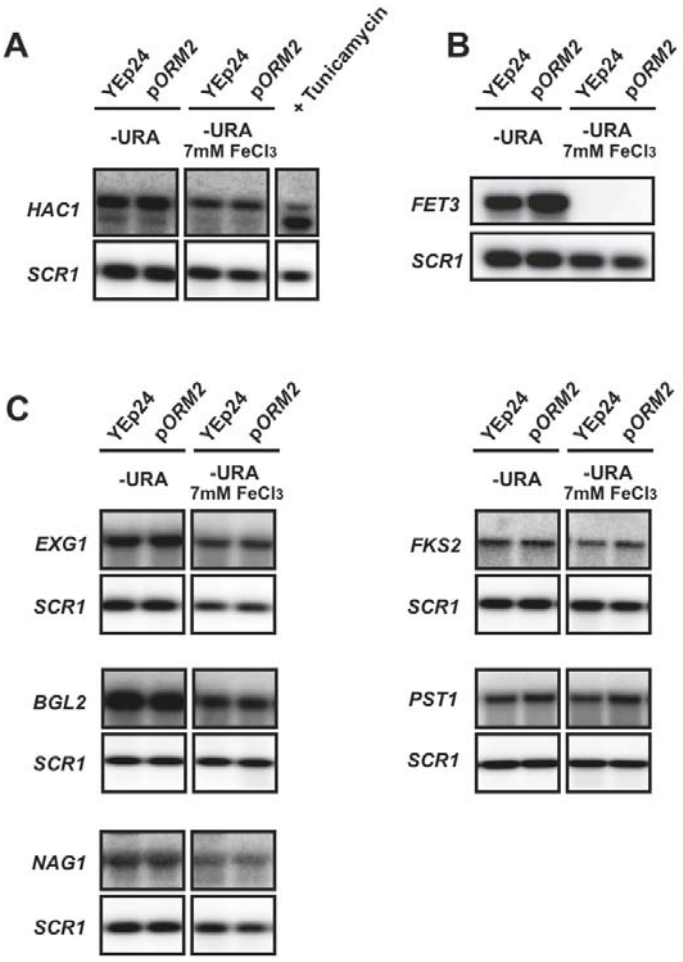

Figure S2 (related to Figures 1, 3 and 4). Analysis of *HAC1* Splicing, *FET3* mRNA and of Mpk1p/High Osmolarity or Cell Wall Target Genes Expression in Normal and High Iron Conditions

Strains were grown on normal (-URA) conditions and incubated for 2 days at 25˚C before collecting for RNA blot analysis. The same strains were also grown on 7mM $FeCl_3$ and incubated for 6 days (p*ORM2*) and 11 days (YEp24) at 25˚C before sampling for RNA analysis. In A, 2 µg/ml of tunicamycin was used to induce ER stress. *SCR1* was used as loading control.

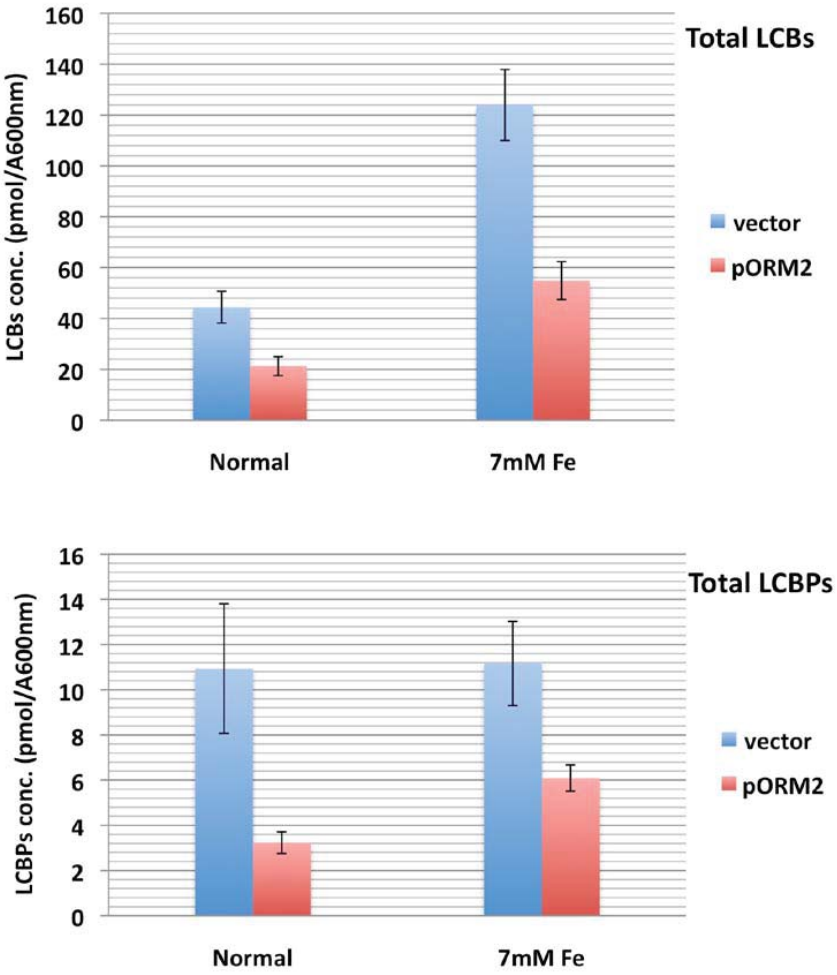

Figure S3 (related to Figure 3). Reproducibility of the Effect of High Iron Conditions and *ORM2* Overexpression on LCB Analysis

Shown are the average values of duplicate samples with the S.D. indicated. These data and those shown in Fig. 3B were obtained from independent experiments.

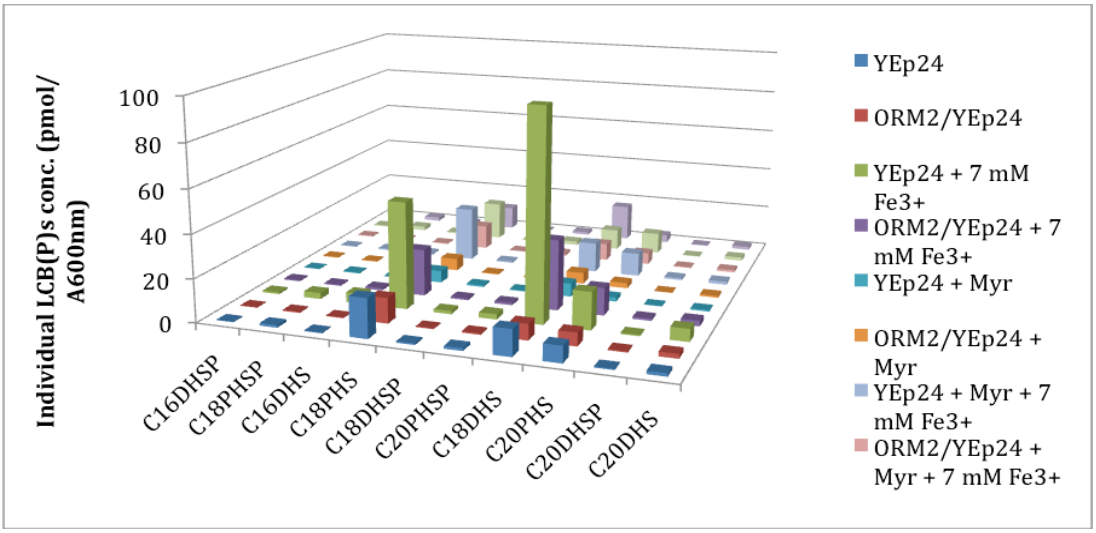

Figure S4 (related to Figure 3B). Detailed Sphingolipid Analysis in Normal and High Iron Conditions in Wild-Type or *ORM2ox* Cells

Strains were grown on normal, 7mM $FeCl_3$, 200ng/ml myriocin, 7mM$FeCl_3$+200ng/ml myriocin and incubated at 25˚C until cells reach to similar size before scraped for LCBs analysis. Shown are the levels of inidividual LCB and LCBPs analyzed in the different conditions.

Table S1. Statistical Analysis of LCB Levels

p-value analysis (two tailed t-test)	Sum LCBs	Sum LCBPs
YEp24 + 7 mM Fe *vs.* YEp24	0.00061063	0.02695004
YEp24 + 7 mM Fe + Myr *vs.* YEp24 + 7 mM Fe	0.000604519	0.002389936
ORM2/YEp24 + 7 mM Fe *vs.* YEp24 + 7 mM Fe	0.000511298	0.01329189
ORM2/YEp24 *vs.* YEp24	0.017172147	0.213779098
YEp24 + Myr *vs.* YEp24	0.001600603	0.183916011
YEp24 + 2 mM Cu *vs.* YEp24	0.984899384	0.506265705

p-value analysis (two tailed t-test)		
Strain/Treatment	**Sum LCBs**	**Sum LCBPs**
YEp24 *vs. ORM2*	0.017172147	0.213779098
YEp24 *vs.* YEp24 + 7 mM Fe	0.00061063	0.02695004
YEp24 + 7 mM Fe *vs. ORM2*+ 7 mM Fe	0.000511298	0.01329189
YEp24 *vs.* Myr	0.001600603	0.183916011
YEp24 + 7 mM Fe *vs.* Myr+ 7 mM Fe	0.000604519	0.002389936
YEp24 *vs.* 2 mM Cu	0.984899384	0.506265705
ORM2 vs. Myr + *ORM2*	0.016856584	0.14505376
ORM2+ 7 mM Fe *vs. ORM2* + Myr + 7 mM Fe	0.000577672	0.189078319
ORM2 vs. ORM2 + 2 mM Cu	0.309257017	0.070071713
2 mM Cu *vs. ORM2* + 2 mM Cu	0.339760011	0.39047349

CHAPTER 3

VACUOLAR AUTOPHAGY OF RNA POLYMERASE I DURING ZINC DEFICIENCY

Vacuolar Autophagy of RNA Polymerase I during Zinc Deficiency

Yueh-Jung Lee, Chrissie Young Lee, Agnieszka Grzechnik, Fernando Gonzales-Zubiate, Ajay A. Vashisht, Albert Lee, James Wohlschlegel & Guillaume Chanfreau

ABSTRACT

Divalent metals such as zinc are required for the function of many cellular proteins and enzymes, in particular for RNA polymerases during transcription. Because of this requirement, organisms have developed elaborate pathways to spare metals in conditions of metals deficiency. Here we show that RNA polymerase I (RNAPI) and some associated proteins are degraded by vacuolar autophagy during zinc deficiency. This downregulation is mediated by export of the RNAPI complex into the vacuole and degradation by vacuolar proteases. Export of RNAPI out of the nucleus requires the exportin Xpo1p and the de-ubiquitination of the Rpa190p subunit by the Ubp2p and Ubp4p ubiquitin proteases. RNAPI downregulation kinetics are influenced by the integrity of specific zinc binding subunits of the enzyme, suggesting a potential mechanism of zinc sensing. Degradation of RNAPI might be linked to the recovery of the zinc bound to the subunits in the vacuole for redistribution to other proteins during zinc deficiency. These results show that zinc deficiency

triggers degradation of the most active cellular transcriptional machinery and underscores the importance of zinc economy in eukaryotic cell metabolism.

INTRODUCTION

Cells need to regulate their intracellular metal content within reasonable range. Metals are required cofactors for many cellular proteins and enzymes but many of these metals are not readily available. Thus most organisms have developed mechanisms to uptake and spare metals in conditions of metal deficiency. In particular, unicellular microorganisms express transporters that uptake metals from the extracellular medium, and redistribute metals from storage compartments (Simm et al., 2007; Van Ho et al., 2002). During metal deficiency downregulation of specific metalloproteins occurs, which facilitates metal sparing for proteins whose functions are prioritized during the adverse conditions generated by the starvation. This also switches metabolic functions to other proteins that work similarly, but that are dependent upon metals other than the one being present in reduced amounts (Kaplan et al., 2006). This regulation can occur by active degradation of the proteins (Merchant and Bogorad, 1986), repression of the transcription of genes encoding these proteins (Bird et al., 2006; Panina et al., 2003; Shakoury-Elizeh et al., 2003), or degradation of the RNAs encoding these proteins (Puig et al., 2005).

Ribosome biogenesis is a very energetically costly process (Warner, 1999). Therefore its regulation is tightly connected to cellular demand, nutrient abundance and stress conditions. Not surprisingly, many regulatory steps affecting ribosome biogenesis regulation involve

regulation of transcription of the ribosomal DNA (rDNA) by RNA polymerase I (RNAPI). The most frequent mechanism of regulation of RNAPI activity affects the initiation stage of transcription (reviewed in (Grummt, 2003; Moss, 2004)). This regulation usually involves modulating the number of RNAPI core complexes associated with transcription factors that direct the binding of the polymerase to its promoter target. In addition, additional work has shown that RNAPI transcription can also be regulated at the elongation stage (Stefanovsky et al., 2006). Negative regulation of RNAPI activity is frequently observed when cells are exposed to nutrient deprivation or suboptimal growth conditions (Grummt, 2003; Moss, 2004; Moss et al., 2007; Warner, 1999). The signal transduction cascade for some of these regulations has been established. For instance, nutrient deprivation-mediated down regulation of RNAPI transcriptional activity is mediated by the Target Of Rapamycin (TOR) signal transduction pathway (Mayer and Grummt, 2006; Powers and Walter, 1999), while the decrease in rRNA synthesis in secretion-defective yeast cells is mediated by the PKC signaling pathway (Li et al., 2000). RNAPI is also affected by stresses that affect the integrity of the cellular components, such as DNA damage. Induction of DNA damage in mammalian cells triggers the ATM signal transduction pathway resulting in an inhibition of RNAPI activity (Kruhlak et al., 2007). Exposure of mammalian cells to oxidative stress triggers the cytoplasmic export of transcription factor TIF-IA through the JNK2 kinase pathway (Mayer et al., 2005), which results in a downregulation of ribosomal RNA synthesis through a

reduction of the number of RNAPI core complexes associated with TIF-IA in the nucleus.

In general, the regulation of RNAPI-driven transcription during stress conditions does not affect the overall levels of polymerase complexes, but rather the amount of complexes that are competent for transcription initiation or are engaged in initiation or elongation. However, the fact that RNAPI activity is regulated during the cell cycle and in conditions of DNA damage underscores the importance of coupling RNAPI activity to cellular activity and integrity. In this study, we report the unexpected finding that RNA polymerase I complexes are down-regulated during zinc deficiency through their export to the vacuole and degradation. We propose that the export of RNAPI to the vacuole and subsequent degradation provides cells with a source of zinc that can be redistributed to other proteins whose functions are prioritized during zinc deficiency.

RESULTS

Downregulation of RNA polymerase I subunits and associated nucleolar proteins during Zinc deficiency

We showed previously that the yeast RNase III Rnt1p cleaves a number of mRNAs encoding iron uptake and mobilization proteins, possibly to prevent their accumulation in iron-replete conditions (Lee et al., 2005). To investigate a possible regulation of Rnt1p during iron deficiency, we assessed the accumulation of Rnt1p by immunoblots of protein extracts prepared from cells shifted into a medium containing the non-permeable metal chelator bathophenanthroline-sulfonate (BPS), which is commonly used to chelate iron. Strikingly, Rnt1p levels started to decrease by 6 hours of exposure to BPS and the protein became virtually undetectable after 8 hours (Fig.1A). To investigate the specificity of this down-regulation, we analyzed the levels of a subset of nuclear and nucleolar proteins in the same conditions. We probed several subunits of RNA polymerases I, II and III, using C-terminally Tandem-Affinity Purification (TAP)-tagged strains (Fig.1B). This analysis showed that all RNA polymerase I (RNAPI) subunits tested were also down-regulated with kinetics similar to that exhibited by Rnt1p (Fig.1B). This effect was not specific to TAP-tagged subunits, as a plasmid-borne HA-tagged Rpa135 (Naryshkina et al., 2003) or untagged Rpa135p detected with an anti-Rpa135 monoclonal antibody were also down-regulated (Fig.1B). In contrast, most RNAPII-specific subunits did not exhibit any

change in accumulation (Fig.1B). The only exception was the large subunit of RNAPII Rpb1p, which was apparently down-regulated based on immunoblot analysis using the monoclonal antibody 8WG16. To test whether this decrease of accumulation of the epitope recognized by this antibody (the unphosphorylated C-terminal domain YSPTSPS heptads, CTD) is due to a degradation of the entire Rpb1p subunit, or rather to a cleavage of the CTD, we used the N200 antibody (Chen and Hahn, 2004) that recognizes the N-terminus of Rpb1p (Fig.1A). This analysis showed that a shorter fragment of Rpb1p accumulates during BPS treatment, suggesting that the CTD heptad repeats, or a larger C-terminal fragment containing these heptads, is cleaved. In agreement with this hypothesis, we observed a small proteolytic fragment on high percentage polyacrylamide gels detected by 8WG16 specifically upon BPS treatment, which might correspond to the CTD or a slightly larger fragment (Fig.1C). Experiments described in Supplemental materials showed that Rpb1p CTD cleavage in cells shifted in BPS was the result of a proteolytic artifact occurring during extracts preparation (Suppl.Fig.S1). Thus, RNAPII remains intact in these conditions.

The previous data showed that Rnt1p and RNAPI are down-regulated during Zinc deficiency. Previous studies had shown that Rnt1p processing of the pre-rRNA is co-transcriptional (Allmang and Tollervey, 1998; Henras et al., 2004), and that Rnt1p physically associates with RNAPI (Catala et al., 2008). To investigate if other proteins that associate with RNAPI are regulated in a similar manner, we analyzed the levels of several

proteins known to associate with RNAPI (Fath et al., 2000). Strikingly, the RNAPI interacting proteins Reb1p, Fpr3p, Rrp5p and Cbf5p were all down-regulated during Zn deficiency (Fig.S2), showing that this downregulation also affects other proteins that associate with RNAPI. In contrast, the nucleolar marker protein Nop1p and the rDNA factor Fob1p were unaffected by a shift into low zinc medium (Fig.S2), showing that this downregulation does not affect all nucleolar proteins. Other nuclear proteins such as Tfg1p, Smd1p and Smb1p were unaffected as well (Fig.S2). These results show that the downregulation of nucleolar proteins during Zn deficiency is limited to a subset of nucleolar proteins that can associate with RNA polymerase I. Because the downregulation of RNA polymerase subunits were specific to RNAPI and associated proteins, we focused our investigations on the mechanisms and pathways required for this pathway.

BPS is generally used to chelate iron, but it can also chelate zinc (Zhao and Eide, 1996). We found that treatment of cells with another chelator EDTA also resulted in Rpa135 downregulation (Fig.1D and see below), raising the question of which metal deficiency was responsible for the effect observed. To investigate whether iron or zinc starvation were responsible, we prepared media containing low Zn (LZM) or low Fe (LIM) by incubating synthetic medium with chelating beads and adding back all metals, except Fe or Zn. Cells shifted into LZM exhibited downregulation of Rpa190-TAP and Rpa135p (Fig.1E). In contrast, incubation in LIM did not result in RNAPI subunits downregulation (Fig.1E),

showing that the effects observed with BPS and EDTA were due to Zn depletion. The kinetics of Rpa135p downregulation were generally slower in LZM than in chelator-containing media (Fig.1) and showed more variability (data not shown), possibly because LZM still contains traces amounts of zinc that are difficult to consistently remove from the medium because of external contaminations (Kay, 2004). Thus, we performed most of the following experiments by treating cells with the metal chelators BPS or EDTA. In agreement with a Zn-specific effect, we found that cells pre-loaded with Zn by growth in preculture in a minimal medium supplemented with 2mM Zn exhibited a slower down regulation than cells pre-grown in unsupplemented medium (Fig.1F). To further demonstrate that Zn deficiency is responsible for RNAPI down-regulation, we used a strain lacking Zap1p, the main transcription factor that activates low-zinc response genes during zinc starvation (Lyons et al., 2000; Wu et al., 2008). Strains lacking Zap1p are genetically zinc-deficient and we found that they exhibit a faster downregulation of Rpa135p than wild-type cells (Fig.1G). This result shows that RNAPI downregulation does not require the Zap1p-mediated transcriptional response that occurs during zinc starvation, but that genetically depriving the cells of zinc accelerate the kinetics of down-regulation. Taken together, these results demonstrate that the downregulation of RNAPI subunits is specifically due to zinc deprivation.

RNAPI downregulation is not related to cell death or to known stress pathways

Transcription of rDNA and RNAPI activity are affected by a number of stress conditions (reviewed in (Grummt, 2003; Warner, 1999)). To investigate whether the downregulation of RNA Polymerase I during zinc deficiency is mechanistically linked to stress conditions previously known to affect its activity, we monitored RNAPI levels in a variety of conditions or in mutants known to affect rDNA transcription. First we found that RNAPI levels were unaffected by amino acids starvation (Fig.S3A) although it has been shown that these conditions result in a reduction in rDNA transcription. RNAPI activity has also been shown to be affected by defects in secretion and a pathway dependent on the Wsc family of putative plasma membrane sensors and the Pkc1p protein kinase (Li et al., 2000; Nierras and Warner, 1999). To investigate if the downregulation of RNAPI observed in zinc deficiency is mechanistically connected to this response, we investigated the kinetics of downregulation of Rpa135p in a *pkc1Δ* strain. We found that although a Pkc1p-deficient strain exhibited lower levels of RNAPI, it did not result in an inhibition of RNAPI downregulation (Fig.S3B). Similarly, RNAPI downregulation occurred with normal kinetics in *wsc* mutants (Fig.S3C), showing that RNAPI downregulation during zinc deficiency is unrelated to the response that occurs during plasma membrane synthesis or secretory defects (Li et al., 2000; Nierras and Warner, 1999).

Previous studies had found that the downregulation of RNAPI transcriptional activity during nutrient deprivation is mediated by the target of rapamycin (TOR) signal transduction

pathway (Claypool et al., 2003; Powers and Walter, 1999). To investigate if the downregulation of RNAPI during zinc deficiency is mechanistically related to the TOR pathway, we used *tor1Δ* or *fpr1Δ* deletion strains that are deficient in TOR signaling. We found that RNAPI downregulation does not require an intact TOR pathway, as it occurs normally in *tor1Δ* or *fpr1Δ* mutants (Fig.S3D). Taken together, these results show that RNAPI downregulation during zinc deficiency is unrelated to multiple regulatory pathways previously described to affect ribosome biogenesis or integrity.

To investigate if RNAPI downregulation results from cellular death following prolonged exposure to low zinc conditions, we investigated its reversibility. After a 10 hour shift to low zinc medium, cells were shifted back to normal zinc medium and the growth and levels of Rpa135p and Rpa190 were assessed upon shifting back the cells (Fig.S4). Cells quickly resumed growth after a shift back to normal conditions (Fig.S4A), showing that most of the cells in the culture did not die during the shift to low zinc conditions. In parallel, Rpa135p and Rpa190p levels were quickly restored to normal levels upon this shift back to normal zinc medium (Fig.S4B). Overall these results show that RNAPI downregulation is not due to cellular death and is unrelated to known stress conditions previously documented to affect ribosome biogenesis and RNAPI activity.

RNAPI downregulation is rescued in vacuolar proteases mutants

The downregulation of RNA polymerase I subunits could be due to either transcriptional downregulation of the genes encoding RNAPI subunits or to post-transcriptional processes. We monitored the mRNA levels of genes encoding three RNAPI subunits (*RPA135*, *RPA49* and *RPA43*) and found that their levels were unaffected during a shift to low zinc medium (Figure 2A). This result shows that RNAPI downregulation does not involve transcriptional repression of RNAPI subunit genes, or degradation of their mRNAs. We next hypothesized that this downregulation occurred by increased protein turnover and searched for proteases whose expression is changed during zinc deficiency. Some vacuolar proteases were previously shown to be upregulated during zinc deficiency (Lyons et al., 2000). To test the involvement of these proteases in RNAPI down-regulation, we monitored Rpa135p levels in *prb1Δ*, *pep4Δ* or *prc1Δ* vacuolar protease mutant strains during a shift in low Zn medium. Fig.2B shows that Rpa135p levels can be rescued in low Zn conditions by inactivation of the vacuolar proteases Prb1p or Pep4p, but not Prc1p. Similarly, the downregulation of GFP-tagged versions of Rpa135p or Rpa43p was rescued in the *prb1Δ* deletion strain (Fig.2C). To test whether this effect was due to a general involvement of vacuolar proteases in RNAPI subunits stability under normal conditions, we monitored the half-life of the Rpa43p subunit in wild-type and vacuolar protease deficient strains in normal growth conditions. To this end, we used a plasmid expressing Rpa43p under the control of the *MET25* promoter, which is repressed in the presence of methionine. We found that Rpa43p

half-life was identical in wild-type and vacuolar protease mutants (Fig.2D). Thus, the vacuolar proteases Pep4p and Prb1p contribute to the downregulation of RNAPI during zinc deficiency but are not involved in the turnover of RNAPI subunits in normal conditions. We also analyzed the levels of other RNAPI-associated proteins in the *pep4Δ* and *prb1Δ* deletion strains. Immunoblot analysis of TAP-tagged versions of Reb1p, Fpr3p, Rrp5p and Cbf5p showed that the downregulation of these proteins observed during zinc deficiency could be rescued by inactivation of the one or both of the vacuolar proteases Pep4p and Prb1p (Fig.2E). Some RNAPI associated proteins were rescued by depletion of only one protease, suggesting that different proteins of the complex are differentially affected by the activity of each of these two proteases (Fig.2E).

RNAPI is exported to the vacuole as a complex during zinc deficiency

Based on these results, we hypothesized that RNAPI complexes are exported to the vacuole during zinc deficiency where they are degraded by the vacuolar proteases Pep4p and/or Prb1p. To test this hypothesis, we monitored the localization of the RNAPI subunits fused to GFP in wild-type or vacuolar protease mutants grown in normal or low zinc conditions, and assessed vacuolar localization using the vital stain FM4-64 (Vida and Emr, 1995)(Fig. 3). As expected, GFP signal was observed outside of the vacuole in all strains in normal medium. During Zn starvation, we observed a complete loss of GFP signal in wild-type cells, consistent with the

downregulation previously observed by western blotting. In contrast, a predominant accumulation of GFP signal was detected inside the vacuole in the *pep4Δ* strain (Fig.3A). This change of localization pattern was specific to RNAPI subunits, and not due to a global change in the nucleolar structure during Zn deficiency, as evidenced by our lack of observation of any localization change using a Nop1-GFP construct in similar conditions (Fig.3B). These experiments showed that RNAPI is exported to the vacuole during zinc deficiency, and that the rescue of RNAPI subunit levels observed previously in vacuolar protease mutants is directly due to a lack of vacuolar degradation. We renamed the downregulation of RNA polymerase I observed during zinc deficiency "vacuolar autophagy". To confirm that vacuolar proteases are involved in RNAPI autophagy, we analyzed RNAPI subunits levels and localization in the *vps30Δ* mutant, in which vacuolar protein sorting is defective. This mutant exhibits lower vacuolar proteases activity because of defective sorting of these proteases into vacuoles. We observed a delay in RNAPI downregulation in the mutant (Fig.S5A), and found that RNAPI accumulates in the vacuoles in this mutant (Fig.S5B). This experiment confirms that proper sorting of the proteases in the vacuole is required for efficient RNAPI degradation in the vacuole.

We next asked whether RNAPI disassembles prior to export or whether the entire complex is exported to the vacuole for degradation. To investigate this question, we performed a TAP-tag purification of RNAPI complexes using extracts from the *pep4Δ* strain

expressing Rpa135p or Rpa190p fused to a TAP-tag grown in normal medium or prolonged zinc deficiency conditions. As shown in Fig.S6, the pattern of bands obtained during TAP purification was very similar before or after a shift to zinc deficient medium (see also Fig.4A). In addition, we also analyzed these complexes using Multidimensional Protein Indentification Technology (MudPIT) and could detect the presence of all subunits in sub-stoichiometric proportions before and after the shift (Supp.Table S1). Since the majority of RNAPI purified during zinc deficiency in the *pep4Δ* strain is localized in the vacuole (Fig.3A), we conclude that the RNAPI is likely exported as an intact complex without disassembly. This observation also explains why proteins associated with RNAPI are also found to be down-regulated in these conditions (Fig.S2).

Export of RNA Polymerase I into the vacuole requires Xpo1p

We next investigated the mechanism by which RNAPI complexes are exported from the nucleus to be degraded in the vacuole. We first hypothesized that this export requires the formation of nucleus-vacuole junctions, which are observed during piece-meal microautophagy of the nucleus (PMN) in starvation conditions (Kvam and Goldfarb, 2007). We investigated the *nvj1*Δ and *vac8*Δ mutants, which are defective in the PMN pathway, but inactivation of these proteins did not rescue RNAPI downregulation (Fig.S3E), showing that the PMN pathway is not involved in RNAPI vacuolar autophagy. We next investigated the

potential function of the exportin Xpo1p in this process. Xpo1p is the major nuclear export factor for proteins in yeast (Stade et al., 1997). Using the thermosensitive allele *xpo1-1*, we found that genetic inactivation of Xpo1 prior to a shift in low Zn medium resulted in a rescue of the downregulation of RNAPI (Fig.3C). Furthermore, inactivation of Xpo1p also resulted in an inhibition of the vacuolar localization of RNAPI during zinc deficiency, and resulted in an accumulation of RNAPI in the nucleolus (Fig.3D). These results support the idea that Xpo1p mediates the export of RNAPI out of the nucleus for subsequent import into the vacuole.

Downregulation and vacuolar import of RNAPI requires de-ubiquitination of the large subunit Rpa190p

In order to understand the mechanism of vacuolar import of RNAPI during zinc deficiency, we first screened mutant strains defective in known various vacuolar import pathways. A variety of *atg* mutants, which are defective in the autophagy or cytoplasm to vacuole targeting (CVT) pathways (Nair and Klionsky, 2005) were screened for Rpa135p levels in zinc deficiency. However none of these mutations were sufficient to rescue or delay the downregulation of RNAPI subunits during zinc deficiency (Fig.S3F; Table S2). Therefore RNAPI downregulation does not require any the known autophagy or CVT pathways that are known to mediate import of proteins in the vacuole. Because covalent modifications often

trigger a change in the stability or localization of protein complexes, we next probed blots of TAP-purified RNAPI complexes (prepared from a *pep4*Δ strain) during a shift to low Zn with anti-ubiquitin antibody. We detected major high molecular weight (>190 kDa) bands using anti-ubiquitin antibodies from TAP-purified RNAPI complexes (Fig.4A), which, given their mobility are likely to correspond to Rpa190p. Strikingly, the ubiquitinated band detected from purified RNAPI became undetectable after 8 hours in low Zn medium (Fig.4A) showing that Rpa190p becomes deubiquitinated in low Zn conditions. These observations suggested that de-ubiquitination of the large subunit Rpa190p may be required for, or at least correlated with degradation of the RNAPI complexes. To test this hypothesis, we screened a number of ubiquitin protease mutants. We first focused on Ubp2p and Ubp4p, as these ubiquitin proteases were described as required for sorting proteins to the vacuole or to multivesicular bodies (Amerik et al., 2000; Dupre and Haguenauer-Tsapis, 2001; Lam et al., 2009). We found that inactivation of the Ubp2p and Ubp4p deubiquitinases resulted in a higher stability of RNAPI complexes in low zinc conditions (Fig.4B). Recent work showed that ribosomes are degraded during starvation in a process known as ribophagy that is dependent on the Ubp3p ubiquitin protease (Kraft et al., 2008). The kinetics of Rpa135p downregulation were unaffected in a strain lacking Ubp3p (Fig.4B) showing that RNAPI downregulation does not require Ubp3p and likely is not mechanistically related to ribophagy. Similarly, Rpa190p levels were not rescued upon inactivation of two other deubiquitinases Ubp8p and Ubp14p

(Fig.4B), showing that the stabilization observed in the ubp2 and ubp4 strains was specific to these two ubiquitin proteases.

We next tested the effect of the inactivation of Ubp2p and Ubp4p on RNAPI localization during a shift to low zinc conditions. Strikingly, stabilization of RNAPI in these strains correlated with inhibition of vacuolar import, as most of the RNAPI subunits localized outside of the vacuole when these mutant strains were grown in low zinc conditions (Fig.5A). These experiments demonstrate that the Ubp2p and Ubp4p ubiquitin proteases are specifically required for vacuolar import of RNAPI during zinc deficiency. This result is consistent with their demonstrated role in sorting vacuolar proteins and multi-vesicular bodies.

Inactivation of the ubiquitin ligase Rsp5p mediates vacuolar autophagy of RNAPI uncoupled from zinc deficiency

If de-ubiquitination of RNAPI is a major determinant of the RNAPI vacuolar authophagy pathway, we predicted that inactivation of the Rsp5p ubiquitin ligase would also result in a Pep4/Prb1-dependent degradation of RNAPI complexes independent of cellular zinc levels. Indeed, using an *rsp5-1* thermosensitive mutant allele of Rsp5p, we found that the abundance of Rpa190p was quickly decreased during a shift of this allele to non-permissive temperature (Fig.4C). In contrast, the stability of Rpa190p was unaffected by a shift to 37°C in the

wild-type strain. Strikingly, the downregulation of Rpa190p observed upon a shift of the *rsp5-1* mutant to the non-permissive temperature was abolished when the Pep4p protease was inactivated (Fig.4C). This result suggests that the downregulation of RNAPI observed in the *rsp5-1* mutant occurs through vacuolar degradation. To demonstrate unambiguously that this is the case, we followed Rpa190p localization in these strains grown in normal medium, before or after a shift to 37°C. We observed a loss of GFP signal in the *rsp5-1* mutant shifted to non-permissive temperature (Fig.5B), consistent with the downregulation observed by immunoblot analysis. However, when the *rsp5-1 pep4*Δ double mutant was shifted to the same temperature, the GFP signal was recovered and accumulated in both the vacuole and the nucleolus. The vacuolar signal is probably due to the partial inactivation of Rsp5p at restrictive temperature which results in only a fraction of the RNAPI complexes being exported. Taken together, these results show that inactivation of the Rsp5p results in vacuolar autophagy that is similar to what was observed during zinc deficiency, and strongly suggests that de-ubiquitination of Rpa190, or another subunit of the RNAPI complex, is a main determinant in triggering vacuolar export and degradation of the RNAPI complex.

Downregulation of RNAPI during Zinc deficiency dramatically reduces ribosomal RNAs synthesis

Based on the downregulation or cleavage of several RNAPI subunits, (Fig.1), we predicted

that RNAPI transcriptional activity might decrease during prolonged zinc starvation resulting in a decrease in ribosomal RNA production. During a shift to BPS-containing medium, we observed a decrease in mature ribosomal RNAs (Fig.6A) and many pre-rRNAs processing intermediates as shown by northern blotting (Fig.6A). To confirm reduced levels of transcription, wild-type cells were treated with BPS for 10 hours before performing transcriptional pulse-chase analysis using ^{3}H-uracil to monitor the kinetics of rRNAs and tRNAs production (Fig.6B,C). This experiment showed that incorporation of ^{3}H in rRNAs is decreased in wild-type cells treated with BPS compared to cells grown in normal medium, with a decrease in the production of full-length 18S, 25S, and 5.8S rRNAs. Comparison of the incorporation and processing profiles obtained with wild-type cells treated with BPS and of the *rnt1Δ* strain grown in normal medium showed that the level of rRNAs transcription was lower in wild-type cells shifted in BPS than in *rnt1Δ* cells. This result shows that a profound inhibition of RNAPI transcription is observed during zinc deficiency, in agreement with the downregulation of RNAPI complexes. RNA polymerase III activity was also affected, as shown by the decreased production of the 5S rRNA and tRNAs in wild-type cells treated with BPS compared to normal medium (Fig.6C). This observation might be explained by the fact that RNA Polymerase III activity is regulated according to RNAPI activity (Laferte et al., 2006). Overall, these results show that the observed depletion of RNAPI subunit during zinc deficiency results in a marked decrease of ribosomal RNAs production in

these conditions.

RNA Polymerase I downregulation is influenced by the integrity of Zn-finger containing Subunits

We next investigated the mechanisms by which RNAPI might sense zinc deficiency to be targeted to the vacuole. RNAPI binds zinc (Treich et al., 1991) and two of its subunits, Rpa135p and Rpa12p contain Zn-finger motifs (Naryshkina et al., 2003; Van Mullem et al., 2002). In order to assess the importance of Zn finger domains in the downregulation of RNAPI, we first used a version of Rpa135p tagged with the HA epitope and expressing two previously described mutant versions in its zinc finger motif (C1107A and C4); (Naryshkina et al., 2003). Strikingly these mutated versions of Rpa135p were down-regulated with a faster kinetics than the wild-type version (Fig.7A), suggesting that the integrity of the zinc finger domains of Rpa135 is important for the kinetics of down-regulation. We also analyzed a strain lacking Rpa12p, as this small subunit contains two zinc-finger motifs but is non-essential (Van Mullem et al., 2002). In contrast we found that strains lacking Rpa12p exhibit a slower downregulation of Rpa135p. This phenotype was specific to Rpa12p and was not observed in a strain lacking a non-zinc binding, non-essential subunit, Rpa49p (Fig.7B,C). Taken together these results show that the integrity of zinc-finger containing subunits of RNAPI subunits can influence the kinetics of downregulation of RNAPI during zinc

deficiency. This result suggests that one or several of these subunits might serve as a zinc sensor to probe the intracellular zinc content and trigger a sensing mechanism that exposes the RNAPI complex to the action of ubiquitin proteases for vacuolar export.

DISCUSSION

The results presented in this study show that zinc starvation (either induced by BPS or EDTA treatment or in zinc-limited medium) results in vacuolar autophagy of RNAPI subunits and some associated proteins. This regulation dramatically decreases ribosomal RNA and tRNA transcription, which accounts quantitatively for most of the transcriptional activity in rapidly growing cells. Most RNA polymerase II subunits tested in this study were unaffected, suggesting that RNAPII transcription is still functional in low zinc conditions, which allows for the expression of genes induced during zinc deficiency (Lyons et al., 2000). These results are consistent with previous observations in *Euglena* showing that Zn deficiency results in the formation of only one peak of RNA polymerase activity, which is likely to be an alpha-amanitin resistant form of Pol II (Falchuk et al., 1985). Our results might also shed light on older studies showing that rats fed on a zinc-deficient diet show reduced RNA polymerase activity (Terhune and Sandstead, 1972), although these results could be due to zinc depletion from the polymerases rather than to the active degradation mechanism demonstrated here. Thus, it is likely that the results that we present here using yeast illustrate a conserved mechanism of zinc economy.

The mechanisms of RNAPI export and vacuolar import during zinc deficiency

Our results support a model showing that RNAPI (and probably Rpa190) de-ubiquitination

by Ubp2/Ubp4p triggers a nuclear export and vacuolar import of the RNAPI complex. This regulated vacuolar degradation can be recapitulated independently from zinc deficiency using the rsp5-1 mutant strain which is defective for ubiquitination. This result strongly suggests that de-ubiquitination plays a major role in triggering vacuolar import of RNAPI and its degradation. One of the interesting mechanisms that remains to be determined is to understand what triggers the de-ubiquitination, export of RNAPI and the degradation in the vacuole upon a decrease in low zinc. We show in this study that the integrity of some of the zinc finger subunits can influence the kinetics of degradation. These results suggests that the Rpa12p and or Rpa135p subunits might serve as a zinc sensor to probe the intracellular zinc content and trigger a sensing mechanism that exposes the RNAPI complex to the action of ubiquitin proteases for vacuolar export. Such a mechanism might involve conformational changes in the RNAPI complex upon a loss of zinc by the zinc binding subunits, which might trigger the binding of Ubp2p or Ubp4p.

Why degrade RNA Polymerase I during Zinc Deficiency?

It has been shown previously that cells reduce the expression of or degrade proteins containing certain metals during starvation of the corresponding metals (Bird et al., 2006; Merchant and Bogorad, 1986; Puig et al., 2005), in order to spare these particular metals and/or redistribute them to other proteins. Biochemical and structural studies have shown that

many subunits of all three eukaryotic RNA polymerases contain multiple zinc atoms (Cramer et al., 2001; Donaldson and Friesen, 2000; Naryshkina et al., 2003; Treich et al., 1991). Therefore, degradation of RNA polymerase might provide a last-resort zinc reservoir during prolonged zinc deficiency. Interestingly, the vacuole is not only the site of degradation of RNA polymerase subunits but also the site of zinc storage and redistribution (Simm et al., 2007). The degradation of RNA polymerase subunits during zinc deficiency might represent an extreme example of metal sparing, which seems to indicate that the function of other cellular zinc-binding proteins are prioritized compared to those involved in ribosomal RNAs production. In addition, downregulation of RNAPI and of rRNA transcription might ultimately result in ribosome depletion and turnover, which could also provide a source of zinc given the abundance of zinc bound by Zn-finger proteins in ribosomes. Because this downregulation is quickly reversible (Fig.S4), it provides cells with the ability to quickly restore translational activity when zinc is re-introduced to cells. Nevertheless, our observation that yeast cells degrade the most active transcriptional machinery during zinc deficiency underscores the importance of zinc economy in cellular metabolism.

Acknowledgements. We thank M. Oakes and M. Nomura for the generous gift of anti-Rpa135p monoclonal antibody; M. Danin-Kreiselman for affinity purification of

anti-Rnt1p antibodies; A.Goldfarb, S.Hahn, C. Guthrie, E. Jones, M. Lund, K. Severinov, J. Warner and C.Woolford, for generous gifts of plasmids, strains or antibodies, M. Carey, S. Merchant, M. Clement, E. Gralla and J. Valentine for helpful discussions, and D. Eide for sharing results prior to publication. C.Y.L was supported by a Ruth L. Kirschstein National Research Service Award GM07185 and by a UCLA Dissertation Year Fellowship. A.L. was supported by the UCLA Chemistry-Biology Interface training program and by a Fellowship from the American Heart Association Western States Affiliate. Supported by NIH grant GM61518 to G.C. and GM089778 to J.W.

EXPERIMENTAL PROCEDURES

Yeast strains, Plasmids and Media

All yeast strains and plasmids used in this study are shown in strains & plasmids table. For low zinc condition, cells were grown to log phase in synthetic defined (SD) media, washed twice with sterile water and shifted to SD media containing either 50uM BPS or 1mM EDTA for the indicated times. For the temperature sensitive mutants, cells were first grown in SD media to log phase at 25°C and shifted to 37°C for the indicated times. For the temperature sensitive mutants in low zinc condition, cells were grown to log phase at 25°C and shifted to 37°C for two hours. Cells were then washed twice with pre-warmed (37°C) sterile water and shifted to pre-warmed low Zn media for the indicated times.

Western Blot Analysis

Cells were harvested and resuspended in the lysis buffer (200mM Tris-HCl pH 8.0; 320mM Ammonium sulfate; 5mM MgCl2; 10mM EGTA pH 8.0; 20mM EDTA pH 8.0; 1mMDTT; 20% glycerol; 1mM PMSF; 2mM benzamidine HCl and protease inhibitor cocktail) and vortex with glass beads for 8 min at 4°C. Supernatants were collected by centrifugation and total protein concentration was measured using the Bradford method. Samples were analyzed by 8% SDS-PAGE and transferred to PVDF membrane for Western blot analysis. Antibodies

used for probing Westerns include anti-Rpa135 (1:5000; gift from M. Oakes and M. Nomura), anti-Rnt1 (gift from M. Danin-Kreiselman), 8WG16 (1:5000; obtained from Covance), anti-GFP (1:10000; monoclonal antibody JL-8 obtained from Clontech), peroxidase anti-peroxidase (1:1000; obtained from Rockland), anti-HA (1:10000; obtained from Santa Cruz Biotechnology), anti-Nop1 (1:10000; obtained from EnCor Biotechnology), and anti-Ubiquitinylated proteins (1:5000; clone FK2 obtained from Millipore).

Northern Blot Analysis -

RNA extraction was performed as described previously (Chanfreau et al., 1998). 5 µg of total RNA were glyoxal denatured and resolved on a 1.2% agarose gel. Northern hybridization was performed as described previously (Sayani et al, 2008). All probes were generated by PCR products and hybridization was performed at 65°C overnight.

Tandem Affinity Purification

TAP purification was performed as described previously (Rigaut et al., 1999) with the following modifications. First, cells were harvested and resuspended in IPP50 or IPP150 buffer with 25% glycerol. Cell suspension was immediately frozen by liquid nitrogen and stored at -80°C. Cells were lysed by manual grinding with pre-chilled mortar and pestle for 10 min in liquid nitrogen. The grinding-freezing was repeated until the cells became

power-like and lysate was thawed on ice before centrifugation. Second, Calmodulin beads were incubated with elution buffer at 4°C for 30min before samples were eluted.

Vacuolar Membrane Staining and Localization Microscopy–

Cells containing Pol I-GFP fusion proteins were grown to log phase and harvested. Cells were resuspended in fresh medium and labeled with the vacuolar membrane dye FM4-64 (20μM, Invitrogen). Cells were incubated (shaking) at 30°C for 20 min and washed with fresh media twice to remove excess dye. The labeled cells were then put back into fresh media to grow at 30°C for 2 hours. Live cells were visualized immediately after labeling by fluorescent microscope. For low zinc or non-permissive temperature shift, cells were first shifted to low zinc media or non-permissive temperature. Two hours prior to the indicated times, cells were harvested and labeled with FM4-64 dye as described above for two hours and visualized immediately after by fluorescent microscope.

FIGURES

Figure 1. Downregulation of yeast nucleolar proteins during Zinc deficiency

A. Western blot analysis of Rnt1p after a shift into BPS-containing medium. The same membrane was probed with an anti-Rnt1p antibody and an anti-hexokinase antibody. Extract from a *rnt1*D strain was included as a negative control.

B. Western blot analysis of RNA polymerase subunits during BPS treatment. TAP-tagged strains were used, except for Rpb1, for which a wild-type strain was used and the 8WG16 mAb (CTD) or N200 antibodies (NTD) was used, and for Rpa135 for which a monoclonal anti-Rpa135p antibody was used.

C. The CTD of Rpb1 is cleaved during BPS treatment. Shown is a western blot analysis of Rpb1 using 8WG16 and a high percentage acrylamide gel (lower panel).

D. The Rpa135 Pol. I subunit is degraded. Shown is a western analysis of an N-terminally HA-tagged version of Rpa135.

E. Downregulation of RNA polymerase subunits is due to zinc limitation. Shown are western blots of Rpb1 (8WG16) or Rpa190-TAP in low zinc medium (LZM) or low iron medium (LIM).

G. Rpa135p downregulation occurs faster in a strain genetically deficient for zinc. Shown is an Rpa135 western analysis in wild-type and *zap1*Δ strains.

Figure 1

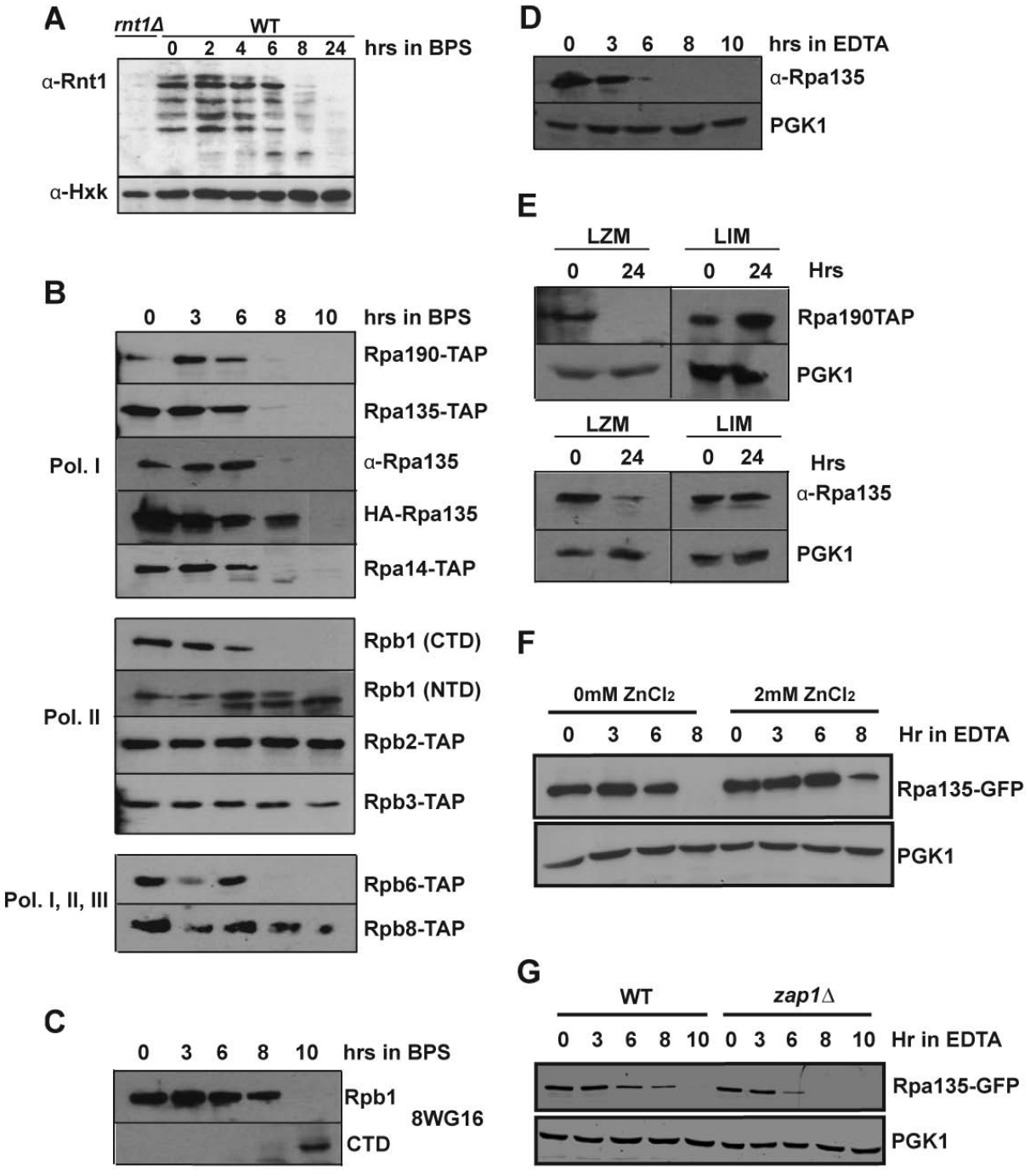
A
rnt1Δ
WT
0 2 4 6 8 24
hrs in BPS
α-Rnt1
α-Hxk
B
0 3 6 8 10
hrs in BPS
Rpa190-TAP
Rpa135-TAP
α-Rpa135
HA-Rpa135
Rpa14-TAP
Pol. I
Rpb1 (CTD)
Rpb1 (NTD)
Rpb2-TAP
Rpb3-TAP
Pol. II
Rpb6-TAP
Rpb8-TAP
Pol. I, II, III
C
0 3 6 8 10
hrs in BPS
Rpb1
CTD
8WG16
D
0 3 6 8 10
hrs in EDTA
α-Rpa135
PGK1
E
LZM
LIM
0 24 0 24
Hrs
Rpa190TAP
PGK1
LZM
LIM
0 24 0 24
Hrs
α-Rpa135
PGK1
F
0mM ZnCl2
2mM ZnCl2
0 3 6 8 0 3 6 8
Hr in EDTA
Rpa135-GFP
PGK1
G
WT
zap1Δ
0 3 6 8 10 0 3 6 8 10
Hr in EDTA
Rpa135-GFP
PGK1

Figure 2. Stabilization of RNAPI subunits during zinc deficiency in vacuolar protease mutants.

A. Northern analysis of RNAPI subunit mRNAs during zinc deficiency. **B.** Immunoblot analysis of Rpa135p in wild-type and vacuolar protease mutants. **C,** same as B except that Rpa135-GFP and Rpa43-GFP were used. **D.** Analysis of Rpa43 half-life in wild-type and vacuolar protease mutants. Cells expressing Rpa43p-GFP under the control of a MET promoter (repressed by Methionine) were pregrown in the absence of Met, and shifted for the indicated times in a Met-containing medium. Rpa43p-GFP levels were analyzed using anti-GFP antibodies. **E.** Immunoblot analysis of RNAPI-associated protein in wild-type and vacuolar protease mutants. Genes encoding Pep4p or Prb1p were disrupted in strains expressing various TAP-tagged proteins, and the level of these tagged subunits assessed during a low zinc shift.

Figure 2

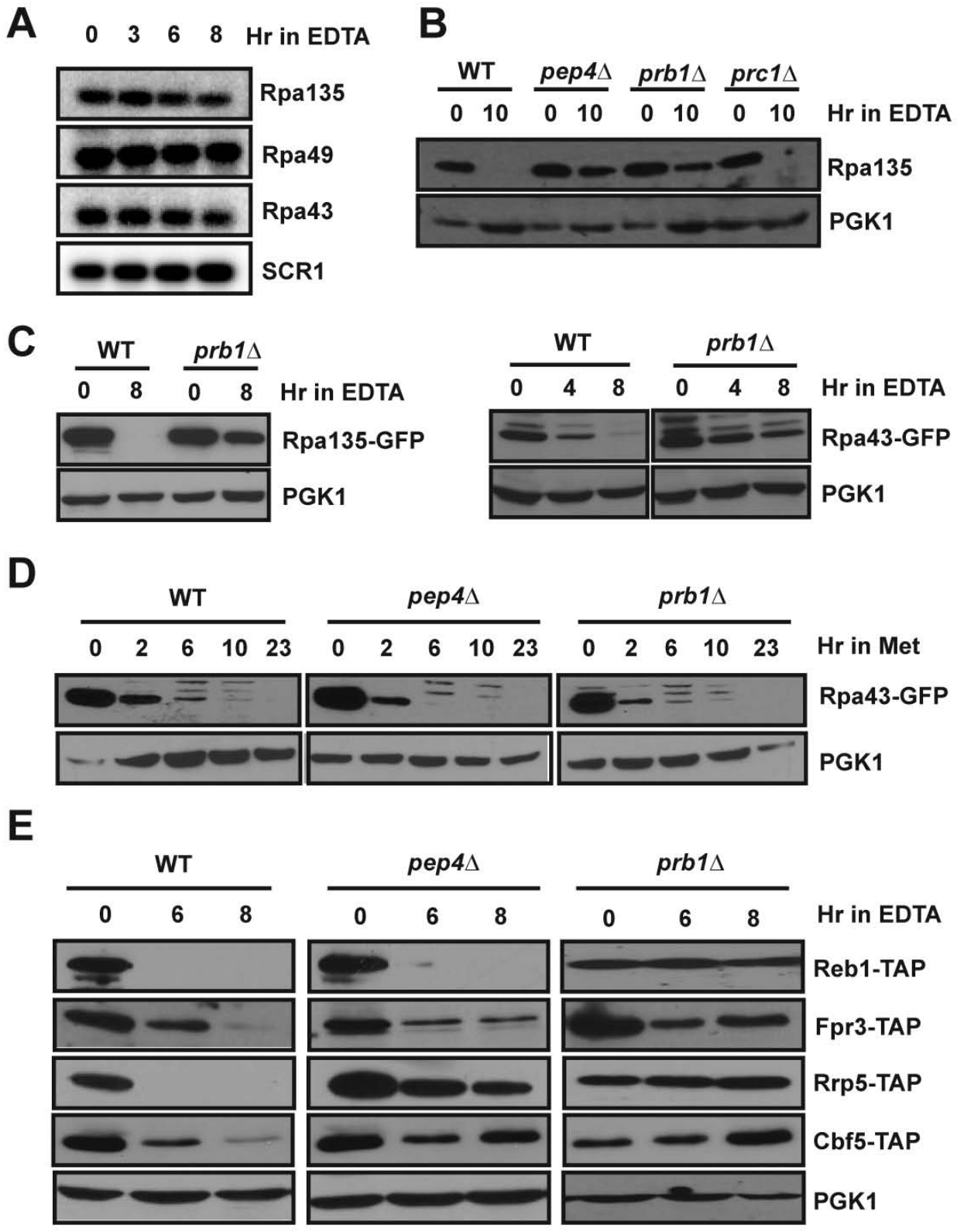
A
0 3 6 8 Hr in EDTA
Rpa135
Rpa49
Rpa43
SCR1
B
WT pep4Δ prb1Δ prc1Δ
0 10 0 10 0 10 0 10 Hr in EDTA
Rpa135
PGK1
C
WT prb1Δ
0 8 0 8 Hr in EDTA
Rpa135-GFP
PGK1
WT prb1Δ
0 4 8 0 4 8 Hr in EDTA
Rpa43-GFP
PGK1
D
WT pep4Δ prb1Δ
0 2 6 10 23 0 2 6 10 23 0 2 6 10 23 Hr in Met
Rpa43-GFP
PGK1
E
WT pep4Δ prb1Δ
0 6 8 0 6 8 0 6 8 Hr in EDTA
Reb1-TAP
Fpr3-TAP
Rrp5-TAP
Cbf5-TAP
PGK1

Figure 3. Export of RNA polymerase I subunit to the vacuole during zinc deficiency.

A. Localization of Rpa49-GFP in wild-type, *pep4Δ*or *prb1Δ* strains in normal medium (0 hrs in EDTA) or after 8 hours in low zinc medium. Green, Rpa49-GFP localization. The vacuole was stained with the FM4-64 dye (red).

B. Localization of Nop1-GFP in normal and low zinc conditions. Legends as in A, except that the strains were transformed with a plasmid expressing Nop1-GFP.

C. Genetic Inactivation of Xpo1p rescues RNAPI down-regulation. Wild-type or Xpo1-1 cells were shifted for 2 hours at 37°C before a shift to low zinc medium.

Figure 3

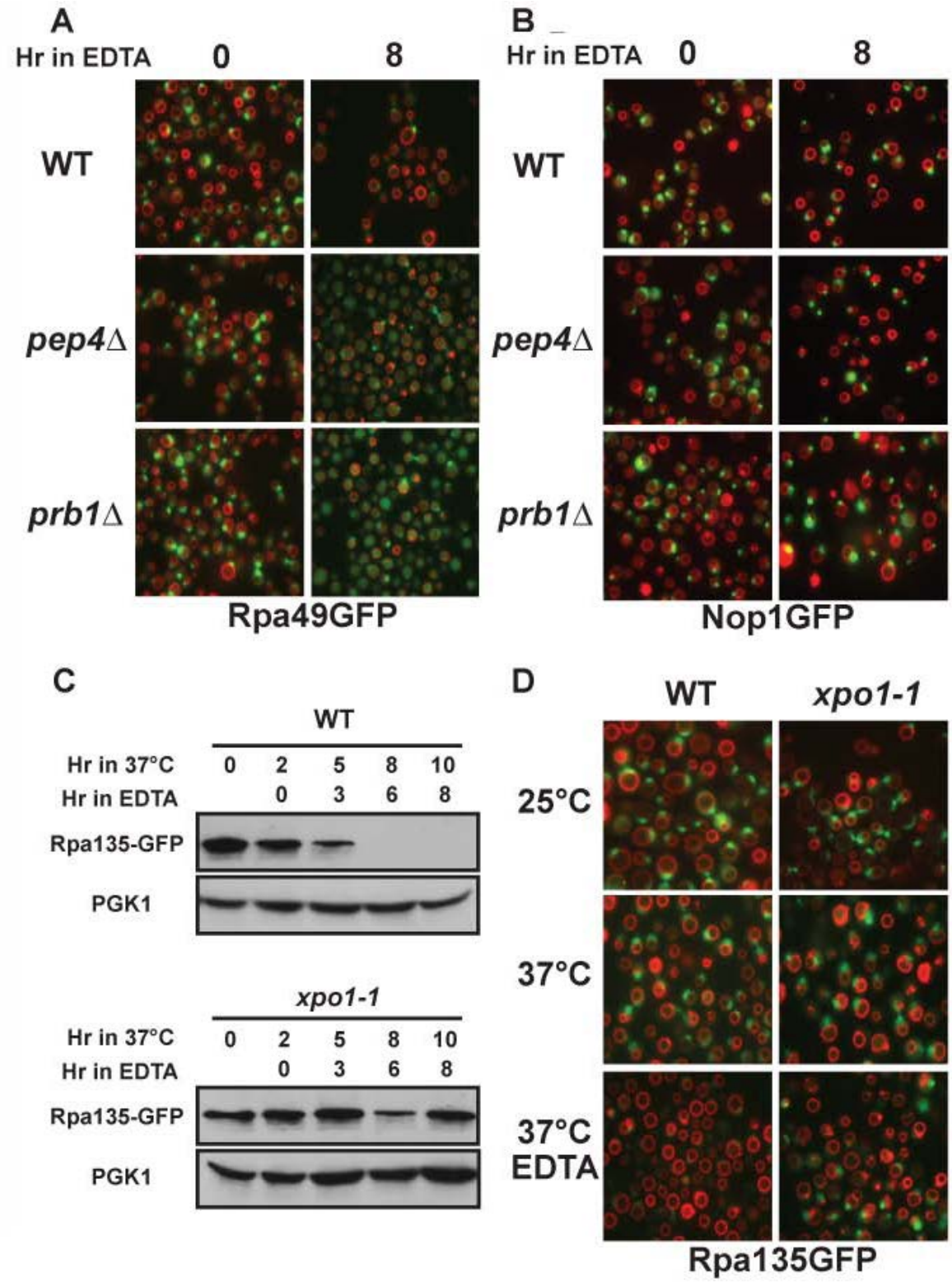
A
Hr in EDTA 0 8
WT
pep4Δ
prb1Δ
Rpa49GFP
B
Hr in EDTA 0 8
WT
pep4Δ
prb1Δ
Nop1GFP
C
WT
Hr in 37°C 0 2 5 8 10
Hr in EDTA 0 3 6 8
Rpa135-GFP
PGK1
xpo1-1
Hr in 37°C 0 2 5 8 10
Hr in EDTA 0 3 6 8
Rpa135-GFP
PGK1
D
WT
xpo1-1
25°C
37°C
37°C EDTA
Rpa135GFP

Figure 4. Loss of Ubiquitination of Rpa190 triggers RNAPI downregulation

A. Analysis of Ubiquitin in purified RNAPI preparations. RNAPI was TAP-purified from pep4*Δ* cells expressing a TAP-tagged version of Rpa190p grown in normal medium or after 4 or 8 hours in a low zinc medium. TAP purified RNAPI complexes were visualized by Sypro-Ruby staining (right), or analyzed by immunoblot using anti-Ubiquitin antibody, or anti-Rpa135 monoclonal antibody. Whole cell extracts were analyzed by immunoblot using the anti-Ubiquitin antibody.

Figure 4

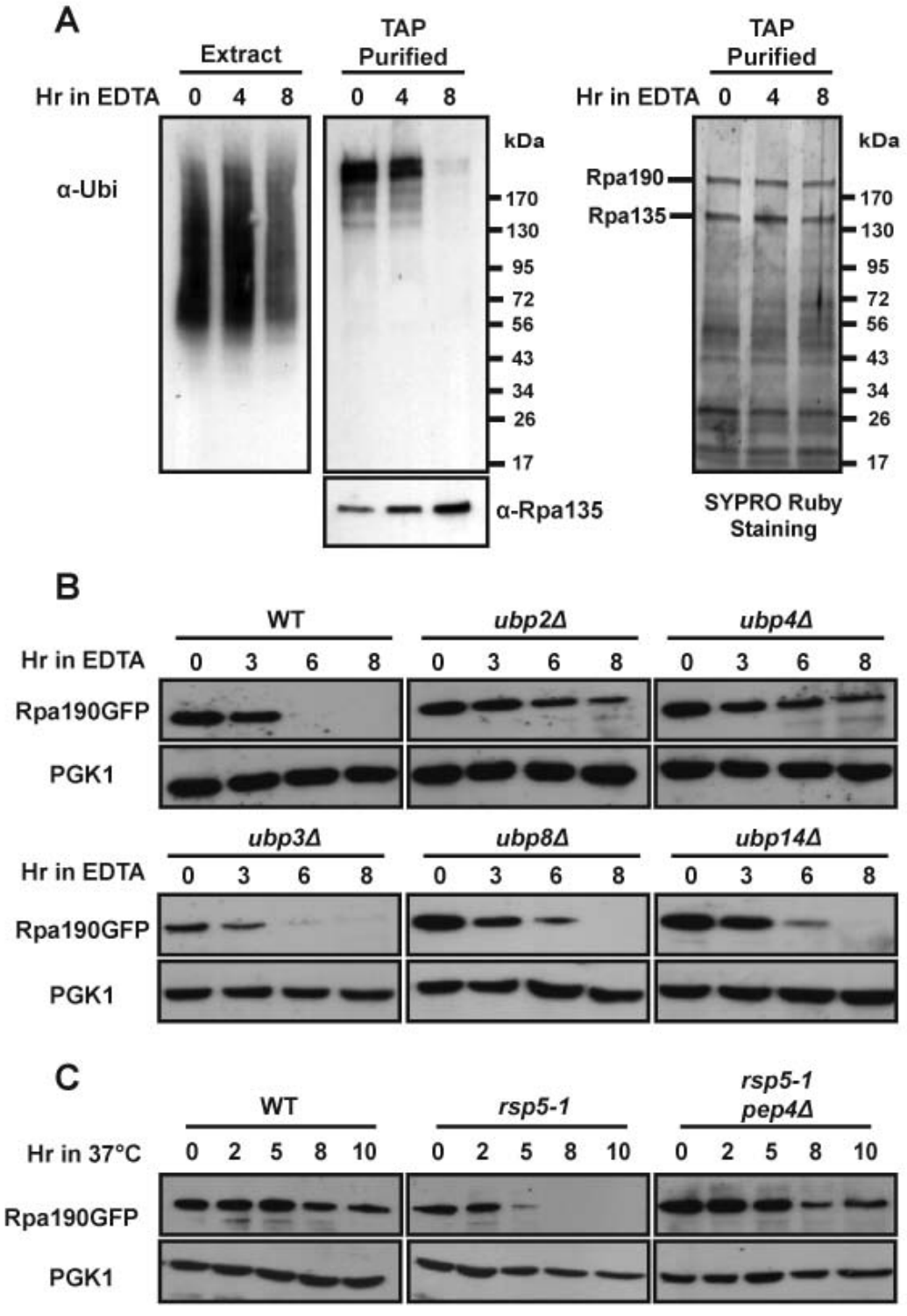
A
Extract
TAP Purified
Hr in EDTA 0 4 8
0 4 8
kDa
α-Ubi
170
130
95
72
56
43
34
26
17
α-Rpa135
TAP Purified
Hr in EDTA 0 4 8
kDa
Rpa190
Rpa135
170
130
95
72
56
43
34
26
17
SYPRO Ruby Staining
B
WT
ubp2Δ
ubp4Δ
Hr in EDTA 0 3 6 8 0 3 6 8 0 3 6 8
Rpa190GFP
PGK1
ubp3Δ
ubp8Δ
ubp14Δ
Hr in EDTA 0 3 6 8 0 3 6 8 0 3 6 8
Rpa190GFP
PGK1
C
WT
rsp5-1
rsp5-1 pep4Δ
Hr in 37°C 0 2 5 8 10 0 2 5 8 10 0 2 5 8 10
Rpa190GFP
PGK1

Figure 5. Localization of RNA Polymerase I subunits in Ubiquitin Proteases and Ligase mutants.

A. Localization of Rpa190-GFP in wild-type, *ubp2Δ* or *ubp4Δ* strains in normal medium (0 hrs in EDTA) or after 8 hours in low zinc medium. Green, Rpa190-GFP localization. The vacuole was stained with the FM4-64 dye (red).

B. Localization of Rpa190-GFP in wild-type and *rsp5-1*strains in normal conditions at 25°C and 37°C. Green, Rpa190-GFP localization. The vacuole was stained with the FM4-64 dye (red).

Figure 5

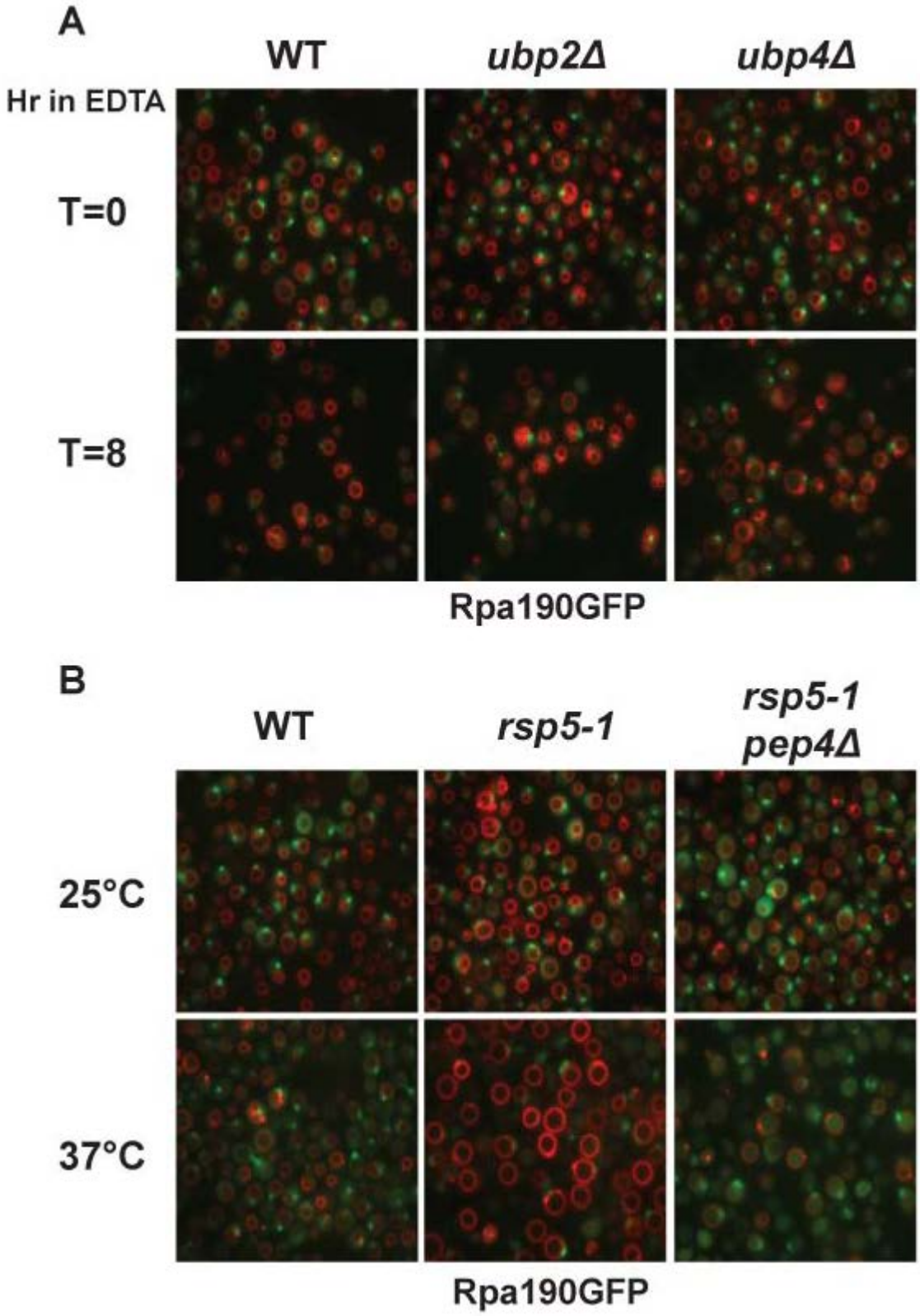
A
WT
ubp2Δ
ubp4Δ
Hr in EDTA
T=0
T=8
Rpa190GFP
B
WT
rsp5-1
rsp5-1
pep4Δ
25°C
37°C
Rpa190GFP

Figure 6. Downregulation of RNAPI transcriptional activity during zinc deficiency.

A. Pulse chase analysis of large RNAs. Shown is the profile of ^{3}H incorporation of pre-rRNAs and rRNAs after chase with unlabeled uracil. An ethidium bromide staining of the gel was performed prior to transfer to the membrane to standardize for loading.

B. Pulse chase analysis of 5.8S, 5S and tRNAs. Shown is the profile of ^{3}H incorporation of small RNAs after chase with unlabeled uracil. Samples were loaded on a polyacrylamide gel and transferred onto a membrane prior to fluorography. The membrane was then hybridized with a ^{32}P probe against the 5.8S rRNA for loading control.

Figure 6

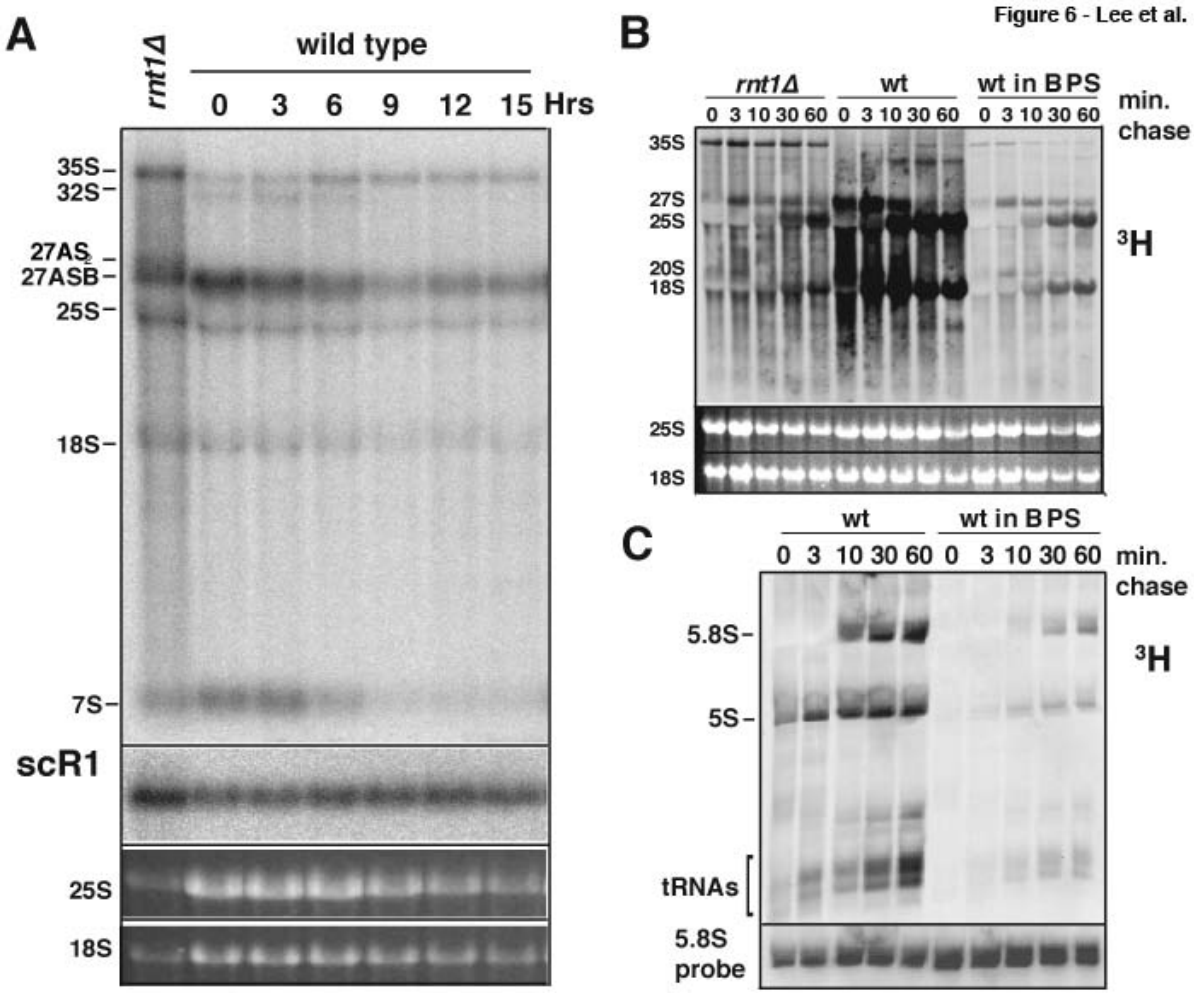
A
rnt1Δ
wild type
0 3 6 9 12 15 Hrs
35S
32S
27AS2
27ASB
25S
18S
7S
scR1
25S
18S
B
Figure 6 - Lee et al.
rnt1Δ
wt
wt in BPS
0 3 10 30 60 0 3 10 30 60 0 3 10 30 60
min. chase
35S
27S
25S
20S
18S
3H
25S
18S
C
wt
wt in BPS
0 3 10 30 60 0 3 10 30 60
min. chase
5.8S
5S
tRNAs
3H
5.8S probe

Figure 7. The kinetics of RNAPI vacuolar autophagy is influenced by the integrity of zinc finger containing subunits.

A. Analysis of Rpa135 Zinc finger mutants. Wild-type or Zinc finger mutant (C1107A or C4) versions of Rpa135 are HA-tagged (Naryshkina et al., 2003), and expressed in wild-type cells expressing endogenous Rpa135p. B. Analysis of Rpa135p levels during zinc deficiency in wild-type and *rpa12Δ* strains. Rpa135p levels were probed using anti-Rpa135p monoclonal antibody. C, Analysis of Rpa135p levels during zinc deficiency in wild-type and *rpa49Δ* strains.

Figure 7

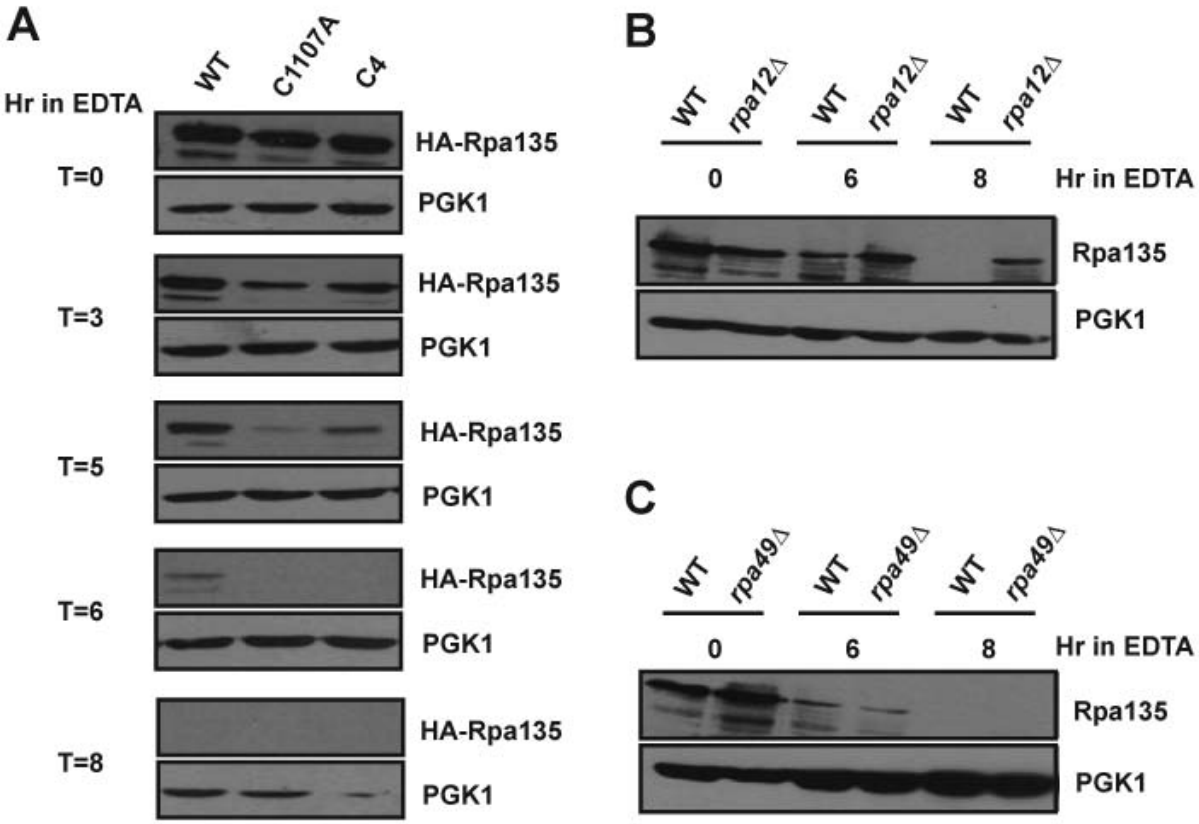
A
WT
C1107A
C4
Hr in EDTA
T=0
HA-Rpa135
PGK1
T=3
HA-Rpa135
PGK1
T=5
HA-Rpa135
PGK1
T=6
HA-Rpa135
PGK1
T=8
HA-Rpa135
PGK1
B
WT
rpa12Δ
WT
rpa12Δ
WT
rpa12Δ
0
6
8
Hr in EDTA
Rpa135
PGK1
C
WT
rpa49Δ
WT
rpa49Δ
WT
rpa49Δ
0
6
8
Hr in EDTA
Rpa135
PGK1

SUPPLEMENTAL FIGURES AND TABLE

Figure S1 RNA polymerase II large subunit CTD cleavage is a post-lysis artifact in extracts prepared from cells shifted in BPS-containing medium.

The CTD of Rpb1 is known to be sensitive to proteolytic cleavage during extract preparation and although protease inhibitors were included in our extracts, we could not rule out the possibility that the CTD cleavage observed in extracts prepared from cells shifted in BPS did not occur after cells lysis. To test whether the CTD cleavage is due to in vivo cleavage or rather to a post cells lysis artifact, we mixed cells harvested before (A_0), or after BPS incubation (A_{10}) and prepared protein extracts from these mixed cells (lane $B_{(0+10)}$, Figure S1). If CTD cleavage in BPS-shifted cells is due a proteolytic activity in the extracts, one might expect to see the complete disappearance of the full-length band in this extract prepared from mixed cells. As a control, extracts prepared separately from these two time points were mixed prior to loading ½(A_0+A_{10}). This experiment showed that in the extract prepared from mixed cells, the full-length Rpb1p disappears, demonstrating that CTD cleavage is indeed a proteolytic artifact that occurs post cells lysis. In contrast, Rpa135 was not affected in the extracts prepared from mixed cells, showing that RNA polymerase I subunits degradation occurs *in vivo*.

Figure S1 - related to Figure1. Analysis of Rpb1 and Rpa135 in extracts from cells prepared prior to or after switch to BPS-containing medium.

A_0, extracts prepared prior to shift to BPS; A_{10} extracts prepared after 10 hours in BPS. ½(A_0+A_{10}) samples contain protein extracts from A_0 and A_{10} samples mixed after extract preparation. $B_{(0+10)}$, protein extracts prepared from a mixture of cells harvested either prior or after BPS shift. Membranes were blotted using the indicated antibodies.

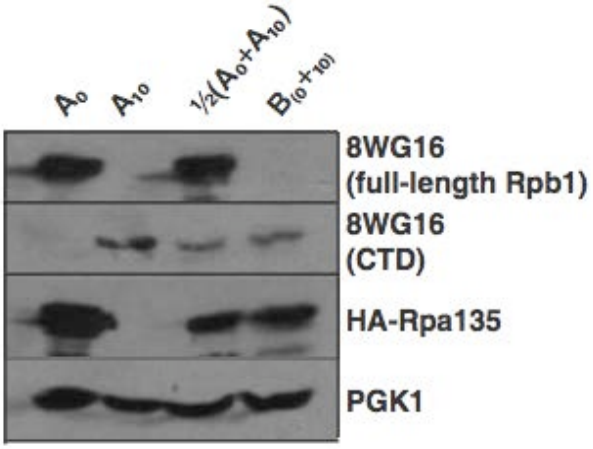

2- Analysis of RNAPI associated proteins and other nuclear proteins during a low zinc shift

Figure S2. Related to Figure 1. Cells expressing TAP-tagged subunits of RNAPI associated proteins (Reb1p, Fpr3p, Rrp5p, Cbf5p), other nucleolar (Fob1p) or nuclear (Tfg1p, Smd1p, Smb1p) proteins were shifted in a medium containing EDTA for the indicated times, and protein levels analyzed using antibodies. Extracts prepared from wild-type cells were also analyzed by immunoblot using anti-Nop1p monoclonal antibodies.

Figure S2

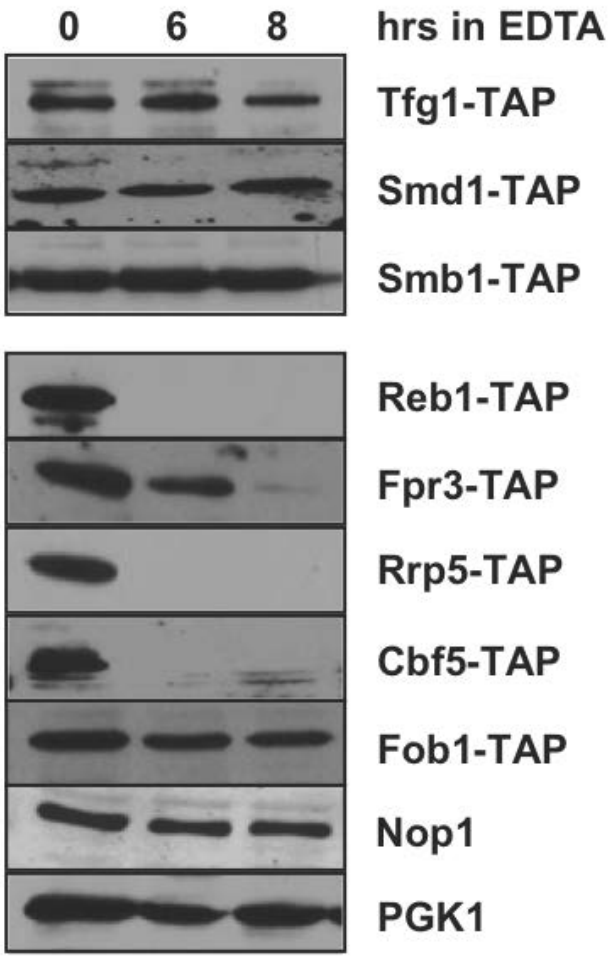
0
6
8
hrs in EDTA
Tfg1-TAP
Smd1-TAP
Smb1-TAP
Reb1-TAP
Fpr3-TAP
Rrp5-TAP
Cbf5-TAP
Fob1-TAP
Nop1
PGK1

3- Down-regulation of RNAPI in low zinc conditions is unrelated to other stresses or mutants previously described to affect RNAPI activity.

Figure S3. Related to Figure 2. **A.** Analysis of Rpa135p during amino acids starvation. **B-F,** analysis of Rpa135p levels in mutant backgrounds. Wild-type or the indicated mutant strains were shifted in a medium containing EDTA for the indicated times, and Rpa135p protein levels analyzed using anti-Rpa135p monoclonal antibody. PGK1 was used as a loading control.

Figure S3

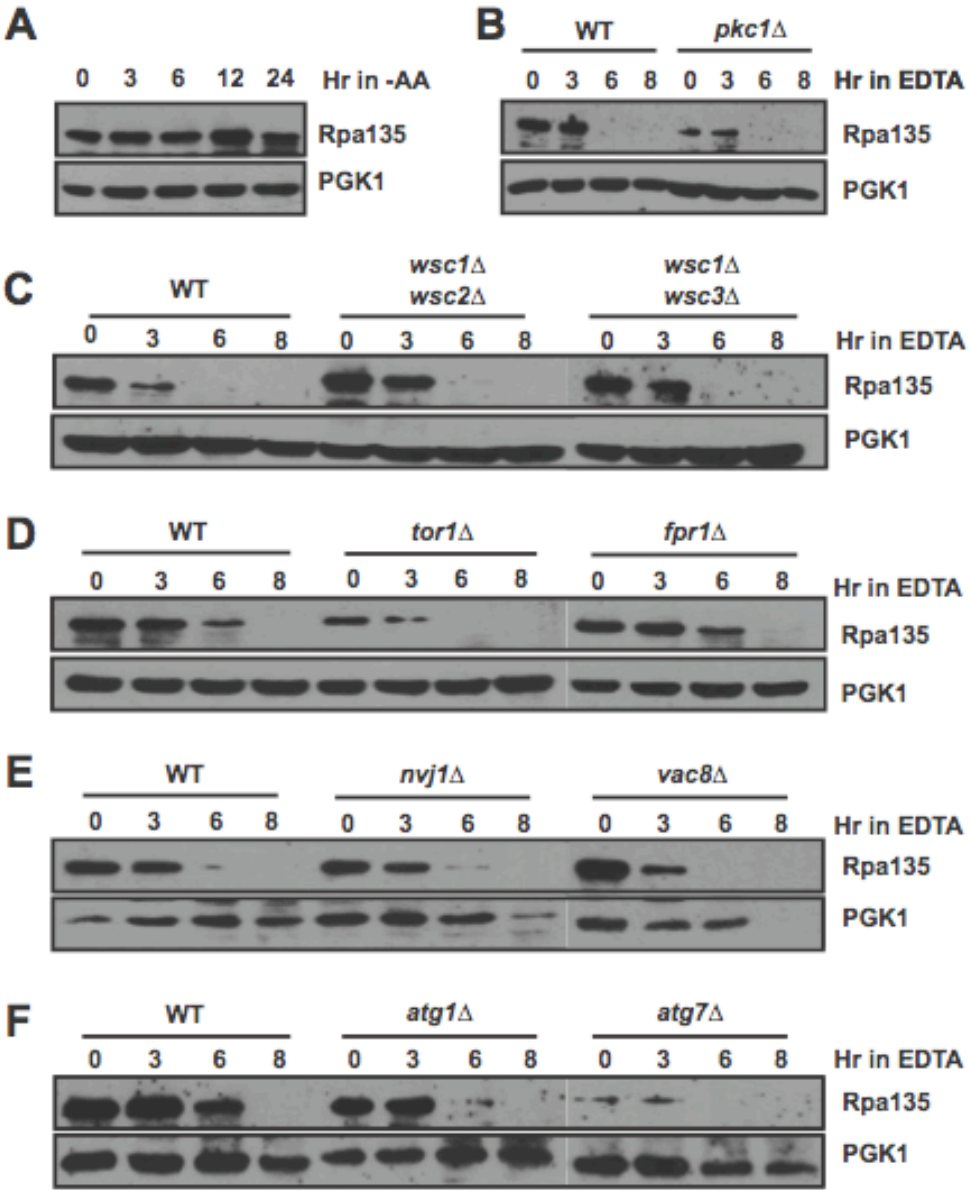
A
0 3 6 12 24 Hr in -AA
Rpa135
PGK1
B
WT
pkc1Δ
0 3 6 8 0 3 6 8 Hr in EDTA
Rpa135
PGK1
C
WT
wsc1Δ wsc2Δ
wsc1Δ wsc3Δ
0 3 6 8 0 3 6 8 0 3 6 8 Hr in EDTA
Rpa135
PGK1
D
WT
tor1Δ
fpr1Δ
0 3 6 8 0 3 6 8 0 3 6 8 Hr in EDTA
Rpa135
PGK1
E
WT
nvj1Δ
vac8Δ
0 3 6 8 0 3 6 8 0 3 6 8 Hr in EDTA
Rpa135
PGK1
F
WT
atg1Δ
atg7Δ
0 3 6 8 0 3 6 8 0 3 6 8 Hr in EDTA
Rpa135
PGK1

4- Down-regulation of RNAPI in low zinc conditions is quickly reversible.

Figure S4. Cells expressing GFP-tagged Rpa135 (dotted line) or Rpa190p (solid line) were shifted in a medium with EDTA for 10 hours. Aliquot samples were taken at time zero, 6 hours and 10 hours. After 10 hours, cells were harvested, washed and returned to normal minimal medium. Aliquots were taken after 30 minutes, 1 hour, 1 hour 30minutes, 2, 3 and 4 hours. The growth curves are shown in panel A, the level of Rpa135-GFP and Rpa190-GFP in panel B.

Figure S4

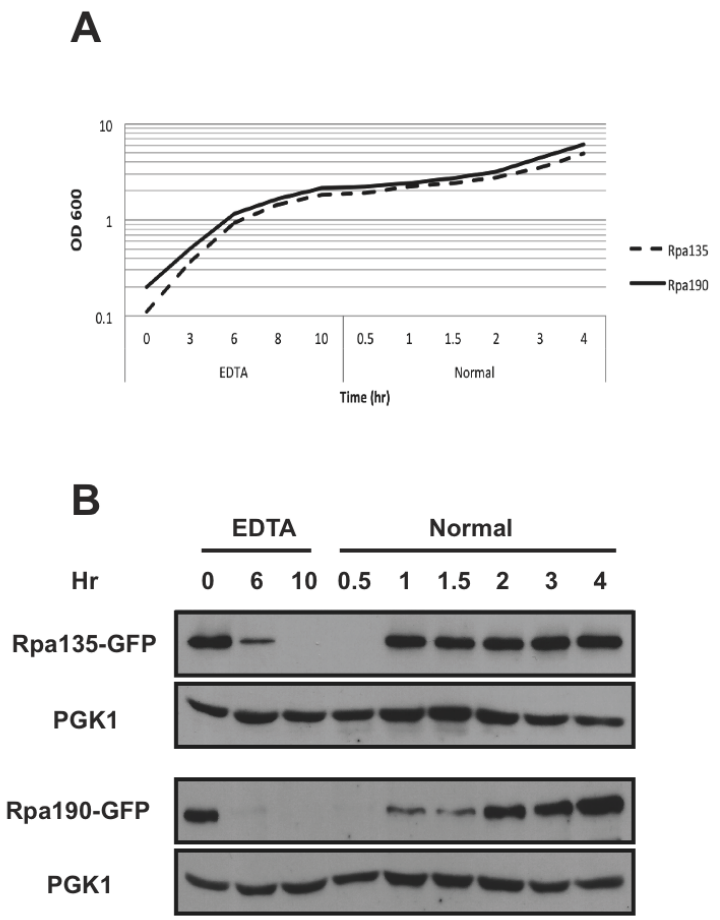
A
10
1
0.1
OD 600
0 3 6 8 10 0.5 1 1.5 2 3 4
EDTA
Normal
Time (hr)
Rpa135
Rpa190
B
EDTA
Normal
Hr
0 6 10 0.5 1 1.5 2 3 4
Rpa135-GFP
PGK1
Rpa190-GFP
PGK1

Figure S5 - Down-regulation of RNAPI is delayed in a *vps30*Δ mutant defective in vacuolar proteases sorting.

Rpa135-GFP levels were analyzed in wild-type and *vps30*Δ mutant defective in vacuolar proteases sorting.strains after a shift in EDTA-containing medium (panel A). In parallel, the localization of Rpa135p was followed and compared to the vacuole (red), revealed by staining with the FM4-64 dye.

Figure S5

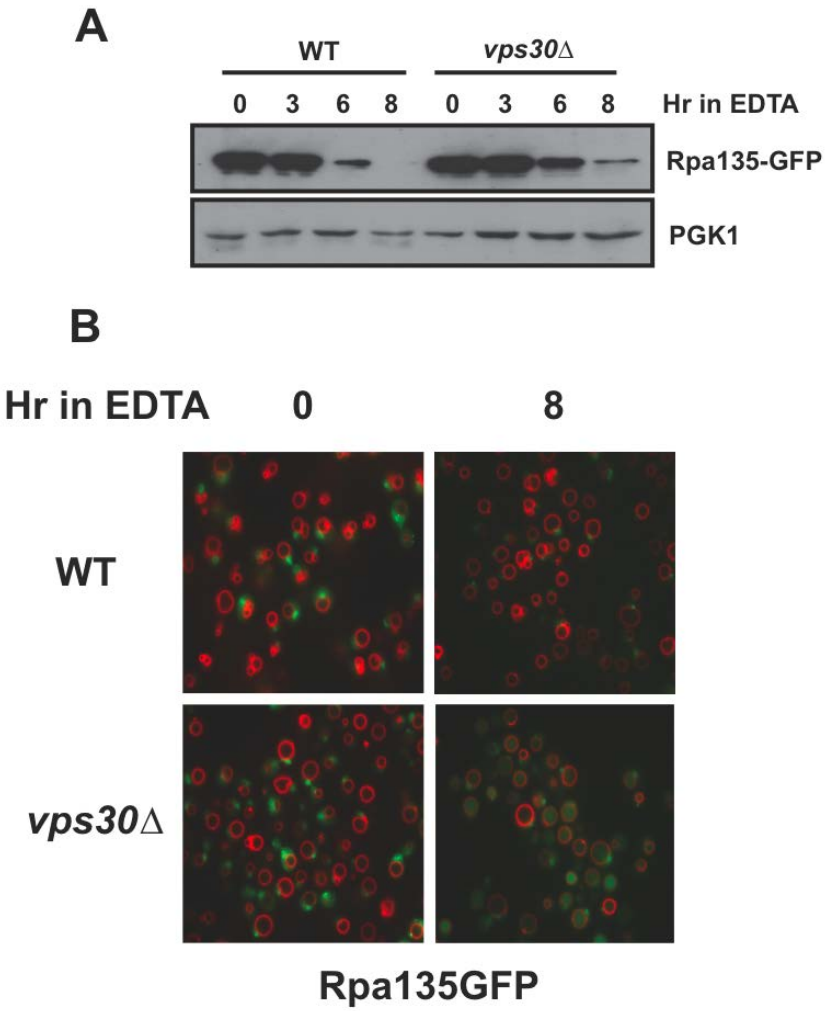
A
WT
vps30Δ
0 3 6 8 0 3 6 8
Hr in EDTA
Rpa135-GFP
PGK1
B
Hr in EDTA 0 8
WT
vps30Δ
Rpa135GFP

6 - TAP purification of RNAPI complexes before or after a shift in low zinc conditions.

Figure S6. Rpa135p and Rpa190p were TAP-tagged in a *pep4*Δ strain, and extracts prepared from strains grown in normal medium or after 8 hours in an EDTA-containing medium were used for TAP purification. Shown are the protein eluates after TAP purification. Proteins were visualized by Sypro-Ruby staining.

Figure S6

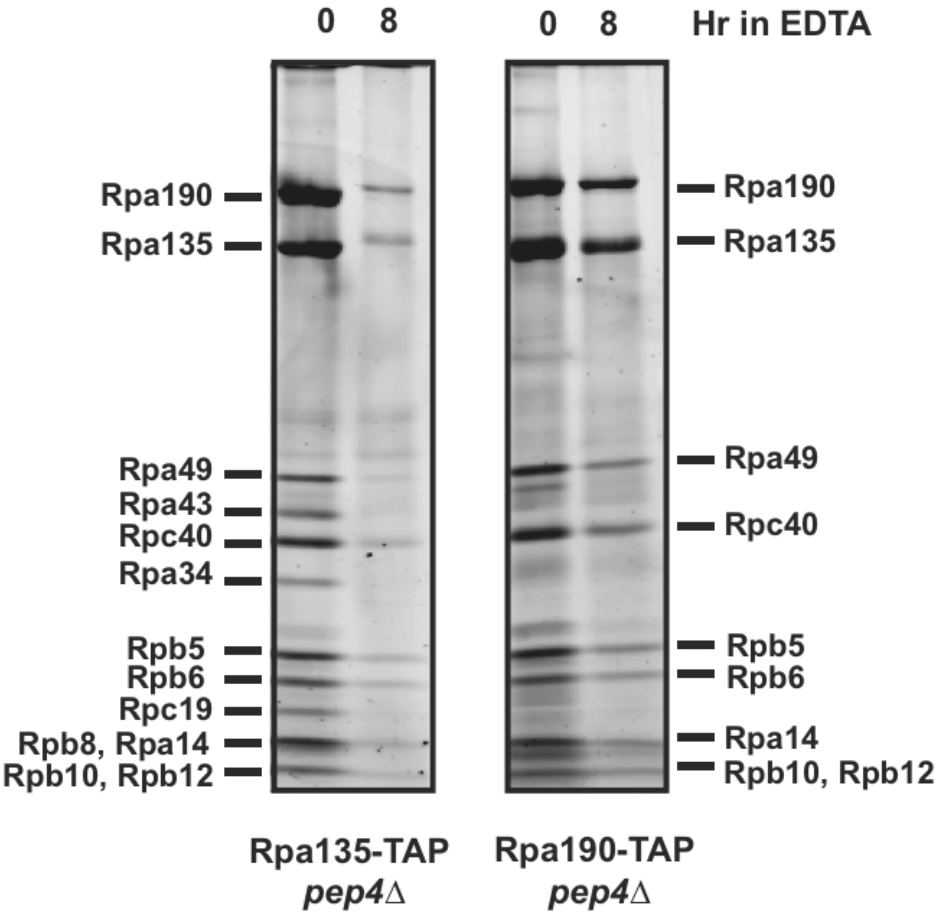
0
8
0
8
Hr in EDTA
Rpa190
Rpa135
Rpa49
Rpa43
Rpc40
Rpa34
Rpb5
Rpb6
Rpc19
Rpb8, Rpa14
Rpb10, Rpb12
Rpa190
Rpa135
Rpa49
Rpc40
Rpb5
Rpb6
Rpa14
Rpb10, Rpb12
Rpa135-TAP
pep4Δ
Rpa190-TAP
pep4Δ

Supplemental Table S1

Mass Spectrometric analysis of RNAPI subunits in normal medium and zinc deficiency conditions. An aliquot of the samples described above purified either using 50mM or 150mM NaCl were analyzed by mass spectrometry. The numbers indicated are normalized spectral abundance factors (NSAF). They correspond to the total number of spectra identified for each protein normalized by the length of each protein and the total number of spectra identified in the run.

Supplemental Table S1

RPA190-TAP				
Salt concentration	150 mM	150 mM	50 mM	50 mM
Hours in EDTA	0	8	0	8
RPA12	8401	6439	5607	3663
RPA135	1754	2632	1278	2054
RPA14	3158	3492	1329	2142
RPA190	1177	5633	2441	5510
RPA34	4068	4188	2518	2620
RPA43	4842	4740	3483	3259
RPA49	2817	4474	871	707
RPB8	791	1300	595	0
RPC10	3349	3688	1708	3690
RPC19	15813	9679	5357	5333
RPC40	5530	8432	3625	2260
RPO26	3345	3576	946	1704

RPA135-TAP				
Salt concentration	150 mM	150 mM	50 mM	50 mM
Hours in EDTA	0	8	0	8
RPA12	10616	14036	3160	2032
RPA135	2384	4418	1380	2596
RPA14	3032	4416	1553	1545
RPA190	1574	10295	2321	2946
RPA34	9334	4154	11941	5704
RPA43	4719	15112	4899	6674
RPA49	3920	1437	1375	1224
RPB8	2744	414	740	695
RPC10	5652	7285	2653	3749
RPC19	12651	12964	10462	8346
RPC40	8055	6372	4253	3866
RPO26	1998	4517	1329	4697

Table S2. Mutant Strains screened for RNAPI down-regulation during zinc deficiency.

Strain	Pol Subunit tested
doa1Δ	Rpa135
vid24Δ	Rpa135
doa3-1	Rpa135
sen3-1	Rpa135
fpr1Δ	Rpa135
tor1Δ	Rpa135
rpd3Δ	Rpa135
rck1Δ	Rpa49
rck2Δ	Rpa135, Rpa49
wsc1Δ,wsc2Δ	Rpa135
wsc1Δ,wsc3Δ	Rpa135
pkc1Δ	Rpa135
vps6Δ	Rpa135
vps21Δ	Rpa135
vps64Δ	Rpa135
vps8Δ	Rpa135
vps4Δ	Rpa135
vps23Δ	Rpa135
vps36Δ	Rpa135
atg1Δ	Rpa135
atg7Δ	Rpa135
atg11Δ	Rpa135
atg17Δ	Rpa135
atg19Δ	Rpa135
vac8Δ	Rpa135
nvj1Δ	Rpa135
ubp3Δ	Rpa135
bre5Δ	Rpa135
ubp1Δ	Rpa135,190
ubp6Δ	Rpa135,190
ubp8Δ	Rpa135,190
ubp14Δ	Rpa135,190
ubi4Δ	Rpa135
erg6Δ	Rpa135

SUB592	Rpa135
fpr3Δ	Rpa135
fpr4Δ	Rpa135
fpr3Δ,fpr4Δ	Rpa135
fpr1Δ,fpr3Δ	Rpa135
fpr1Δ,fpr3Δ,fpr4Δ	Rpa135
def1Δ	Rpa35
ssd1Δ	Rpa135
sec1-1	Rpa135
siz1Δ	Rpa49
siz2Δ	Rpa49
siz1Δ,siz2Δ	Rpa49
zip3Δ	Rpa49
siz1Δ,siz2Δ,zip3Δ	Rpa49
mms21-sp	Rpa135,Rpa49
ulp1Δ	Rpa49
uba2ts	Rpa49
asr1Δ	Rpa49
slx5Δ	Rpa49
slx8Δ	Rpa49
zap1Δ	Rpa135, Rpa49
zrt1Δ	Rpa49
zrc1Δ	Rpa49
zrt1Δzrt2Δ	Rpa190
zrt1Δzrt3Δ	Rpa190
zrt1Δzrc1Δ	Rpa190
mex67-5	Rpa49
mms1Δ	Rpa135
rtt101Δ	Rpa135

REFERENCES

Allmang, C., and Tollervey, D. (1998). The role of the 3' external transcribed spacer in yeast pre-rRNA processing. J Mol Biol *278*, 67-78.

Amerik, A.Y., Nowak, J., Swaminathan, S., and Hochstrasser, M. (2000). The Doa4 deubiquitinating enzyme is functionally linked to the vacuolar protein-sorting and endocytic pathways. Mol Biol Cell *11*, 3365-3380.

Bird, A.J., Gordon, M., Eide, D.J., and Winge, D.R. (2006). Repression of ADH1 and ADH3 during zinc deficiency by Zap1-induced intergenic RNA transcripts. Embo J *25*, 5726-5734.

Catala, M., Tremblay, M., Samson, E., Conconi, A., and Abou Elela, S. (2008). Deletion of Rnt1p alters the proportion of open versus closed rRNA gene repeats in yeast. Mol Cell Biol *28*, 619-629.

Chanfreau, G., Rotondo, G., Legrain, P., and Jacquier, A. (1998). Processing of a dicistronic small nucleolar RNA precursor by the RNA endonuclease Rnt1. EMBO J *17*, 3726-3737.

Chen, H.T., and Hahn, S. (2004). Mapping the location of TFIIB within the RNA polymerase II transcription preinitiation complex: a model for the structure of the PIC. Cell *119*, 169-180.

Claypool, J.A., French, S.L., Johzuka, K., Eliason, K., Vu, L., Dodd, J.A., Beyer, A.L., and Nomura, M. (2003). Tor pathway regulates Rrn3p-dependent recruitment of yeast RNA polymerase I to the promoter but does not participate in alteration of the number of active genes. Mol Biol Cell.

Cramer, P., Bushnell, D.A., and Kornberg, R.D. (2001). Structural basis of transcription: RNA polymerase II at 2.8 angstrom resolution. Science *292*, 1863-1876.

Donaldson, I.M., and Friesen, J.D. (2000). Zinc stoichiometry of yeast RNA polymerase II and characterization of mutations in the zinc-binding domain of the largest subunit. J Biol Chem *275*, 13780-13788.

Dupre, S., and Haguenauer-Tsapis, R. (2001). Deubiquitination step in the endocytic

pathway of yeast plasma membrane proteins: crucial role of Doa4p ubiquitin isopeptidase. Mol Cell Biol *21*, 4482-4494.

Falchuk, K.H., Mazus, B., Ber, E., Ulpino-Lobb, L., and Vallee, B.L. (1985). Zinc deficiency and the Euglena gracilis chromatin: formation of an alpha-amanitin-resistant RNA polymerase II. Biochemistry *24*, 2576-2580.

Fath, S., Milkereit, P., Podtelejnikov, A.V., Bischler, N., Schultz, P., Bier, M., Mann, M., and Tschochner, H. (2000). Association of yeast RNA polymerase I with a nucleolar substructure active in rRNA synthesis and processing. J Cell Biol *149*, 575-590.

Grummt, I. (2003). Life on a planet of its own: regulation of RNA polymerase I transcription in the nucleolus. Genes Dev *17*, 1691-1702.

Henras, A.K., Bertrand, E., and Chanfreau, G. (2004). A cotranscriptional model for 3'-end processing of the Saccharomyces cerevisiae pre-ribosomal RNA precursor. RNA *10*, 1572-1585.

Kaplan, J., McVey Ward, D., Crisp, R.J., and Philpott, C.C. (2006). Iron-dependent metabolic remodeling in S. cerevisiae. Biochim Biophys Acta *1763*, 646-651.

Kay, A.R. (2004). Detecting and minimizing zinc contamination in physiological solutions. BMC Physiol *4*, 4.

Kraft, C., Deplazes, A., Sohrmann, M., and Peter, M. (2008). Mature ribosomes are selectively degraded upon starvation by an autophagy pathway requiring the Ubp3p/Bre5p ubiquitin protease. Nat Cell Biol *10*, 602-610.

Kruhlak, M., Crouch, E.E., Orlov, M., Montano, C., Gorski, S.A., Nussenzweig, A., Misteli, T., Phair, R.D., and Casellas, R. (2007). The ATM repair pathway inhibits RNA polymerase I transcription in response to chromosome breaks. Nature *447*, 730-734.

Kvam, E., and Goldfarb, D.S. (2007). Nucleus-vacuole junctions and piecemeal microautophagy of the nucleus in S. cerevisiae. Autophagy *3*, 85-92.

Laferte, A., Favry, E., Sentenac, A., Riva, M., Carles, C., and Chedin, S. (2006). The transcriptional activity of RNA polymerase I is a key determinant for the level of all ribosome components. Genes Dev *20*, 2030-2040.

Lam, M.H., Urban-Grimal, D., Bugnicourt, A., Greenblatt, J.F., Haguenauer-Tsapis, R., and Emili, A. (2009). Interaction of the deubiquitinating enzyme Ubp2 and the e3 ligase Rsp5 is required for transporter/receptor sorting in the multivesicular body pathway. PLoS One *4*, e4259.

Lee, A., Henras, A.K., and Chanfreau, G. (2005). Multiple RNA surveillance pathways limit aberrant expression of iron uptake mRNAs and prevent iron toxicity in S. cerevisiae. Mol Cell *19*, 39-51.

Li, Y., Moir, R.D., Sethy-Coraci, I.K., Warner, J.R., and Willis, I.M. (2000). Repression of ribosome and tRNA synthesis in secretion-defective cells is signaled by a novel branch of the cell integrity pathway. Mol Cell Biol *20*, 3843-3851.

Lyons, T.J., Gasch, A.P., Gaither, L.A., Botstein, D., Brown, P.O., and Eide, D.J. (2000). Genome-wide characterization of the Zap1p zinc-responsive regulon in yeast. Proc Natl Acad Sci U S A *97*, 7957-7962.

Mayer, C., Bierhoff, H., and Grummt, I. (2005). The nucleolus as a stress sensor: JNK2 inactivates the transcription factor TIF-IA and down-regulates rRNA synthesis. Genes Dev *19*, 933-941.

Mayer, C., and Grummt, I. (2006). Ribosome biogenesis and cell growth: mTOR coordinates transcription by all three classes of nuclear RNA polymerases. Oncogene *25*, 6384-6391.

Merchant, S., and Bogorad, L. (1986). Rapid degradation of apoplastocyanin in Cu(II)-deficient cells of Chlamydomonas reinhardtii. J Biol Chem *261*, 15850-15853.

Moss, T. (2004). At the crossroads of growth control; making ribosomal RNA. Curr Opin Genet Dev *14*, 210-217.

Moss, T., Langlois, F., Gagnon-Kugler, T., and Stefanovsky, V. (2007). A housekeeper with power of attorney: the rRNA genes in ribosome biogenesis. Cell Mol Life Sci *64*, 29-49.

Nair, U., and Klionsky, D.J. (2005). Molecular mechanisms and regulation of specific and nonspecific autophagy pathways in yeast. J Biol Chem *280*, 41785-41788.

Naryshkina, T., Bruning, A., Gadal, O., and Severinov, K. (2003). Role of second-largest RNA polymerase I subunit Zn-binding domain in enzyme assembly. Eukaryot Cell *2*, 1046-1052.

Nierras, C.R., and Warner, J.R. (1999). Protein kinase C enables the regulatory circuit that connects membrane synthesis to ribosome synthesis in Saccharomyces cerevisiae. J Biol Chem *274*, 13235-13241.

Panina, E.M., Mironov, A.A., and Gelfand, M.S. (2003). Comparative genomics of bacterial zinc regulons: enhanced ion transport, pathogenesis, and rearrangement of ribosomal proteins. Proc Natl Acad Sci U S A *100*, 9912-9917.

Powers, T., and Walter, P. (1999). Regulation of ribosome biogenesis by the rapamycin-sensitive TOR-signaling pathway in Saccharomyces cerevisiae. Mol Biol Cell *10*, 987-1000.

Puig, S., Askeland, E., and Thiele, D.J. (2005). Coordinated remodeling of cellular metabolism during iron deficiency through targeted mRNA degradation. Cell *120*, 99-110.

Rigaut, G., Shevchenko, A., Rutz, B., Wilm, M., Mann, M., and Seraphin, B. (1999). A generic protein purification method for protein complex characterization and proteome exploration. Nat. Biotechnol. *17*, 1030-1032.

Shakoury-Elizeh, M., Tiedeman, J., Rashford, J., Ferea, T., Demeter, J., Garcia, E., Rolfes, R., Brown, P.O., Botstein, D., and Philpott, C.C. (2003). Transcriptional Remodeling in Response to Iron Deprivation in Saccharomyces cerevisiae. Mol Biol Cell *15*, 1233-1243.

Simm, C., Lahner, B., Salt, D., LeFurgey, A., Ingram, P., Yandell, B., and Eide, D.J. (2007). Saccharomyces cerevisiae vacuole in zinc storage and intracellular zinc distribution. Eukaryot Cell *6*, 1166-1177.

Stade, K., Ford, C.S., Guthrie, C., and Weis, K. (1997). Exportin 1 (Crm1p) is an essential nuclear export factor. Cell *90*, 1041-1050.

Stefanovsky, V., Langlois, F., Gagnon-Kugler, T., Rothblum, L.I., and Moss, T. (2006). Growth factor signaling regulates elongation of RNA polymerase I transcription in mammals via UBF phosphorylation and r-chromatin remodeling. Mol Cell *21*, 629-639.

Terhune, M.W., and Sandstead, H.H. (1972). Decreased RNA polymerase activity in mammalian zinc deficiency. Science *177*, 68-69.

Treich, I., Riva, M., and Sentenac, A. (1991). Zinc-binding subunits of yeast RNA polymerases. J Biol Chem *266*, 21971-21976.

Van Ho, A., Ward, D.M., and Kaplan, J. (2002). Transition metal transport in yeast. Annu Rev Microbiol *56*, 237-261.

Van Mullem, V., Landrieux, E., Vandenhaute, J., and Thuriaux, P. (2002). Rpa12p, a conserved RNA polymerase I subunit with two functional domains. Mol Microbiol *43*, 1105-1113.

Vida, T.A., and Emr, S.D. (1995). A new vital stain for visualizing vacuolar membrane dynamics and endocytosis in yeast. J Cell Biol *128*, 779-792.

Warner, J.R. (1999). The economics of ribosome biosynthesis in yeast. Trends Biochem Sci *24*, 437-440.

Wu, C.Y., Bird, A.J., Chung, L.M., Newton, M.A., Winge, D.R., and Eide, D.J. (2008). Differential control of Zap1-regulated genes in response to zinc deficiency in Saccharomyces cerevisiae. BMC Genomics *9*, 370.

Zhao, H., and Eide, D. (1996). The ZRT2 gene encodes the low affinity zinc transporter in Saccharomyces cerevisiae. J Biol Chem *271*, 23203-23210.

CHAPTER 4

FUTURE DIRECTIONS

From the work presented in Chapter 2, it is clear that iron toxicity does not result from oxidative stress. Instead, sphingolipid signaling mediates iron toxicity. However, further studies need to be done in order to understand why activation of sphingolipid-mediated signaling in high iron conditions leads to cellular toxicity. Identification of the downstream targets of sphingolipid signaling in high iron conditions can provide insight into why this signaling pathway leads to cellular toxicity. Moreover, further studies on regulation of Orm proteins in high iron conditions can also help us understand the regulation of sphingolipid signaling in response to different iron concentrations. Furthermore, it is important to investigate why excess iron can trigger an increase in sphingolipid synthesis, which leads to cellular toxicity. In other eukaryotes, such as human, Orm proteins inhibit sphingolipid synthesis (Breslow et al, 2010). Therefore, it is important to investigate whether a similar signaling pathway is induced in response to high iron in other eukaryotic cells.

As shown in Chapter 3, we discovered that the RNA polymerase I complex is subject to degradation during zinc deficiency and that this degradation is mediated by the nuclear exportin Xpo1 and vacuolar proteases Pep4 and Prb1. However, the mechanism involved in transporting the RNAPI complex into the vacuole is still unknown. It is important to further investigate the mechanism of the RNAPI complex import into the vacuole in order to provide a complete story of the down-regulation RNAPI complex during zinc starvation. Moreover, we have shown that de-ubiquitination is required for the down-regulation of the RNAPI

complex during zinc starvation. It still remains unknown whether RNAPI subunits or the associated proteins are deubiquitinated during zinc starvation. Therefore, it is important to identify the deubiquitinated protein(s) and the mechanism which triggers the de-ubiquitination during zinc starvation. Furthermore, based on the data shown in Chapter 3, we hypothesize that one of the zinc-binding subunits of RNAPI complex may function as a zinc sensor to trigger the down-regulation of RNAPI during zinc starvation. Therefore, it is important to study whether the zinc-binding domains of RNAPI subunits play important roles in the down-regulation of RNAPI complex during zinc deficiency.

REFERENCES

Breslow, D.K., Collin, S.R., Bodenmiller, B., Aebersold, R., Simon, K., Shevchnko, A., Ejsing, C.S., and Weissman, J.S. (2010) Orm family proteins mediate sphingolipid homeostasis. *Nature* 463(7284):1048-53